Calhoun: The NPS Institutional Archive
DSpace Repository

Theses and Dissertations 1. Thesis and Dissertation Collection, all items

1976-09

An investigation of stress determination for aircraft fatigue life estimation from in-flight strain data.

Horne, George Michael

Monterey, California: Naval Postgraduate School

http://hdl.handle.net/10945/17825

This publication is a work of the U.S. Government as defined in Title 17, United States Code, Section 101. Copyright protection is not available for this work in the United States.

Downloaded from NPS Archive: Calhoun

Calhoun is the Naval Postgraduate School's public access digital repository for research materials and institutional publications created by the NPS community. Calhoun is named for Professor of Mathematics Guy K. Calhoun, NPS's first appointed -- and published -- scholarly author.

Dudley Knox Library / Naval Postgraduate School
411 Dyer Road / 1 University Circle
Monterey, California USA 93943

http://www.nps.edu/library

AN INVESTIGATION OF STRESS DETERMINATION FOR AIRCRAFT FATIGUE LIFE ESTIMATION FROM IN-FLIGHT STRAIN DATA

George Michael Horne

DUDLEY KNOX LIBRARY
NAVAL POSTGRADUATE SCHOOL
MONTEREY, CALIFORNIA 93940

NAVAL POSTGRADUATE SCHOOL

Monterey, California

THESIS

An Investigation of Stress Determination for Aircraft Fatigue Life Estimation from In-Flight Strain Data

by

George Michael Horne

September 1976

Thesis Advisor: G. H. Lindsey

Approved for public release; distribution unlimited.

T175042

REPORT DOCUMENTATION PAGE	READ INSTRUCTIONS BEFORE COMPLETING FORM
1. REPORT NUMBER | 2. GOVT ACCESSION NO.	3. RECIPIENT'S CATALOG NUMBER
4. TITLE (and Subtitle) An Investigation of Stress Determination for Aircraft Fatigue Life Estimation from In-Flight Strain Data	5. TYPE OF REPORT & PERIOD COVERED Master's Thesis September 1976 6. PERFORMING ORG. REPORT NUMBER
7. AUTHOR(s) George Michael Horne	8. CONTRACT OR GRANT NUMBER(s)
9. PERFORMING ORGANIZATION NAME AND ADDRESS Naval Postgraduate School Monterey, CA 93940	10. PROGRAM ELEMENT, PROJECT, TASK AREA & WORK UNIT NUMBERS
11. CONTROLLING OFFICE NAME AND ADDRESS Naval Postgraduate School Monterey, CA 93940	12. REPORT DATE September 1976 13. NUMBER OF PAGES 139
14. MONITORING AGENCY NAME & ADDRESS (if different from Controlling Office) Naval Postgraduate School Monterey, CA 93940	15. SECURITY CLASS. (of this report) UNCLASSIFIED 15a. DECLASSIFICATION/DOWNGRADING SCHEDULE

16. DISTRIBUTION STATEMENT (of this Report)

Approved for public release; distribution unlimited.

17. DISTRIBUTION STATEMENT (of the abstract entered in Block 20, if different from Report)

18. SUPPLEMENTARY NOTES

19. KEY WORDS (Continue on reverse side if necessary and identify by block number)

Stress determination, aircraft structures, stress relaxation

20. ABSTRACT (Continue on reverse side if necessary and identify by block number)

A thorough knowledge of localized stresses due to geometric effects is necessary for accurate fatigue life estimation in aircraft structures. The Department of Aeronautics, Naval Postgraduate School, Monterey, California, has developed a strain monitoring system that provides data on nominal stresses experienced by aircraft structures, which can be applied to

DD FORM 1 JAN 73 1473 EDITION OF 1 NOV 65 IS OBSOLETE
(Page 1) S/N 0102-014-6601 |

20. Abstract (continued)

obtain local stresses at a stress concentration, provided a local stress vs. nominal strain relationship is available. A theory proposed by Neuber lends itself to development of a method by which local stress can be obtained with knowledge of nominal strain and material properties alone.

Neuber's theory was evaluated by comparison of experimental stress concentration factors with theoretical values for plates with central holes and was found to be a valid basis for obtaining local stress from nominal strain.

Stress relaxation behavior was obtained for two cyclic loading histories of plate specimens in an effort to extend the monotonic local stress vs. nominal strain relationships into practical use for fatigue life estimation of aircraft structures.

An Investigation of Stress Determination for Aircraft Fatigue Life Estimation from In-Flight Strain Data

by

George Michael Horne
Lieutenant, United States Navy
B.S., Mississippi State University, 1968

Submitted in partial fulfillment of the
requirements for the degree of

MASTER OF SCIENCE IN AERONAUTICAL ENGINEERING

from the

NAVAL POSTGRADUATE SCHOOL
September 1976

Thesis
H8024
c.1

DUDLEY KNOX LIBRARY
NAVAL POSTGRADUATE SCHOOL
MONTEREY, CALIFORNIA 93940

ABSTRACT

A thorough knowledge of localized stresses due to geometric effects is necessary for accurate fatigue life estimation in aircraft structures. The Department of Aeronautics, Naval Postgraduate School, Monterey, California, has developed a strain monitoring system that provides data on nominal stresses experienced by aircraft structures, which can be applied to obtain local stresses at a stress concentration, provided a local stress vs. nominal strain relationship is available. A theory proposed by Neuber lends itself to development of a method by which local stress can be obtained with knowledge of nominal strain and material properties alone.

Neuber's theory was evaluated by comparison of experimental stress concentration factors with theoretical values for plates with central holes and was found to be a valid basis for obtaining local stress from nominal strain.

Stress relaxation behavior was obtained for two cyclic loading histories of plate specimens in an effort to extend the monotonic local stress vs. nominal strain relationships into practical use for fatigue life estimation of aircraft structures.

TABLE OF CONTENTS

I. INTRODUCTION AND LITERATURE SURVEY ---------------- 9

II. STRESS-STRAIN DATA ON UNIAXIAL SPECIMENS OF 7075 T-6 ALUMINUM ---------------------------------- 13

- A. INTRODUCTION ---------------------------------- 13
- B. CYCLIC STRESS-STRAIN CURVE TEST -------------- 21
  - 1. Description of Test --------------------- 21
  - 2. Test Results ---------------------------- 27
- C. SINGLE AMPLITUDE CYCLIC LOADING TEST --------- 31
  - 1. Description of Test --------------------- 31
  - 2. Test Results ---------------------------- 31
- D. DUAL AMPLITUDE CYCLIC LOADING TEST ----------- 33
  - 1. Description of Test --------------------- 33
  - 2. Test Results ---------------------------- 43
- E. DISCUSSION OF TEST RESULTS ------------------ 46

III. LOCAL STRESS-STRAIN BEHAVIOR ---------------------- 50

- A. INTRODUCTION ---------------------------------- 50
- B. CALCULATION OF LOCAL STRESS ON INITIAL LOADING --------------------------------------- 51
- C. EVALUATION OF STRAIN GAGE PLACEMENT ---------- 52
- D. CYCLIC LOADING TESTS ------------------------- 58
  - 1. Single Amplitude Cyclic Loading Test ---- 59
  - 2. Single Amplitude Cyclic Loading Test Results --------------------------------- 60
  - 3. Dual Amplitude Cyclic Loading Test ------ 65
  - 4. Dual Amplitude Cyclic Loading Test Results --------------------------------- 66
  - 5. Discussion of Test Results -------------- 69

E. STRESS RELAXATION BEHAVIOR ------------------ 71

1. Introduction and Theory ---------------- 71

2. Single Amplitude Cyclic Loading Test Results ---------------------------------- 76

3. Dual Amplitude Cyclic Loading Test Results ---------------------------------- 82

4. Discussion of Test Results ------------- 88

IV. CONCLUSIONS ON TEST RESULTS --------------------- 92

APPENDIX A - TABULAR DATA ---------------------------- 95

REFERENCES -- 137

INITIAL DISTRIBUTION LIST ------------------------------ 139

LIST OF FIGURES

1. Photograph of plate with a central hole ---------- 14

2. Diagram of plate with a central hole ------------ 15

3. Photograph of uniaxial specimen ---------------- 16

4. Diagram of uniaxial specimen ------------------- 17

5. Photograph of MTS System ----------------------- 19

6. Photograph of MTS System ----------------------- 20

7. Diagram of beat phenomena waveform -------------- 23

8. Diagram of hysteresis loops for cyclic stress-strain curve ---------------------------- 26

9. Cyclic and monotonic stress-strain curves -------- 28

10. Monotonic stress-strain curve (cyclic stress-strain curve test) ---------------------- 29

11. $\sigma\varepsilon$-σ curve (cyclic stress-strain curve test) ----- 30

12. Monotonic stress-strain curves (single and dual amplitude cyclic loading tests on uniaxial specimens ------------------------------- 32

13. $\sigma\varepsilon$-σ curve (single amplitude cyclic loading test on a uniaxial specimen) -------------------------- 34

14. σ-N curve (single amplitude cyclic loading test on a uniaxial specimen) -------------------------- 35

15. Dual amplitude input function ------------------ 37

16. $\sigma\varepsilon$-σ curve (dual amplitude cyclic loading test on a uniaxial specimen) -------------------------- 44

17. σ-N curve (dual amplitude cyclic loading test on a uniaxial specimen) -------------------------- 45

18. Center section of plate with central hole -------- 53

19. Monotonic σ-e curve (single amplitude cyclic loading test on a plate) ------------------------ 64

20. Monotonic σ-e curve (dual amplitude cyclic loading test on a plate) ------------------------ 68

21. Stress and strain relationships for relaxation theory -- 73

22. σ-N curve (single amplitude cyclic loading test on plate E = 10.67×10^6 lbf/in^2)------------------ 79

23. σ-N curve (single amplitude cyclic loading test on plate E = 10.0×10^6 lbf/in^2) ------------------ 80

24. σ-N curve (dual amplitude cyclic loading test on plate E = 10.67×10^6 lbf/in^2) ----------------- 85

25. σ-N curve (dual amplitude cyclic loading test on plate E = 10.19×10^6 lbf/in^2) ----------------- 86

26. Initial stress vs. relaxation rate parameter - all tests -- 90

I. INTRODUCTION AND LITERATURE SURVEY

The ability to predict the fatigue life of aircraft structures accurately and with reliability is of prime concern to structural engineers.

Prior to any attempt to derive a valid fatigue life theory one basic requirement must be satisfied. A thorough knowledge of localized stresses due to geometric effects is necessary and, because these stresses can not be measured directly, an accurate method of determining them analytically must be found which is applicable to a variety of loading situations and configurations. From a more realistic and practical standpoint fatigue life estimation would be greatly facilitated if stresses could be calculated based on actual inflight strain histories, data that are quite easily obtained in realistic situations but difficult to simulate in a laboratory. Specifically, if a relationship between the nominal strain in a structural component and the local stress at a stress raiser could be developed based on structural configuration, then the easily measured nominal strain would provide a local stress. Knowledge of this local stress is critical to fatigue life estimation, since fatigue failures originate at the stress raiser.

In a survey of the literature to determine if a satisfactory method for determining local stress exists, and if such a method would be adequate with only nominal strain and

the material properties known, one relationship was frequently encountered. This relationship, postulated by Neuber (Ref. 1), states that the geometric mean of the stress concentration factor, K_σ, and the strain concentration factor, K_ε, is equivalent to the elastic stress concentration factor, K_t, even in nonlinear stress-strain regions, or

$$K_t^2 = K_\sigma \; K_\varepsilon$$

where

$$K_\sigma = \frac{\text{local stress}}{\text{nominal stress}} = \frac{\sigma}{s}$$

and

$$K_\varepsilon = \frac{\text{local strain}}{\text{nominal strain}} = \frac{\varepsilon}{e}$$

Numerous examples of the adequacy of this relationship in calculating stress-strain curves were found. Crews used a modified form of the relationship in loading sequence tests (Ref. 2), and in a study of stress-strain behavior at notch roots (Ref. 3), and found the stresses thus calculated correlated very closely with experimentally determined stresses. Wetzel studied the accuracy of the relationship with three different types of data taken in experiments involving smooth specimen simulation of fatigue behavior of notches (Ref. 4). Morrow et al., also confirm the validity of the equation by comparison of fatigue failures at different stress concentration factors (Ref. 5). Since the Neuber relationship involved the factors of interest in this investigation and in light of

past results, it appeared that Neuber's theory might prove to be a satisfactory basis on which to establish a method for calculating local stress using nominal strain.

During the course of this study the requirement for a stress-strain relationship was expected. However, due to the dependence of fatigue on cyclic loading a monotonic stress-strain relationship alone appeared to be insufficient and a cyclic-stress-strain curve would be required in addition to the monotonic one. Landgraf et al., conducted a literature survey to determine whether an exact definition of a cyclic stress-strain curve existed and found none (Ref. 6). They did, however, propose an incremental step test method for determining a cyclic stress-strain curve whereby a uniaxial specimen is taken into tensile yield, then compressive yield, then cycled in tension and compression to decreasing values of strain. The locus of the maximum values of strain obtained from the resulting hysteresis loops forms the cyclic stress-strain curve. This method was adopted for use in this study.

Because the local stress-nominal strain relationships expected to be developed from this study would eventually be applied to actual aircraft structures under fatigue analysis, a specimen representing a realistic structural component was sought. A plate with a central hole was decided upon due to its commonality in almost all aircraft structures. The plate specimen was expected to provide local and nominal stress and

strain data which would be representative of that found in actual structural components.

During the literature survey a dependence of fatigue on loading history was shown by Crews (Ref. 2), Naumann (Refs. 7 and 8), Schijve (Refs. 9 and 10), and Potter (Ref. 11). In order to establish a basic foundation of knowledge from which to extend into more sophisticated loading histories, two simple loading situations were proposed. Single and dual, or repetitive high-low, amplitude loading programs were chosen to compare the effects of different loading histories on stress relaxation behavior, a necessary factor in the determination of local stress in cyclic loading situations. In the tests proposed, the requirement for compressive loading of the plates was ruled out on the basis that in actual aircraft structures such loads, in the higher stress regions to be encountered, would cause buckling and change the nature of the investigation entirely.

In summary, this investigation was directed toward determining a method whereby local stress can be calculated from knowledge of nominal strain and material properties alone. Local stress relaxation behavior was examined in order to extend the local stress vs. nominal strain relationship to the determination of local stress under cyclic loading and thereby give it practicality in future fatigue life determination studies.

II. STRESS-STRAIN DATA ON UNIAXIAL SPECIMENS OF 7075 T-6 ALUMINUM

A. INTRODUCTION

In order to provide a sound data base for comparison with data obtained in tests on plate specimens with central holes (Figs. 1 and 2), uniaxial specimens of 7075 T-6 aluminum (Figs. 3 and 4) were subjected to three different tests. The first test was designed to obtain monotonic and cyclic stress-strain curves. The second and third were single and dual amplitude cyclic loading tests, which were designed to obtain monotonic stress-strain curves and stress relaxation data under two different types of loading. The single amplitude cyclic loading test was designed to repeatedly load the specimen to a predetermined strain, which remained constant throughout the test. The dual amplitude cyclic loading test was designed to alternately load the specimen to two predetermined strains, one approximately twice the magnitude of the other.

The data obtained from the uniaxial specimens were considered indicative of the properties of the material at the location of stress concentration factor (Ref. 3) and would provide a consistent and readily duplicated basis for determining behavior of other specimens of the same material but of arbitrary geometry and stress concentration factors.

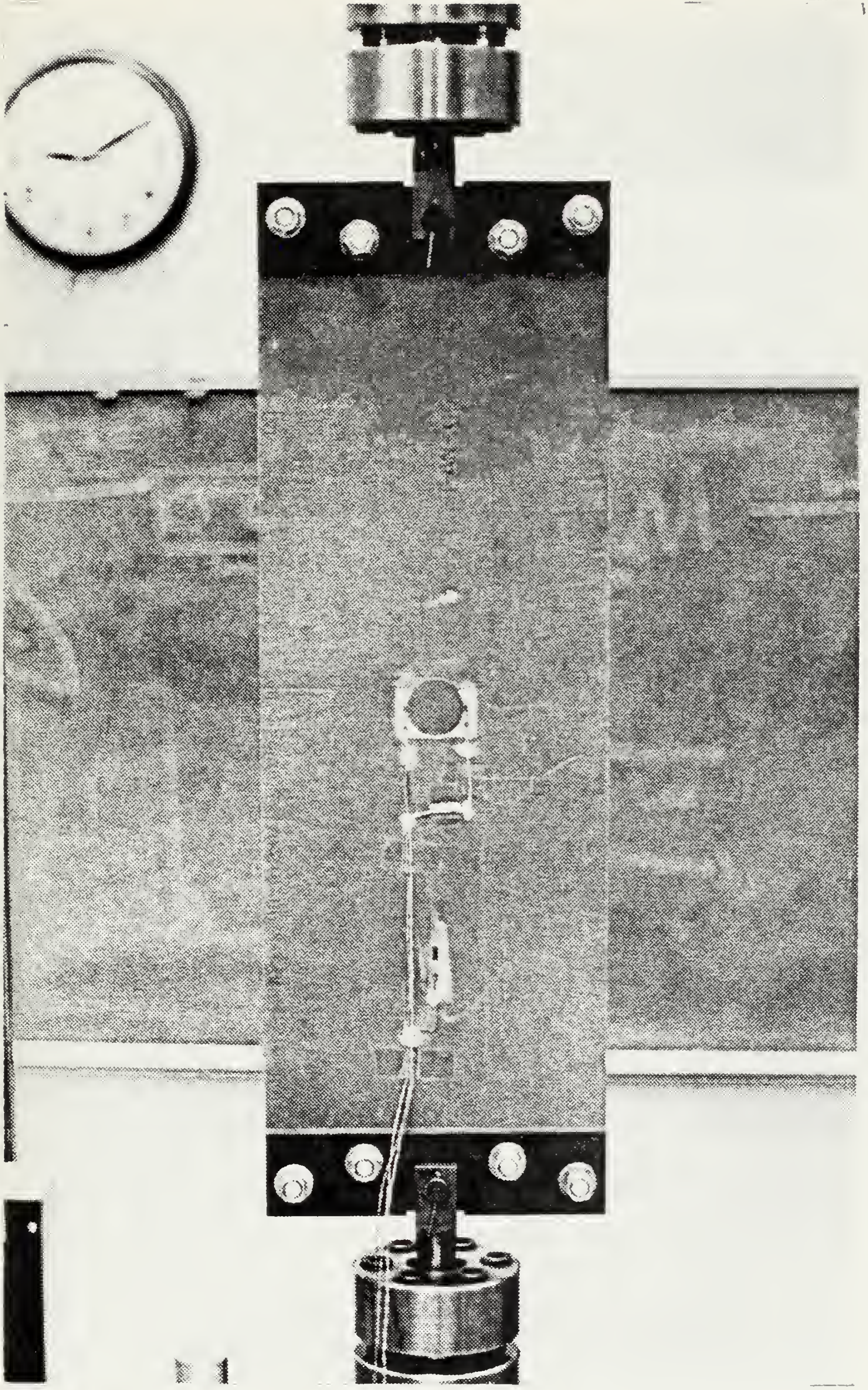

Figure 1

Photo of Plate Specimen

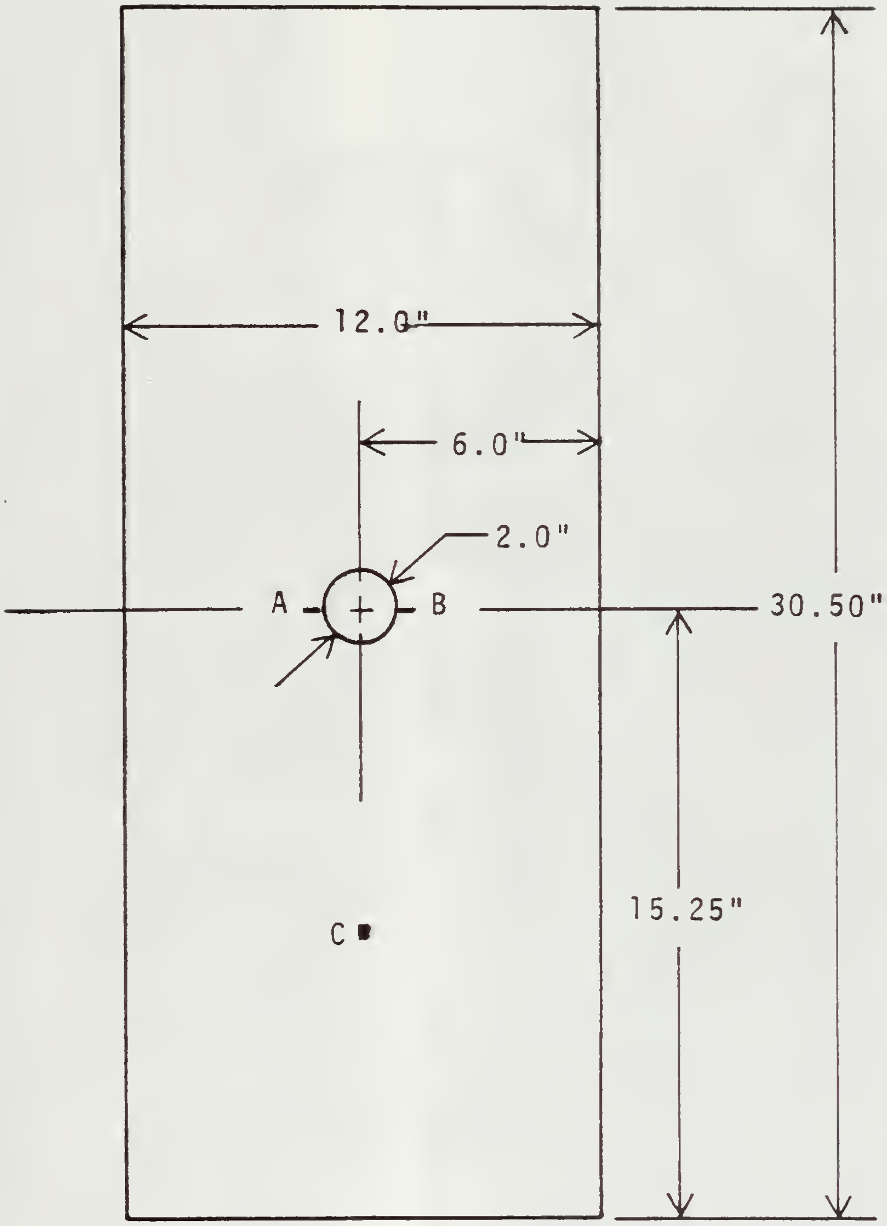

Figure 2

Plate specimen with central hole constructed of 7075 T-6 aluminum

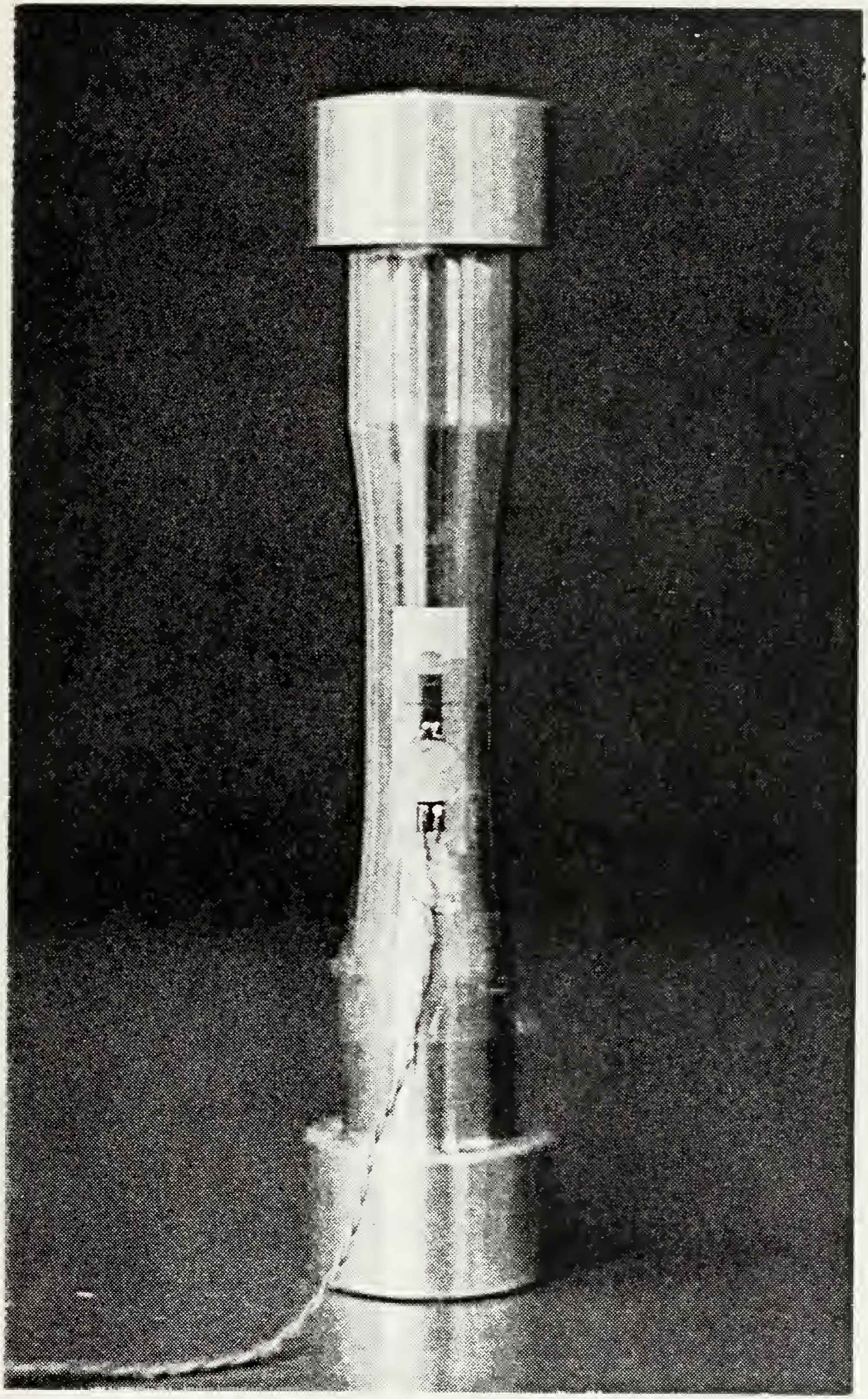

Figure 3

Photo of Uniaxial Specimen

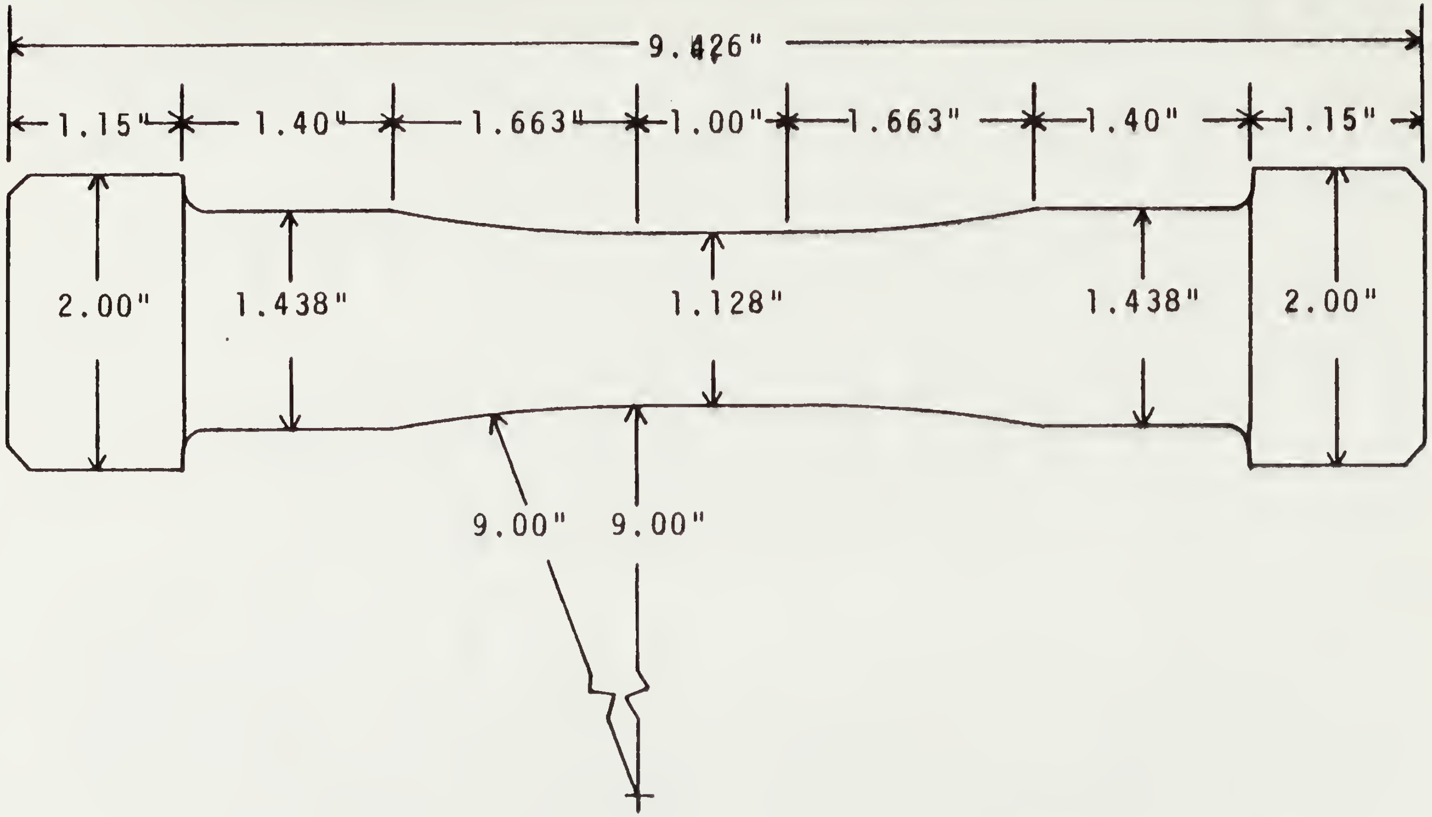

Figure 4

Uniaxial Specimen
7075 T-6 Aluminum

The testing of the uniaxial specimens was done using an MTS Systems Corporation closed-loop, servo-controlled testing system (Figs. 5 and 6). The system was driven under strain control by an internal function generator or by an Electronics Associates, Incorporated PACE TR-20 analog computer. Outputs of voltages representing load and strain on the specimen being tested were input to a Hewlett-Packard X-Y recorder and a Hewlett-Packard dual trace strip chart recorder.

The uniaxial specimens used in the tests were constructed of 7075 T-6 aluminum in accordance with ASTM recommendations (Ref. 12). Each specimen had a test section cross-sectional area of one square inch in order that load might be interpreted directly as stress on the specimen. Strain gages were mounted as shown in Figure 3.

Prior to the actual tests, an alignment check, as described by ASTM (Ref. 12), was performed on the load cell test bed to ensure that strains due to bending from misalignment would not be introduced into the specimens. The maximum percent bending ranged from 2.37 to 4.43 percent (Table 1), with the average being 3.30 percent. This is within the 5.0 percent maximum allowable bending moment recommended by ASTM.

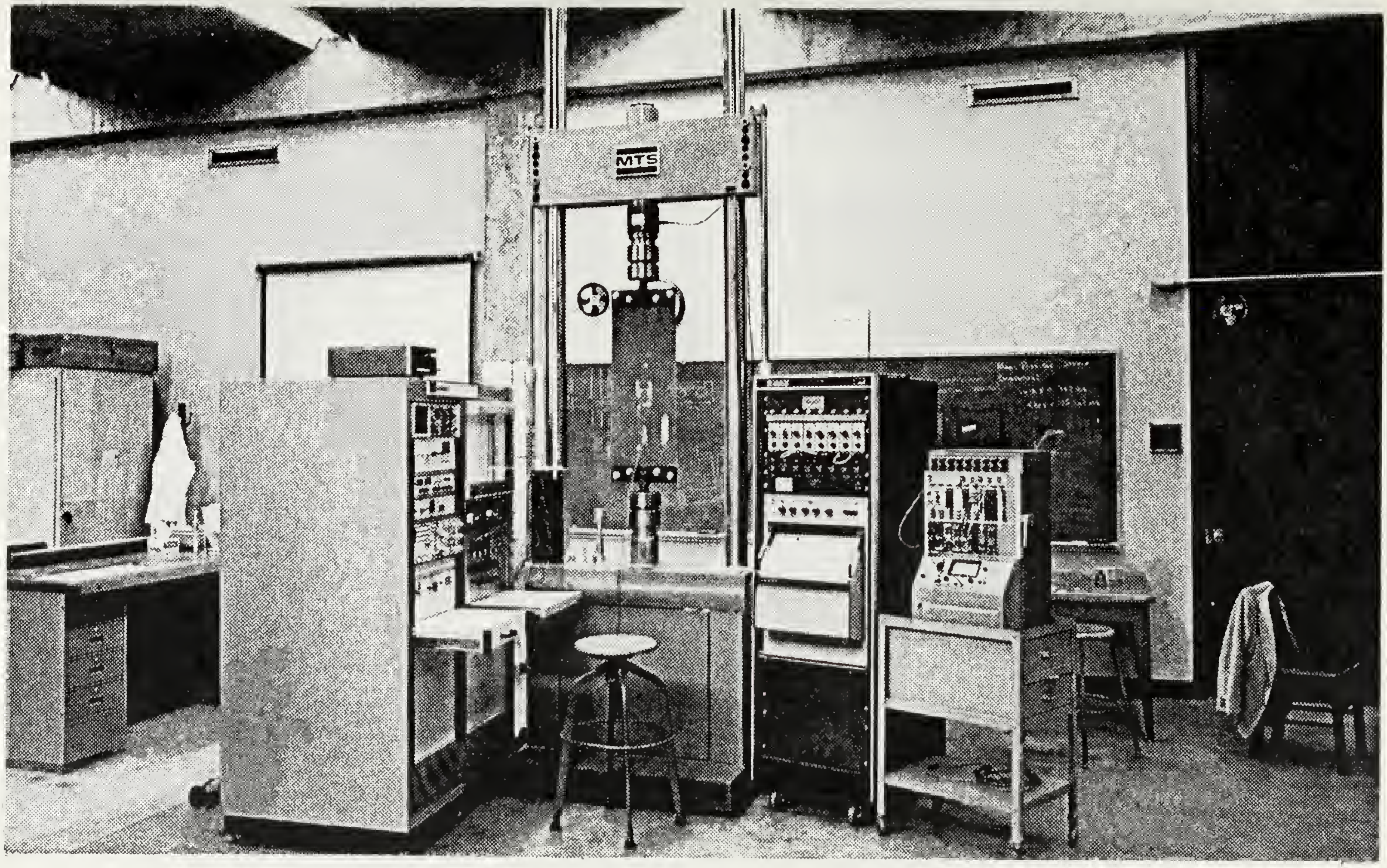

Figure 5
Photo of MTS System

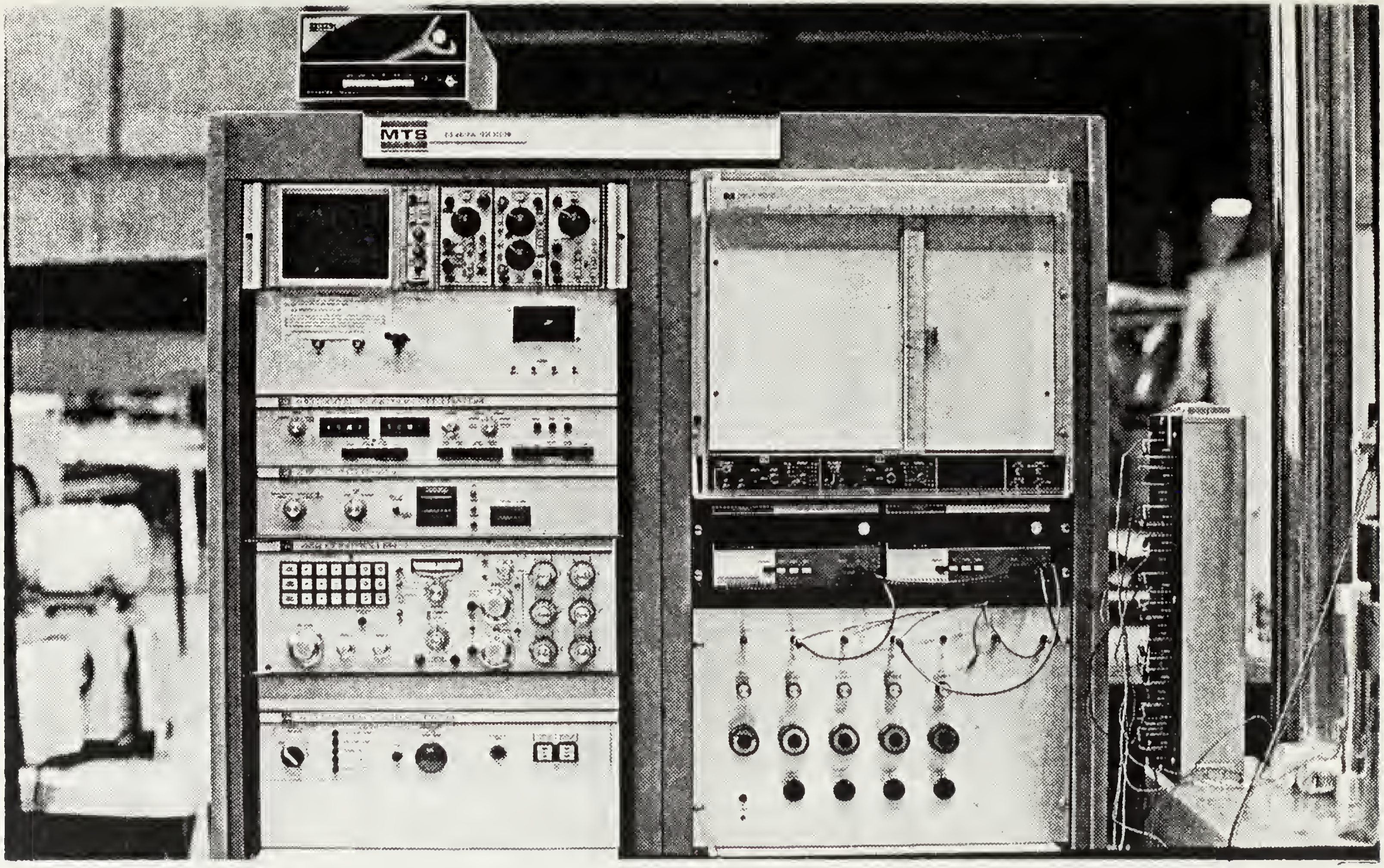

Figure 6
Photo of MTS System

Specimens were mounted and secured in the test system in accordance with current MTS Corporation instructions (Ref. 13). Care was taken to ensure that each specimen was not damaged nor yielded prior to any test.

Before each test was begun, strain gages mounted on the specimen were zeroed and calibrated while the specimen was hanging unattached in the machine, and according to standard practice. The load cell output voltage was also zeroed at this time. All recorders in use for a particular test were calibrated with a known input voltage to ensure accurate reproduction of voltage outputs from the test system.

B. CYCLIC STRESS-STRAIN CURVE TESTS

1. Description of Test

To obtain the desired monotonic and cyclic stress-strain curves for 7075 T-6 aluminum, an incremental step test similar to that proposed by Landgraf et al. (Ref. 6) was utilized.

The closed-loop, servo-controlled material testing system used did not have a function generator capable of providing a periodic, decreasing amplitude function required for the incremental step test. To obtain such a function to drive the testing system, an analog computer and the beat phenomena, obtained from summing two sinusoidal functions, were employed (Ref. 14).

Two sinusoidal functions

$$X_1(t) = R_1 \cos(\omega_1 t)$$

and

$$X_2(t) = R_2 \cos(\omega_2 t)$$

generated by an analog computer and summed provide a resultant output of

$$X(t) = R_1 \cos\omega_1 t + R_2 \cos[(\omega_1 - \Delta\omega)t]$$

or

$$X(t) = R \cos(\omega_1 t + \phi)$$

where

$$R = R_1 + R_2,\ \omega_1 > \omega_2,\ \omega_1 \neq \omega_2,\ \Delta\omega = \omega_1 - \omega_2,$$

and

$$\emptyset = \mathrm{Tan}^{-1}\left[-\frac{R_2 \sin(\Delta\omega t)}{R_1 + R_2 \cos(\Delta\omega t)}\right].$$

By appropriate selection of the variables R_1, R_2, ω_1, and ω_2 the resultant output will oscillate at ω_1 between $R_1 + R_2$ and $R_1 - R_2$ at a rate of $\Delta\omega$ (Fig. 7). Beginning at the maximum amplitude and continuing for approximately one half the beat period, $\frac{\Delta t}{2}$, a cyclic decreasing amplitude function is obtained.

Both the analog computer and the material testing system operate on ± 10.0 VDC. To utilize the full capability of the system, a maximum amplitude of $R = \pm$ 10.0 VDC and a minimum of $R = 0.0$ VDC were desired. Thus, $R_1 = 5.0$ VDC and $R_2 = 5.0$ VDC were chosen for maximum input amplitudes. A beat period of $\Delta t = 80$ s/c was selected and considered

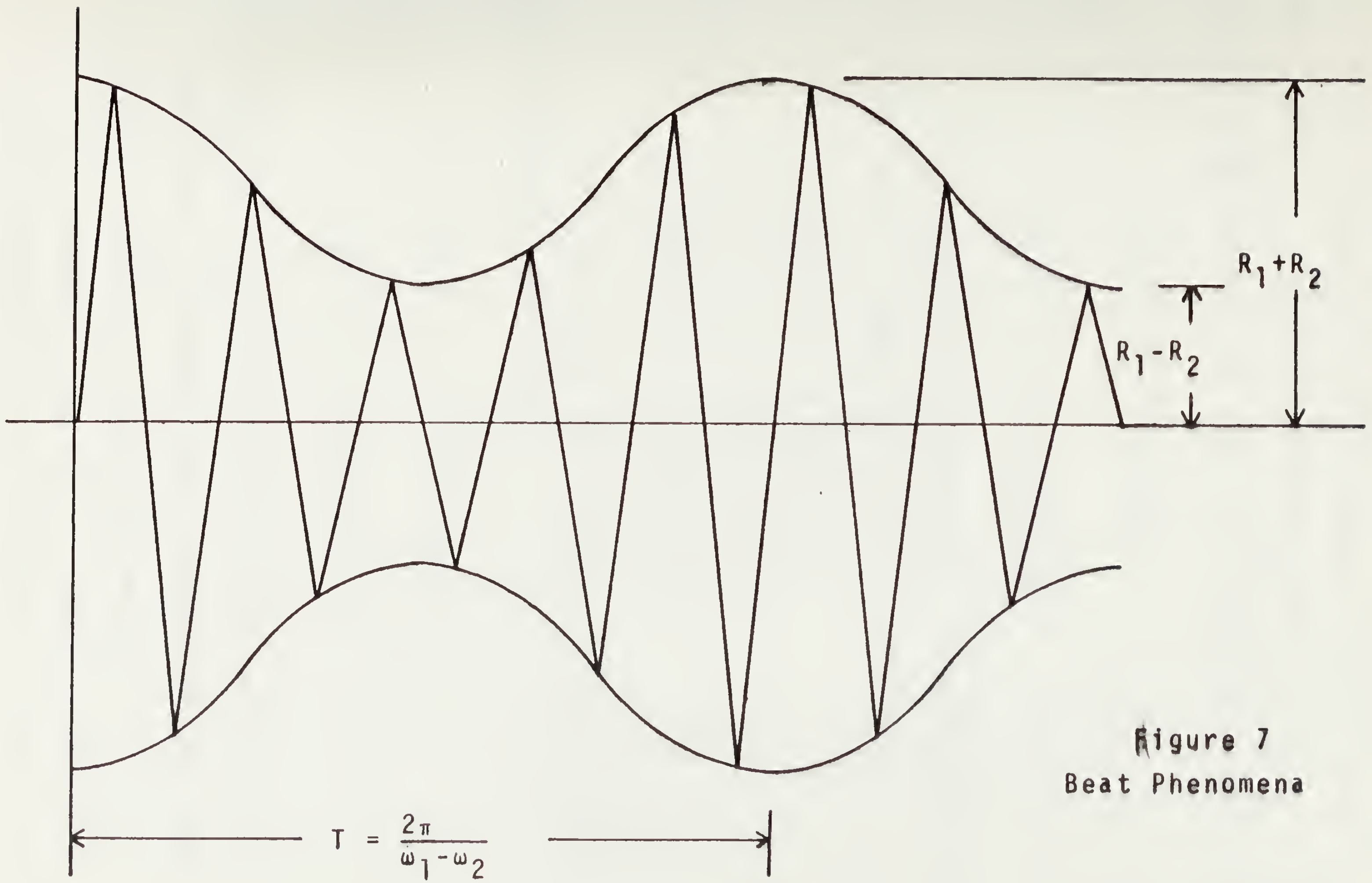

Figure 7
Beat Phenomena

adequate to remain within testing system and recorder limitations. Likewise, a cyclic frequency of $f = \frac{1}{4}$ c/s was desired to provide the cyclic output function period of 4 c/s. Thus, $\omega_1 = \frac{\pi}{2}$ rad/s was assumed, fixing $\omega_2 = \frac{19}{40}\pi$ rad/s since $\Delta w = \frac{\pi}{40}$ rad/s. The two input functions used were

$$X_1(t) = 5.0 \operatorname{Cos} \left(\frac{\pi}{2}t\right)$$

and

$$X_2(t) = 5.0 \operatorname{Cos} \left(\frac{19}{40}\pi t\right).$$

To produce these functions, differential equations for analog solution were programmed as follows:

$$\ddot{X}_1(t) = - 2.4674\ X_1(t)$$

and

$$\ddot{X}_2(t) = - 2.2268\ X_2(t).$$

In constructing the scaled analog solution, the actual equations used were

$$\ddot{X}_1(t) = - 0.24674\ X_1(t)$$

and

$$\ddot{X}_2(t) = - 0.22268\ X_2(t).$$

These provided a more satisfactory beat period of $\Delta t = 252.95$ s/c. Thus the cyclic period became 12.65 s/c or twenty oscillations in one beat period.

The output of the analog computer was supplied as input to the controller of the material testing system under strain control. Initially the output amplitude of the analog

computer was set to zero by zeroing the initial conditions on the input functions. By manually increasing the initial conditions on each input function to the values calculated for solution, the output was increased to + 10.0 VDC, putting the specimen into tensile yield. Reversing the procedure and manually decreasing the initial conditions to zero, reversing the polarity of the output and manually increasing the initial conditions to the calculated values, produced a - 10.0 VDC output which placed the specimen in a compressive yield condition with the strain equal to the initial tensile yield strain. This was done to provide a symmetric cyclic stress-strain curve.

The analog computer was activated with the specimen in compressive yield and allowed to cycle until the load-strain curve plotted by the X-Y recorder became linear through the origin, at which time the test was terminated (Fig. 8). This occurred after approximately nine cyclic oscillations.

Output voltages representing load and strain on the specimen were input to an X-Y recorder to provide a series of load, or stress, versus strain curves throughout the test. The uniaxial specimen was constructed with a test section cross-sectional area of one square inch, thus allowing load to be interpreted directly as stress, and load-strain curves as stress-strain curves.

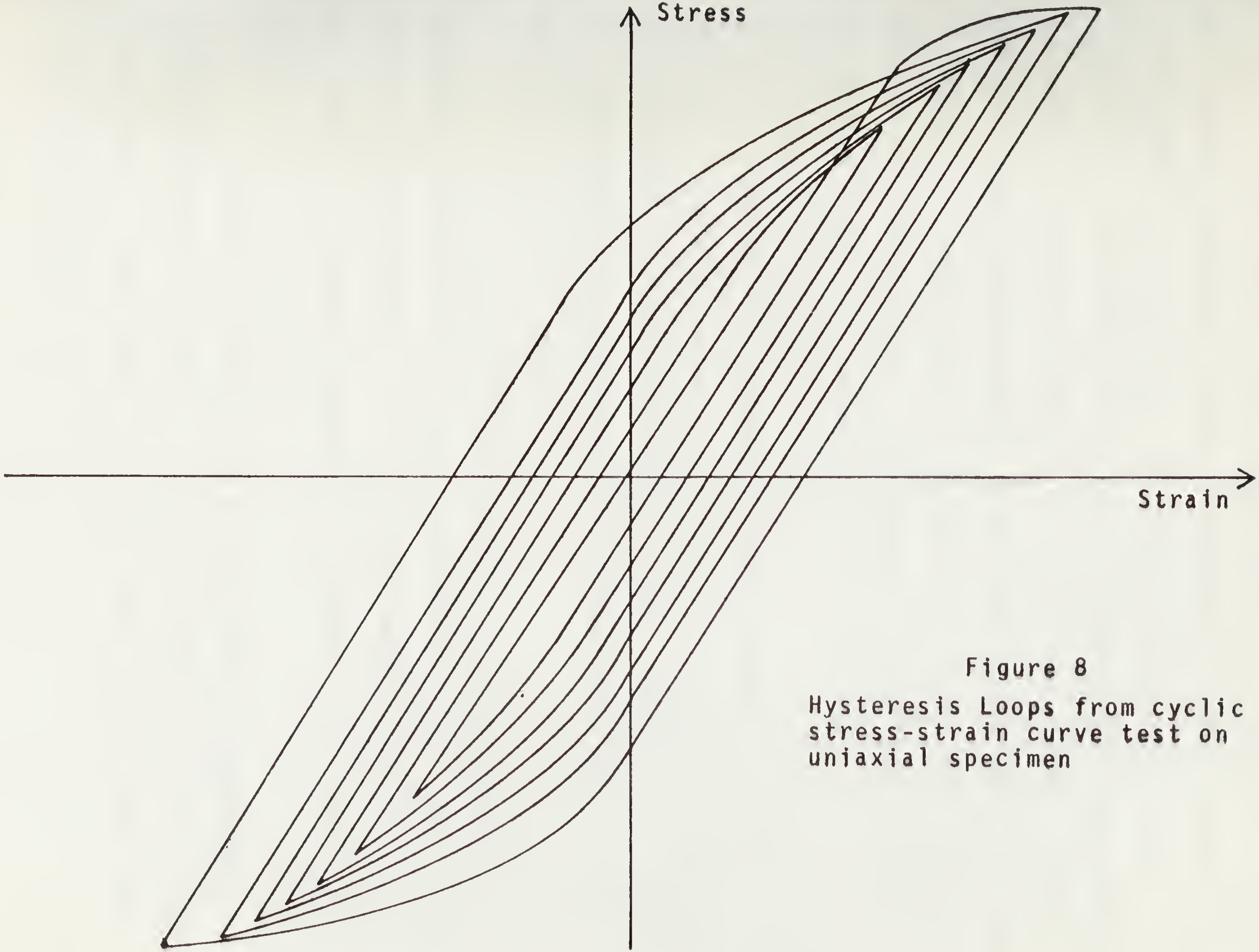

Figure 8

Hysteresis Loops from cyclic stress-strain curve test on uniaxial specimen

2. Test Results

The X-Y recorder plot of output voltages of stress and strain provided a series of hysteresis loops, each with a maximum strain amplitude less than the preceding loop (Fig. 8). The locus of the tips of these loops, when plotted in terms of stress in Lbf/in^2 and strain in μin/in, is the desired cyclic stress-strain curve (Fig. 9 and Table 2). The slightly "S" shaped curve is symmetrical about the origin in tension and compression. The modulus of elasticity calculated from the linear portion of the curve was $E = 10.18 \times 10^6$ Lbf/in^2.

The initial loading of the specimen provided voltage outputs of stress and strain with which to construct the monotonic stress-strain curve (Figs. 9 and 10 and Table 3). The modulus of elasticity calculated from this curve was $E = 10.67 \times 10^6$ Lbf/in^2.

The two percent yield stress obtained from the monotonic stress-strain curve is 78,000 Lbf/in^2. This yield stress and the modulus of elasticity compare favorably with the theoretical values generally accepted to be 77,000 Lbf/in^2 and $E = 10.3 \times 10^6$ Lbf/in^2.

Values of stress and strain from the monotonic curve were used to produce a stress x strain ($\sigma\varepsilon$) vs. stress curve (Fig. 11 and Table 3). This curve was for later use in the plate tests.

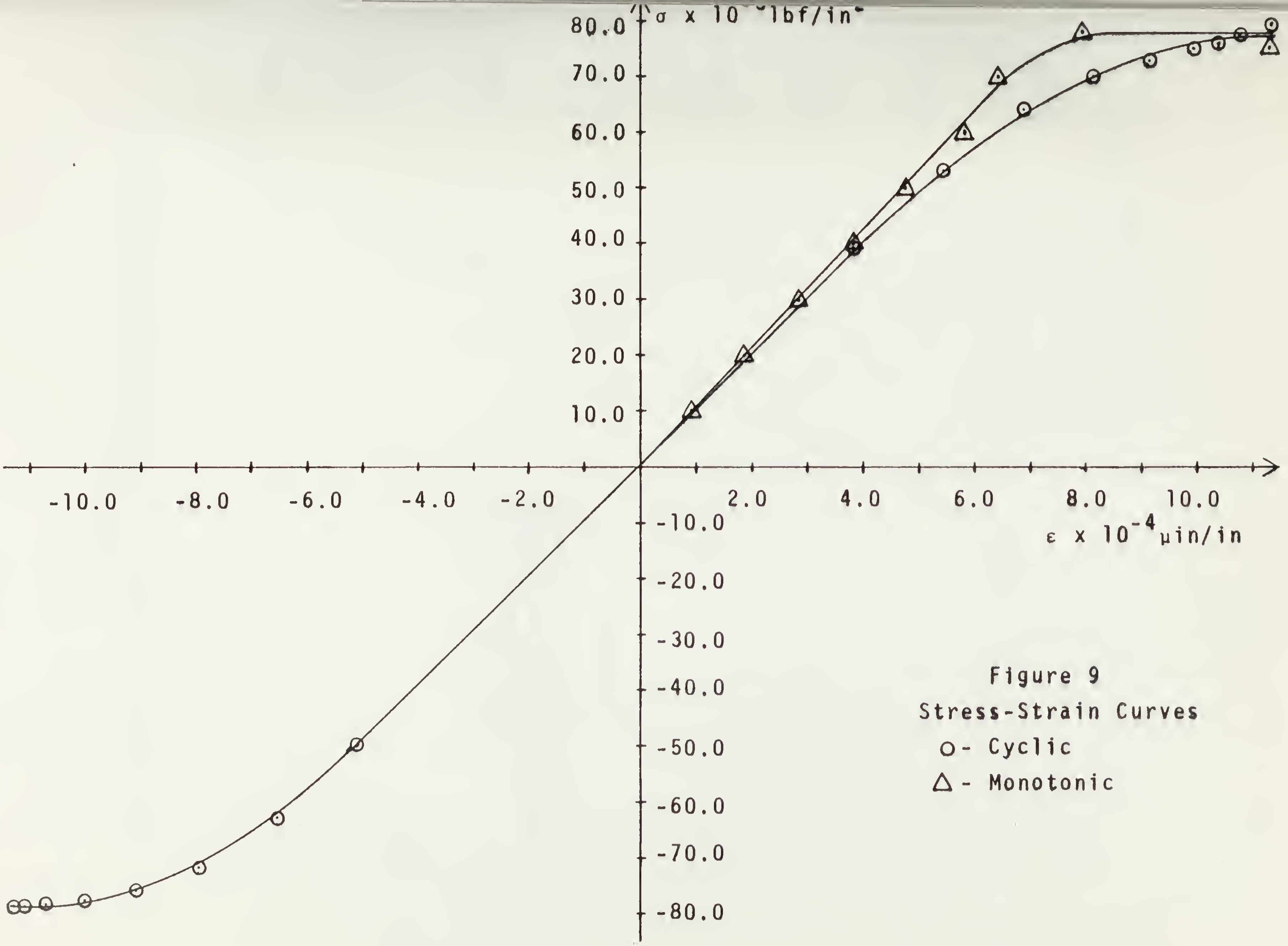

Figure 9
Stress-Strain Curves
○- Cyclic
△ - Monotonic

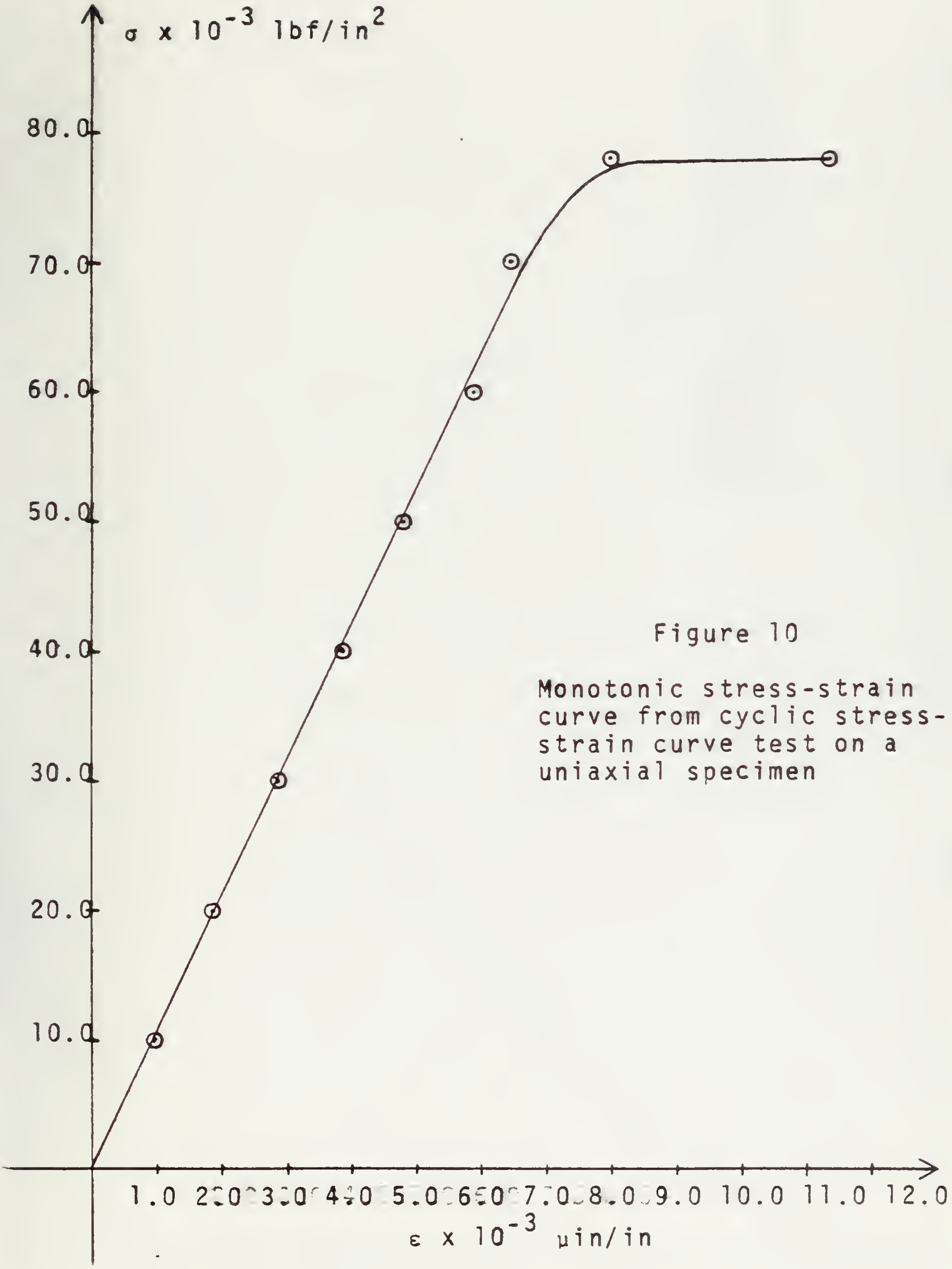

Figure 10

Monotonic stress-strain curve from cyclic stress-strain curve test on a uniaxial specimen

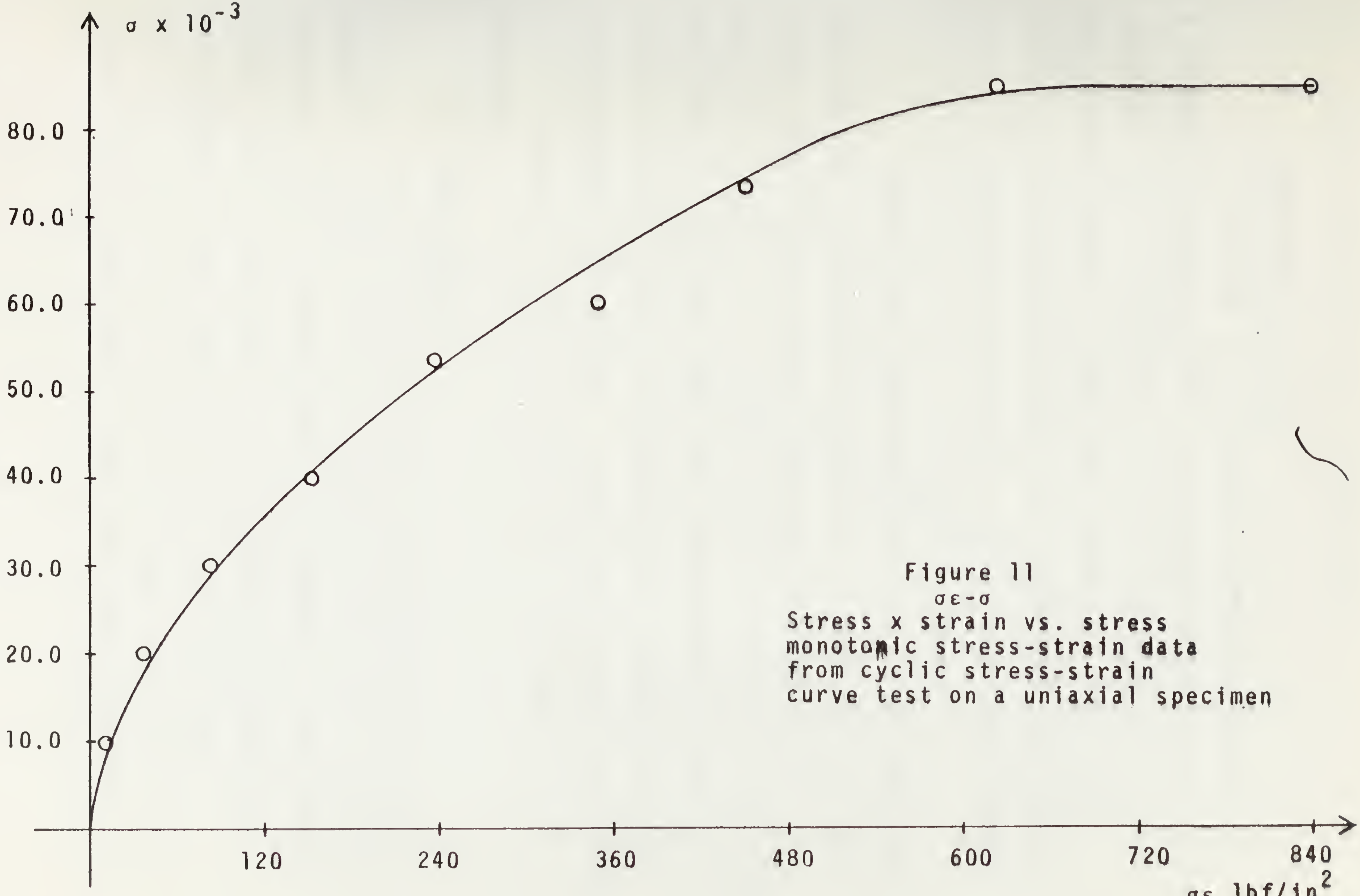

Figure 11
σε-σ
Stress x strain vs. stress
monotomic stress-strain data
from cyclic stress-strain
curve test on a uniaxial specimen

C. SINGLE AMPLITUDE CYCLIC LOADING TEST

1. Description of Test

A knowledge of the stress relaxation behavior in a uniaxial specimen of 7075 T-6 aluminum subjected to single amplitude cyclic loading was required for comparison with relaxation behavior in the plate specimens. The initial loading cycle furnished stress and strain data for construction of a monotonic stress-strain curve, which was compared with other similar curves previously mentioned.

The function generator installed in the MTS system was capable of producing a haversine function to drive the system under strain control. Maximum amplitude of the haversine function was set to provide 7.3 VDC of the 10.0 VDC available. This input amplitude corresponded to 11167 μ in/in strain in the specimen. The specimen was cycled 275 times to the maximum strain value. A dual trace strip recorder and an X-Y recorder were used to plot load and strain output voltages.

2. Test Results

The plot of stress and strain provided by the X-Y recorder allowed calculation of data points from the initial loading cycle for construction of a monotonic stress-strain curve (Fig. 12 and Table 4). The modulus of elasticity calculated from the linear portion of the curve was $E = 10.0 \times 10^6$ lbf/in^2. The yield stress was found to be 80,000 lbf/in^2. Values of stress and strain from this curve

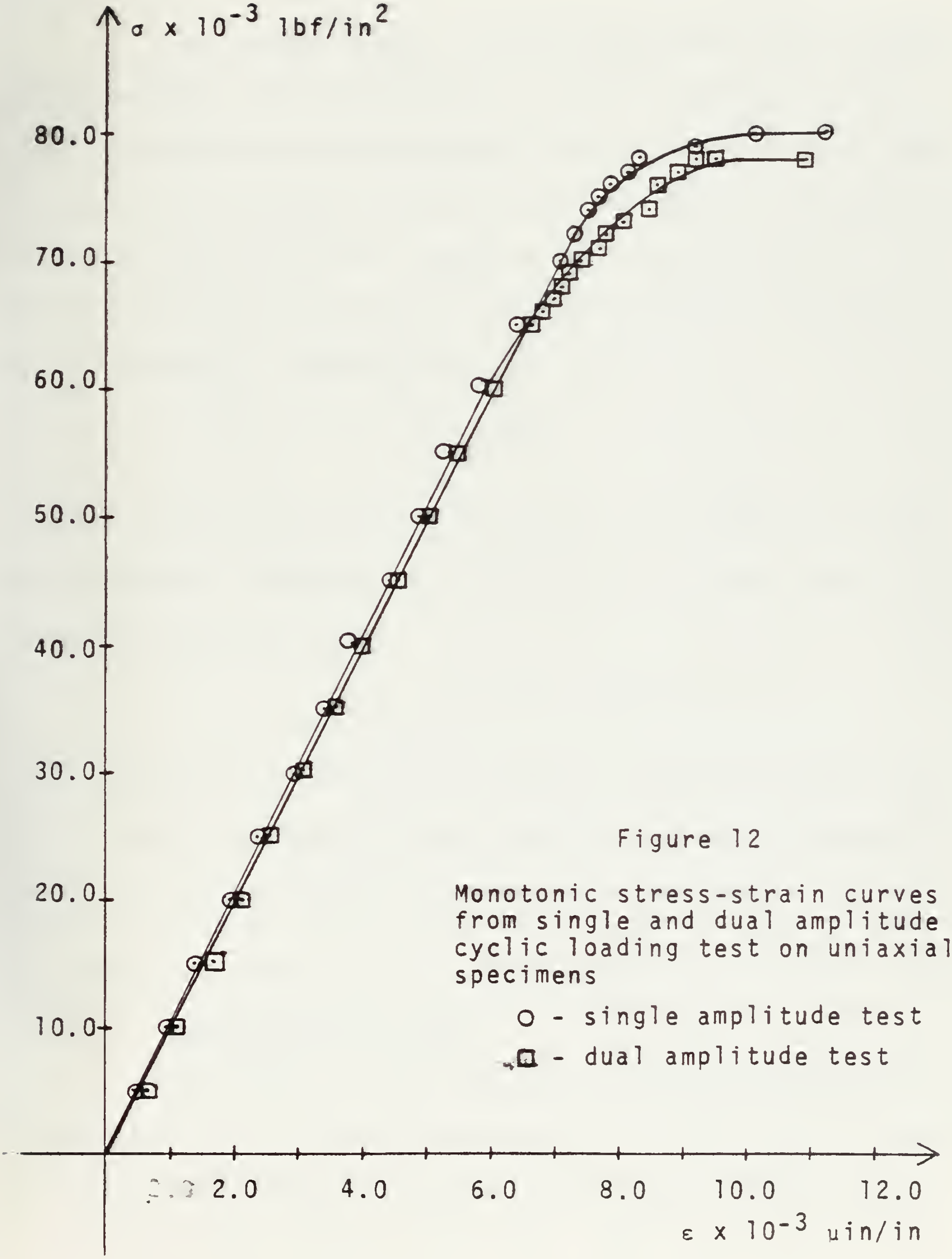

Figure 12

Monotonic stress-strain curves from single and dual amplitude cyclic loading test on uniaxial specimens

○ - single amplitude test

□ - dual amplitude test

were used to construct a stress x strain ($\sigma\varepsilon$) vs. stress curve (Fig. 13 and Table 4) for later use in the plate tests and for comparison with those of the other uniaxial specimen tests.

The stress output voltages obtained from the dual trace recorder were converted to lbf/in^2 (Table 5) and plotted against the cycle number, N, on semilog graph paper (Fig. 14) to indicate stress relaxation behavior graphically. The locus of data points appeared to form a straight line indicating stress relaxation behavior could be represented by an exponential equation of the form

$$\sigma = \sigma_o e^{-bN} .$$

A least squares exponential curve fit calculator algorithm was applied to the data on 253 points out of 275 taken. The resulting equation was

$$\sigma = 73160 \ e^{-(3.177 \times 10^{-3})N} .$$

A correlation coefficient of 0.994 was calculated for the fit. Thus the relaxed stress value at any cycle number, N, could be obtained with a high degree of accuracy.

D. DUAL AMPLITUDE CYCLIC LOADING TEST

1. Description of Test

Knowledge of the effects of dual amplitude cyclic loading on stress relaxation behavior in uniaxial specimens of 7075 T-6 aluminum was desired for comparison with the

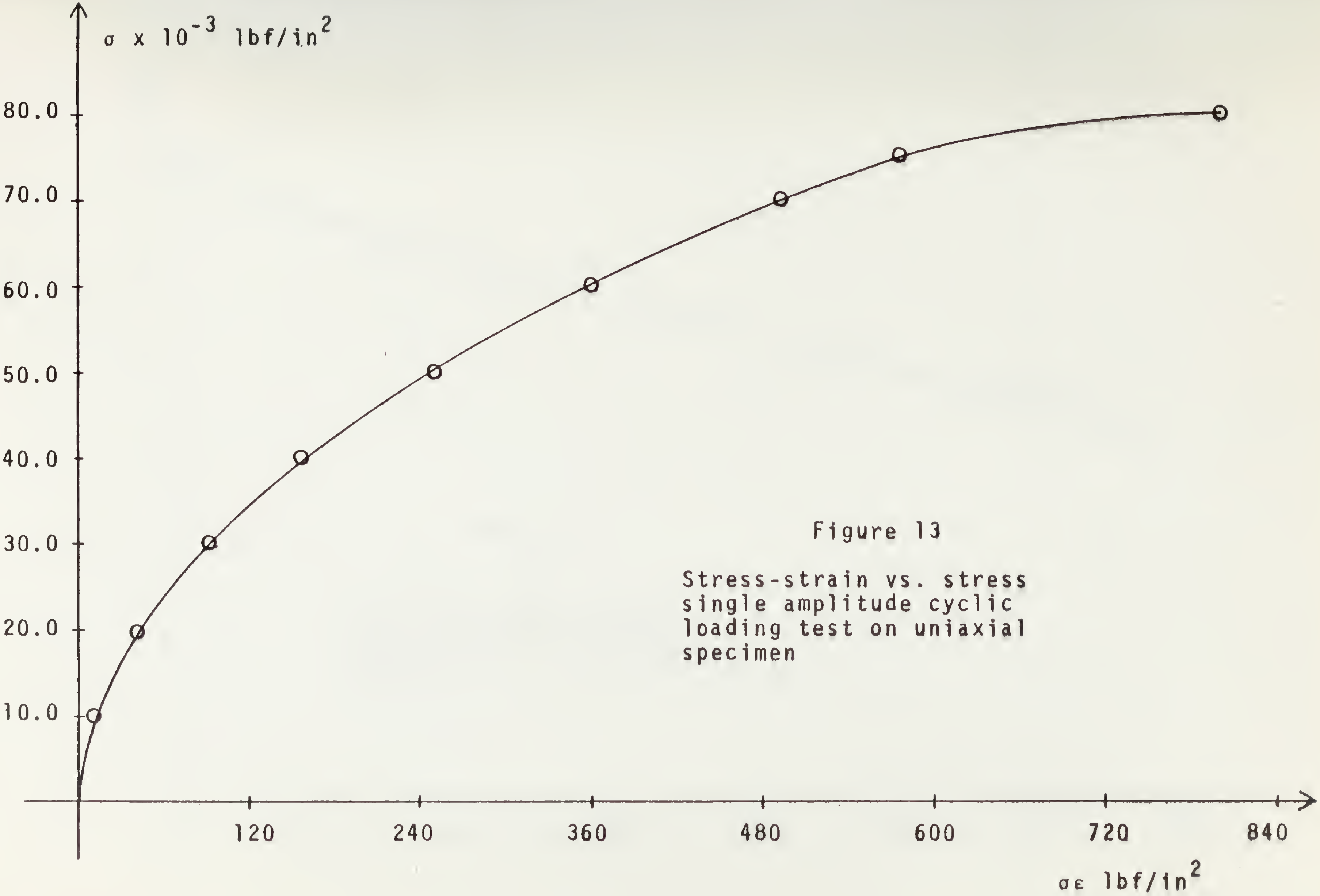

Figure 13

Stress-strain vs. stress single amplitude cyclic loading test on uniaxial specimen

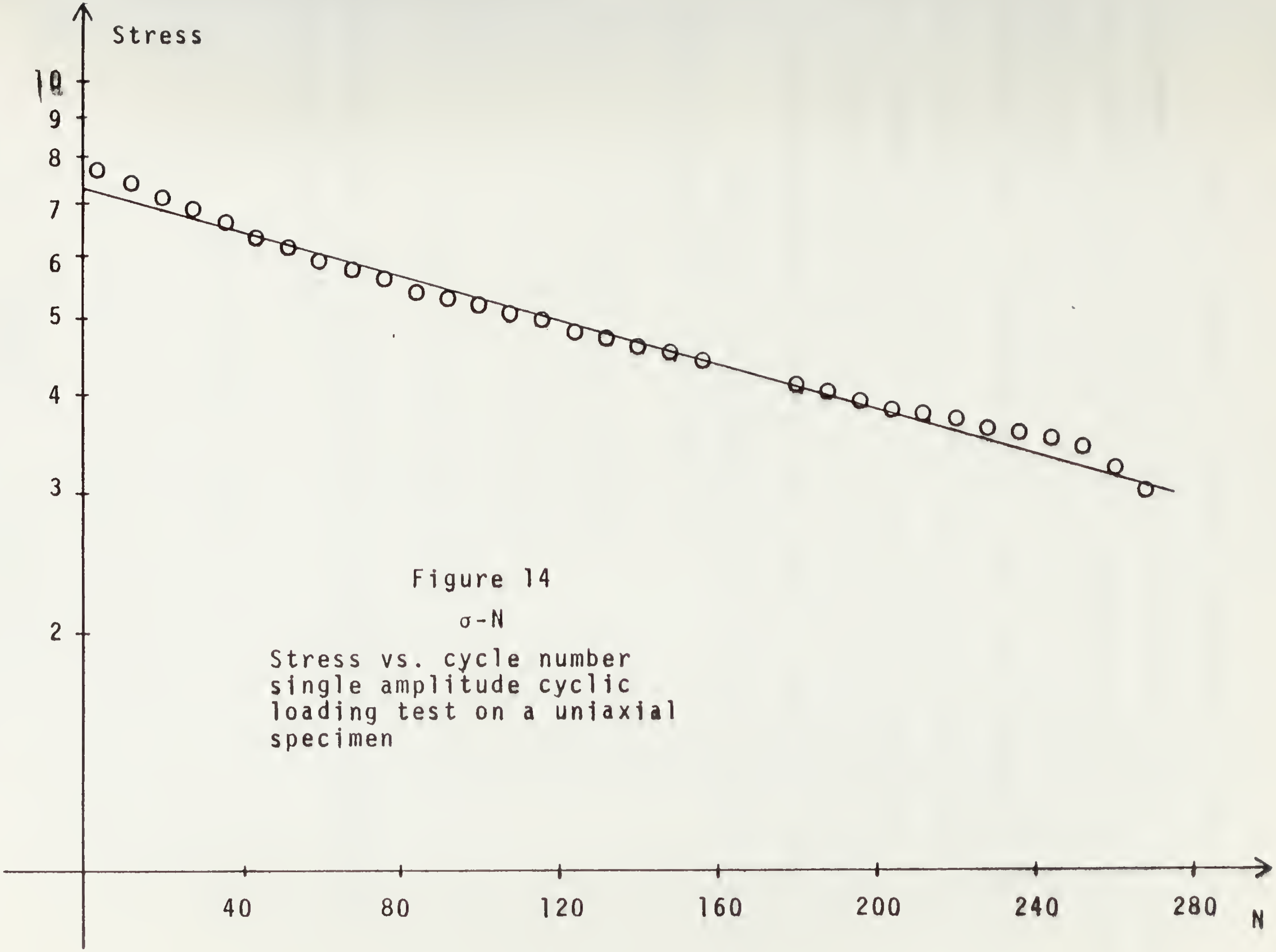

Figure 14

σ-N

Stress vs. cycle number
single amplitude cyclic
loading test on a uniaxial
specimen

results of the single amplitude cyclic loading test on a uniaxial specimen and the plate tests.

The MTS system's function generator did not have the capability of producing a dual amplitude, cyclic function. The analog computer and the beat phenomena used in the cyclic stress-strain curve test were applied to the problem in a modified form. A function with a low, positive amplitude of one half that of the high amplitude was desired (Fig. 15). For optimum utilization of the system this required a maximum high amplitude output voltage of + 10.0 VDC, thus fixing the maximum low amplitude output voltage of + 5.0 VDC.

From the development of the function for the cyclic stress-strain curve test (Ref. 14)

$$X_1(t) = R_1 \text{ Cos } (\omega_1 t)$$

$$X_2(t) = R_2 \text{ Cos } (\omega_2 t)$$

and

$$X(t) = R \text{ Cos } (\omega_1 t + \phi).$$

Summing of the two functions, $X_1(t)$ and $X_2(t)$, produced the resultant, $X(t)$, where

$$X(t) = X_1(t) + X_2(t)$$

Also,

$$R = [R_1^2 + R_2^2 + 2 R_1 R_2 \text{ Cos } (\Delta\omega t)]^{\frac{1}{2}},$$

and

$$\text{TAN } \emptyset = \frac{R \text{ Sin } \emptyset}{R \text{ Cos } \emptyset} = \frac{-R_2 \text{ Sin } (\Delta\omega t)}{R_1 + R_2 \text{ Cos } (\Delta\omega t)}$$

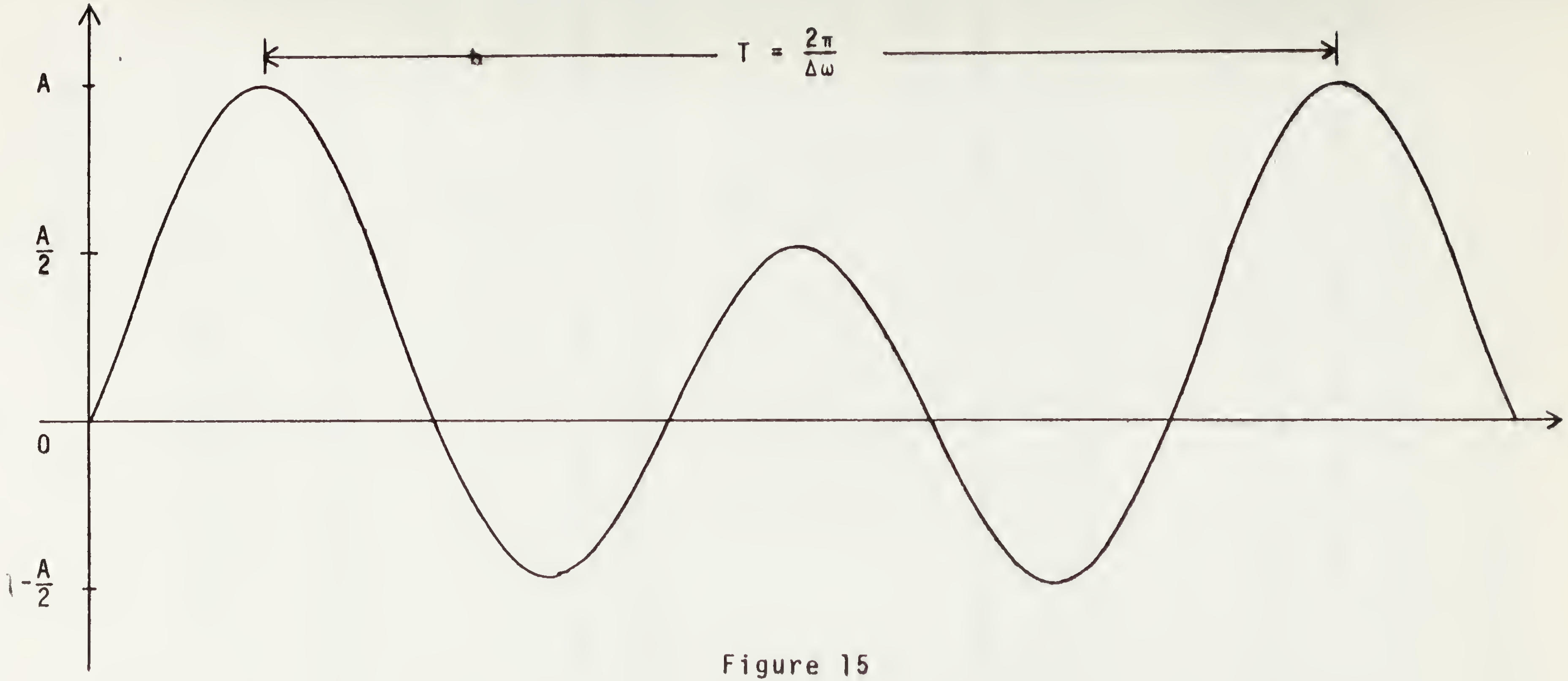

Figure 15

Dual amplitude input function

where

$\Delta\omega = \omega_1 - \omega_2$ and $T = 2\pi/\Delta\omega$ can be written.

Consideration of Figure 15 and the conditions that $R = 10.0$ at the high amplitude output and $R = 5.0$ at the low amplitude output allowed constraint equations to be written in the form

$$X(t) + \Delta = R$$

where Δ was a constant voltage added to give an additional degree of freedom with which to force the resultant output into a dual amplitude wave form. The constraint equations obtained were

$$X(0) + \Delta = 10$$

and

$$X(\tfrac{T}{2}) + \Delta = 5.$$

An additional constraint equation was obtained from the negative portion of the desired waveform, where $R = -5.0$ was arbitrarily chosen such that

$$X(\tfrac{T}{4}) + \Delta = -5.$$

The application of

$$R(t) = [R_1^2 + R_2^2 + 2 R_1 R_2 \text{Cos} (\Delta\omega t)]^{\frac{1}{2}}$$

$$\emptyset (t) = \text{Tan}^{-1} [\frac{-R_2 \text{Sin} (\Delta\omega t)}{R_1 + R_2 \text{Cos} (\Delta\omega t)}]$$

and

$$X(t) = R(t) \text{Cos} (\omega_1 t + \emptyset)$$

to the above constraint equations at $t = 0$, $t = \frac{T}{4}$, and $t = \frac{T}{2}$ gave rise to three equations in three unknowns for solution. For these calculations $\omega_1 = 2\Delta\omega$ was desired for only two amplitudes to be produced per cycle.

At $t = 0$,

$$\phi(0) = 0,\ R(0) = R_1 + R_2, \text{ and } X(0) = R(0) = R_1 + R_2$$

and

$$R_1 + R_2 + \Delta = 10.$$

At $t = \frac{T}{4}$,

$$\Delta\omega t = \Delta\omega\frac{T}{4} = \frac{\pi}{2}, \text{ and } \omega_1 t = \pi,$$

then,

$$\phi(\tfrac{T}{4}) = \frac{-R_2}{R_1},\ R(\tfrac{T}{4}) = [R_1^2 + R_2^2]^{\frac{1}{2}} \text{ and}$$

$$X(\tfrac{T}{4}) = -[R_1^2 + R_2^2]^{\frac{1}{2}} \text{Cos}\ [\pi + \phi\ (\tfrac{T}{4})].$$

By use of a trigonometric identity the equation

$$X(\tfrac{T}{4}) = -\ [R_1^2 + R_2^2]^{\frac{1}{2}} \text{Cos}\ \phi\ (\tfrac{T}{4})$$

could be written. Then, if a right triangle is constructed with R_1 and R_2 as sides and $[R_1^2 + R_2^2]^{\frac{1}{2}}$ as the hypotenuse, $\phi(t)$ is the angle between the hypotenuse and R_1. Therefore,

$$\text{Cos}\ \phi(t) = \frac{R_1}{[R_1^2 + R_2^2]^{\frac{1}{2}}},$$

which, when substituted into the equation for $X(\frac{T}{4})$, yielded

$$X(\frac{T}{4}) = - R_1 .$$

Then,

$$- R_1 + \Delta = - 5.0$$

could be written.

$$\text{At } t = \frac{T}{2}, \ \Delta\omega t = \Delta\omega\frac{T}{2} = \pi, \text{ and } \omega_1 t = 2\pi,$$

then,

$$\phi(\frac{T}{2}) = 0, \ R(\frac{T}{2}) = R_1 - R_2, \text{ and } X(\frac{T}{2}) = R_1 - R_2 .$$

Then,

$$R_1 - R_2 + \Delta = 5.$$

Thus, three equations

$$R_1 + R_2 + \Delta = 10$$

$$- R_1 + \Delta = - 5$$

$$R_1 - R_2 + \Delta = 5$$

were available for solution to obtain R_1, R_2, and Δ. Simultaneous solution of the equations gave values of $R_1 = 6.25$, $R_2 = 2.50$, and $\Delta = 1.25$. During the solution for these values it was noted that if $R_1 = 6.50$, $R_2 = 2.50$, and $\Delta = 1.0$ were substituted in the equations the only change in the output function would be the maximum amplitude of the negative cycle, such that

$$X(0) + \Delta = 10$$

$$X(\tfrac{T}{4}) + \Delta = - 5.5$$

and

$$X(\tfrac{T}{2}) + \Delta = 5.$$

Because such a change would not alter the original function's high and low positive amplitudes, which were of prime concern, and because the negative amplitude value was arbitrarily chosen as - 5.0 initially, the latter values were chosen for convenience in setting the initial conditions on the analog computer.

Having established the amplitudes required to generate the desired function, the frequencies ω_1 and ω_2 were considered next. The requirement to keep the periodic output function rate low to remain within system and recorder limitations led to the selection of $\omega_1 = \pi/5$ rad/s. Having assumed $\omega_1 = 2\Delta\omega$, $\Delta\omega = \pi/10$ rad/s and $\omega_2 = \pi/10$ rad/s followed. This established the beat frequency, f, at $f = 0.05$ c/s and $\tau = 20$ s/c. Thus, the period for one local oscillation, from high peak amplitude to the next corresponding low peak amplitude, was $\tau_1 = 10$ s/c.

The input functions thus obtained were

$$X_1(t) = 6.5 \text{ Cos } (\Delta\pi/5t)$$

and

$$X_2(t) = 2.5 \text{ Cos } (\pi/10t).$$

To produce these functions, differential equations for analog solution were programmed as follows:

$$\ddot{X}_1(t) = - 0.3948 \; X_1(t)$$

and

$$\ddot{X}_2(t) = - 0.09870 \; X_2(t).$$

The two input functions were summed with Δ = 1.0 VDC at the final stage, prior to input of the resulting function to the controller of the MTS system, to provide alternating, maximum positive amplitude peak output voltages of + 10.0 VDC and + 5.0 VDC.

To prevent compressive yield in the specimen due to the - 5.0 VDC output on each cycle of the function, the reference voltage, or local zero, of the system was set such that, under strain control, the negative voltage output caused the specimen to be placed in a state of zero strain. Maximum strain was set to 7.0 VDC output of the 10.0 VDC available. This corresponded to 10737 μ in/in strain in the specimen on the high amplitude cycle and 6168 μ in/in strain on the low amplitude cycle.

As in the cyclic stress-strain curve test, initial conditions were set to zero at the start of this test and then brought up to the specified values manually with the system under the control of the analog computer. With all initial conditions set in, the specimen was in a maximum strain condition. At this point the analog computer was

activated and allowed to cycle the specimen 140 times. Outputs of strain and load voltages were recorded on both the X-Y recorder and the dual trace strip chart recorder. As in the previous tests, load data were interpreted directly as stress.

2. Test Results

The output voltages of stress and strain plotted by the X-Y recorder provided data points from which a monotonic stress-strain curve was constructed (Fig. 12 and Table 6). The modulus of elasticity calculated for the curve was $E = 10.19 \times 10^6$ lbf/in^2. The yield stress was 78,000 lbf/in^2. Stress and strain data from this curve were used to construct a stress x strain ($\sigma\varepsilon$) vs. stress curve for comparison with those of other uniaxial specimen tests and for later use in the plate tests (Fig. 16 and Table 6).

The dual trace recorder provided stress output voltages from which maximum stress per cycle could be computed (Table 7). The stress data were plotted versus cycle number, N, on semilog graph paper (Fig. 17) to graphically represent stress relaxation behavior. The locus of the low amplitude data points as well as the high amplitude data points appeared to form a straight line, indicating equations for both stress relaxation behaviors would be of the form

$$\sigma = \sigma_0 e^{-bN}.$$

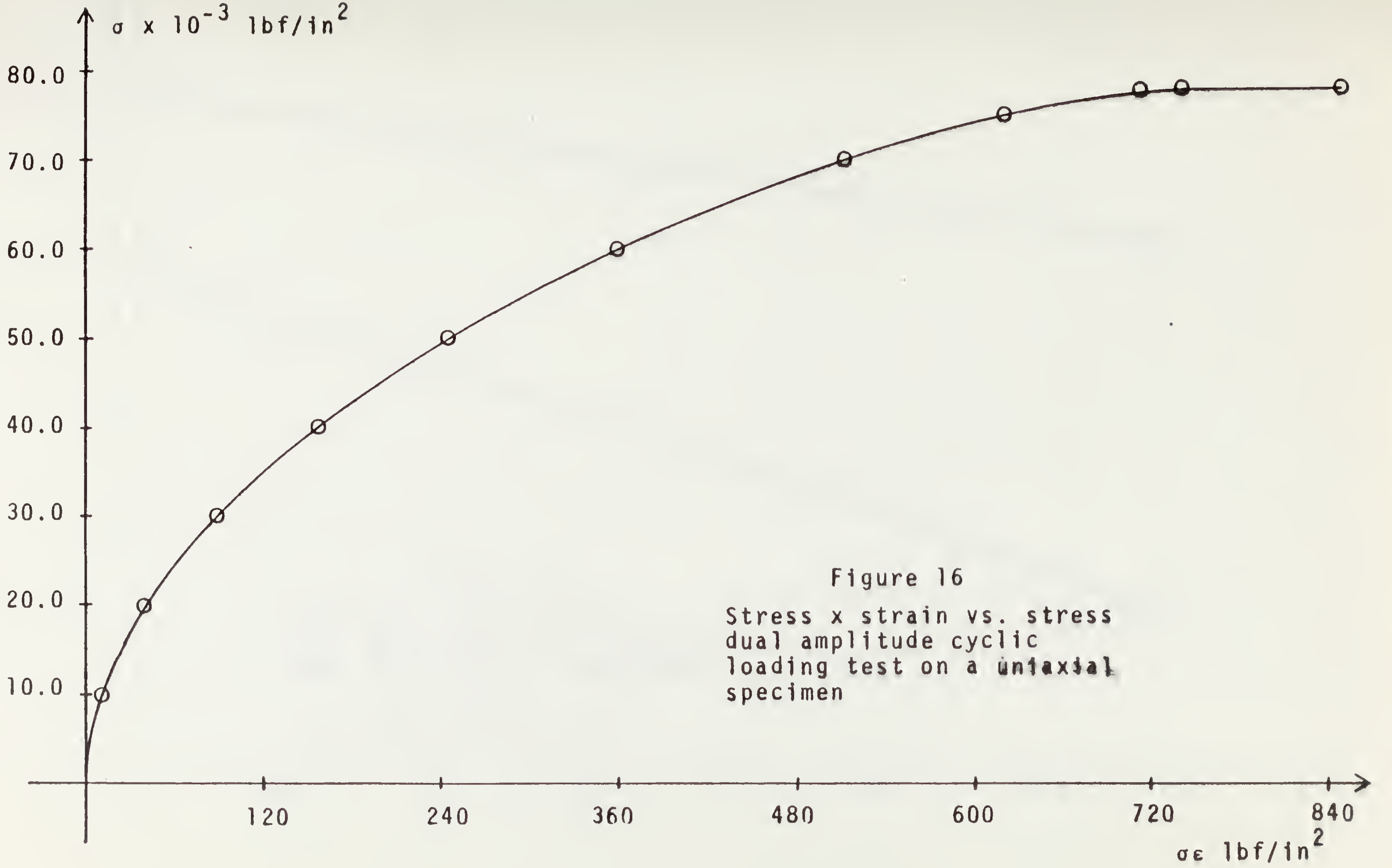

Figure 16

Stress x strain vs. stress dual amplitude cyclic loading test on a uniaxial specimen

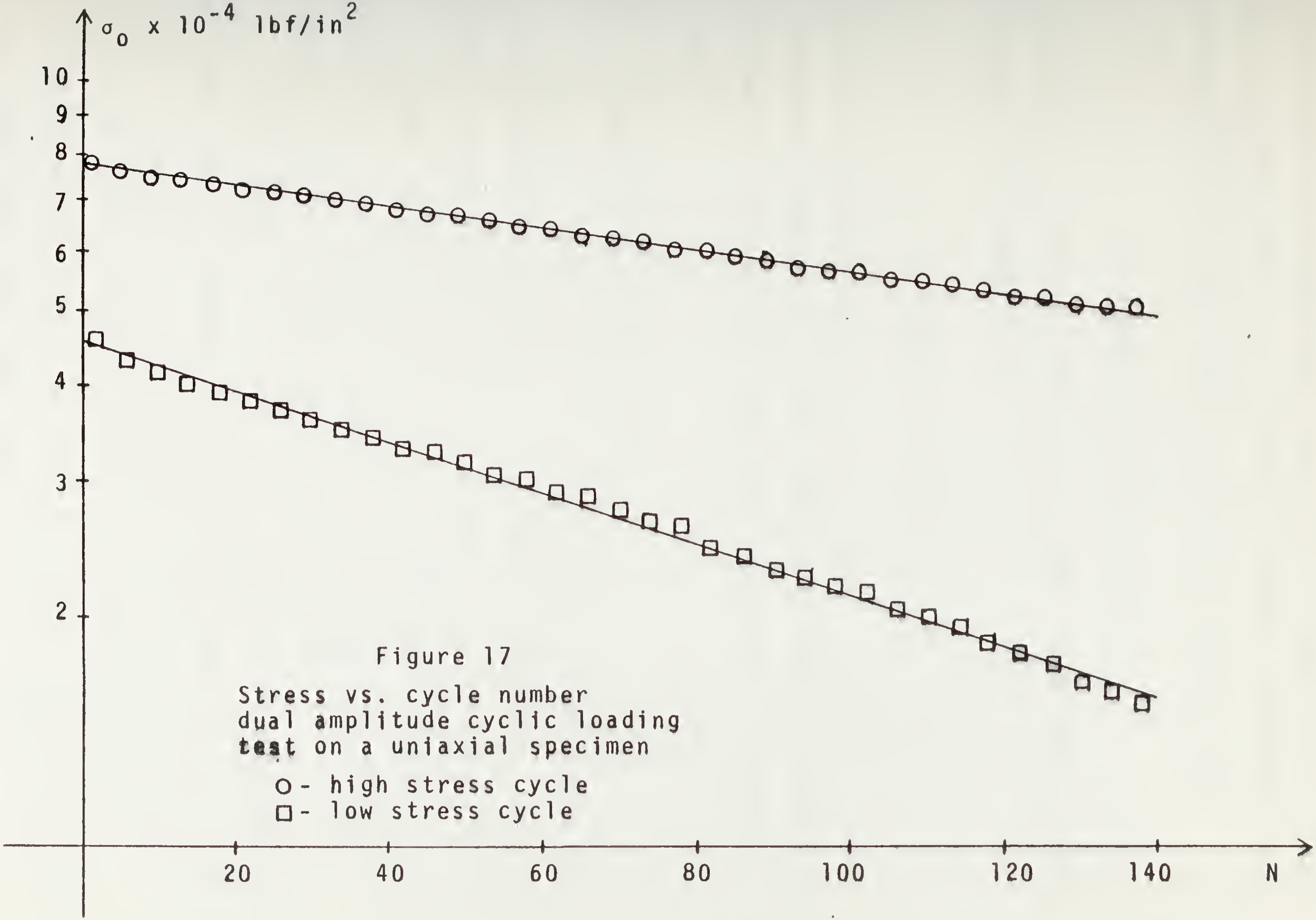

Figure 17

Stress vs. cycle number
dual amplitude cyclic loading
test on a uniaxial specimen

○ - high stress cycle
□ - low stress cycle

A least squares exponential curve fit was applied to 70 high stress points and to 70 low stress points. The resulting equation for the high stress relaxation behavior was

$$\sigma = 76930\ e^{-(3.168 \times 10^{-3})N}$$

with a correlation coefficient of 0.999. For the low stress situation the equation was

$$\sigma = 45600\ e^{-(7.572 \times 10^{-3})N}$$

with a correlation coefficient of 0.998. Thus the stress relaxation behavior in a dual amplitude loading program was defined in terms of the number of cycles and an initial stress value.

E. DISCUSSION OF TEST RESULTS

The main objective of the uniaxial specimen tests was to provide consistent data in the form of monotonic and cyclic stress-strain curves, stress x strain ($\sigma\varepsilon$) vs. stress curves, and stress relaxation behavior for 7075 T-6 aluminum. These data were to be used for comparison and analysis of data taken in tests on plates with central holes.

Three monotonic stress-strain curves were obtained based on three separate tests of uniaxial specimens (Figs. 10 and 12). The moduli of elasticity for the three tests were $E = 10.67 \times 10^6$ lbf/in^2 for the curve obtained from the cyclic stress-strain curve test, $E = 10.0 \times 10^6$ lbf/in^2 from the single amplitude test, and $E = 10.19 \times 10^6$ lbf/in^2 from

the dual amplitude test. These values are within a maximum of 6.28 percent of each other. The average value of the three moduli of elasticity, E = 10.29 x 10^6 lbf/in^2, is almost identical to the published value for 7075 T-6 aluminum, E = 10.3 x 10^6 lbf/in^2. The maximum deviation of individual values obtained from the published value is 3.48 percent. Comparison of curve shape indicates excellent correlation up to stresses of approximately 60,000 lbf/in^2, after which some deviation of the curves from each other is evident. The monotonic stress-strain curve from the dual amplitude loading test tends to decrease slope more rapidly above 60,000 lbf/in^2 and reaches a limit at a stress level of 78,000 lbf/in^2. The single amplitude loading test curve and the monotonic stress-strain curve from the cyclic stress-strain curve test decrease slope at approximately the same rate but have stress limits of 80,000 lbf/in^2 and 78,000 lbf/in^2, respectively.

Because only one cyclic stress-strain curve was developed (Fig. 9), a comparison for consistency could not be made. However, the modulus of elasticity obtained was E = 10.18 x 10^6 lbf/in^2, which is consistent with the monotonic stress-strain curve values obtained, as it should be. The slope decreases more rapidly in comparison to the monotonic curves and remains below it indicating the material cyclically softens. This is not compatible with the results found by Landgraf et al (Ref. 6), which indicates 7075 T-6

aluminum hardens under cyclic loading. The cyclic stress-strain curve obtained in this test was the only one available for use and therefore would be used, if necessary, while the differences in results were noted.

The stress x strain ($\sigma\varepsilon$) vs. stress curves (Figs. 11, 13 and 16) obtained from the three stress-strain curves conform favorably. The differences noted are due to the differences found in the stress and strain data and perpetuated in the mathematics used to construct them. As in the monotonic cases, and for the same reasons, the stress x strain ($\sigma\varepsilon$) vs. stress curves are acceptable for use in the plate tests.

A comparison of the stress relaxation behavior in the single and dual amplitude loading tests can be made by consideration of the equations obtained previously describing this behavior. The equations take the form

$$\sigma = \sigma_0 e^{-bN} .$$

Of particular interest are the initial stress, σ_0, and the stress relaxation rate parameter, b. The single amplitude loading test produced $\sigma_0 = 73160$ lbf/in^2 and $b = 3.177 \times 10^{-3}$, while the high stress relaxation behavior of the dual amplitude loading test produced $\sigma_0 = 76930$ lbf/in^2 and $b = 3.168 \times 10^{-3}$. The initial stresses differ by 4.8 percent, possibly due to the mathematics of the curve fit routine, and the relaxation rate parameters differ by 0.28 percent. This

correlation seems to be quite good and would indicate the type of loading history does not appreciably affect the relaxation behavior of the material when it is loaded repeatedly beyond the proportional limit. However, because only one low cycle stress was applied between the high stress cycles, further tests with considerably different loading histories would be desirable before concluding this to be the general behavior of the high stress relaxation.

The low stress level relaxation behavior provided an initial stress of $\sigma_o = 45{,}600$ lbf/in^2 and a relaxation rate parameter of $b = 7.572 \times 10^{-3}$. The relaxation rate parameter, b, is significantly higher for the low stress portion of loading than for the high stress portion and indicates a possible association between initial stress and relaxation rate. Because only one dual amplitude loading test was performed at one low stress value, further dual amplitude tests with various low stress values are warranted prior to generalizing this association.

From the three uniaxial specimen tests a sound data base was obtained for use in the analysis of the plate tests.

III. LOCAL STRESS-STRAIN BEHAVIOR

A. INTRODUCTION

General stress analysis indicates aircraft structures are in a state of uniaxial stress in most cases but contain numerous local stress concentrations. The Department of Aeronautics, Naval Postgraduate School, Monterey, California, has developed a strain monitoring system which provides data on the nominal stresses experienced by aircraft structures (Refs. 15, 16, and 17) which could be applied to obtain local strain at the stress concentrations. Practicality prevents such monitoring of the numerous local stress concentrations, while fatigue life estimation requires knowledge of local stresses. A means of relating the readily available nominal strains and the local stresses is required for practical fatigue life estimation in aircraft structures.

In order to obtain relationships between local stress and nominal strain for real structures possessing geometric effects, plates with central holes to model those effects were subjected to single and dual amplitude cyclic loading tests. The local strain and nominal stress and strain data obtained in these tests were used to calculate local stress at the hole in order to determine the suitability of a method, based on a theory proposed by Neuber (Ref. 1), for computing local stress on the basis of knowledge of nominal strain and the material properties alone. In addition, these tests

were expected to show the interactions, if any, between geometric configuration and loading history on the local stress relaxation behavior as compared with the behavior found in uniaxial specimen tests.

B. CALCULATION OF LOCAL STRESS ON INITIAL LOADING

Because stress in a plate can not be measured directly, other analytical methods must be used to determine the stress at points (A) and (B) in Figure 2.

One such method involves a proposal by Neuber (Ref. 1), derived from a study of prismatical bodies. Neuber concluded that the geometric mean of stress concentration factor, K_σ, and strain concentration factor, K_ε, is equal to the elastic stress concentration factor, K_t. In equation form:

$$K_t^2 = K_\sigma K_\varepsilon$$

where K_σ is local stress, σ, divided by nominal stress, S, and K_ε is local strain, ε, divided by nominal strain, e.

This equation can be further reduced to

$$K_t^2 = \frac{\sigma\varepsilon}{Se}$$

or, by assuming nominal stress remains in the linear region and $S = E\,e$,

$$K_t^2 = \frac{\sigma\varepsilon}{E\,e^2} \quad .$$

In this form the stress concentration factor is calculated on the basis of the measured local and nominal strain and

calculated values of local stress, and the modulus of elasticity from the appropriate stress-strain curve. The stress concentration factor thus calculated should be indicative of, in this case, all plates with central holes of the same proportionate dimensions and of the same material. With the stress concentration factor thus calculated

$$\sigma\varepsilon = E\ e^2 K_t^2$$

can be written. Therefore, with the stress concentration for a particular configuration known, the modulus of elasticity for the material, and a stress x strain ($\sigma\varepsilon$) vs. stress curve as calculated in the uniaxial specimen tests, the only requirement is knowledge of the nominal strain, an easily obtained quantity from a practical standpoint. In further discussions this method will be known as the Neuber method.

C. EVALUATION OF STRAIN GAGE PLACEMENT

Prior to conducting tests on the 7075 T-6 aluminum plate specimens, a determination of the validity of strain data obtained from strain gages positioned at points (A) and (B) in Figure 18 was made. A plate specimen of 2024 aluminum was prepared with strain gages mounted at these points. Strain gage (A) provided maximum strain on the notch or hole edge and strain gage (B) provided an average of strain across the area it spanned.

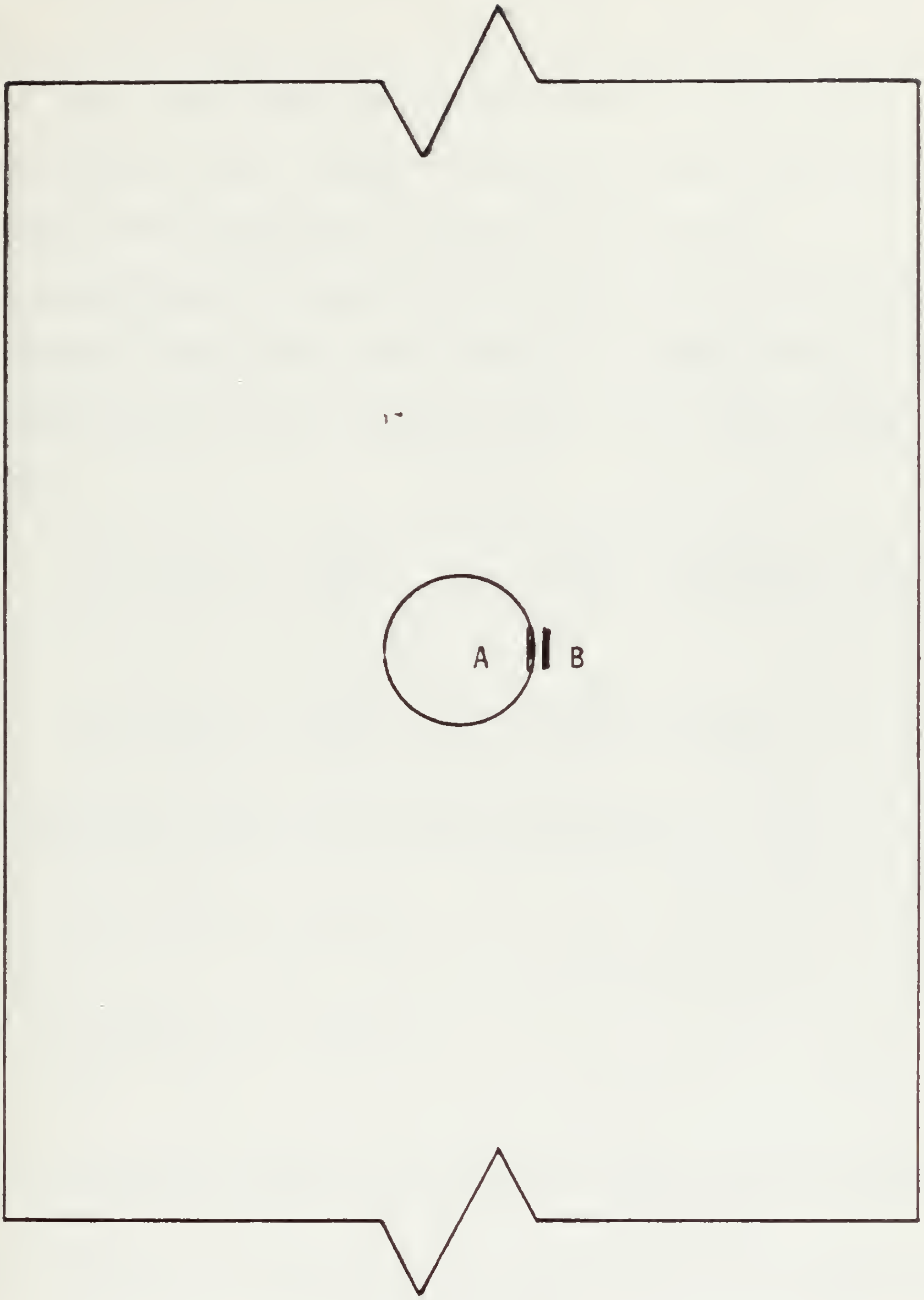

Figure 18

Center section of plate specimen
with locations of strain gages
used in strain gage placement test.

The plate was loaded into tension in load steps of 2000 lbs. up to 18,000 lbs. Strain data from each strain gage and load were recorded at each step. This step was repeated three times. Nominal stress on the plate was calculated from load data (Tables 8, 9, and 10).

To calculate the theoretical values of strain at the two locations the stress and strain solutions for an infinite plate with a hole in the center were used. The stress equations

$$\sigma_r = \frac{\sigma}{2} [(1 - \frac{a^2}{r^2}) - (1 - 4 \frac{a^2}{r^2} + 3 \frac{a^4}{r^4}) \text{ Cos } 2\theta]$$

and

$$\sigma_\theta = \frac{\sigma}{2} [(1 + \frac{a^2}{r^2}) + (1 + 3 \frac{a^4}{r^4}) \text{ Cos } 2\theta]$$

were substituted into the strain equations

$$\varepsilon_r = \frac{1}{E} [\sigma_r - \nu\sigma_\theta]$$

and

$$\varepsilon_\theta = \frac{1}{E} [\sigma_\theta - \nu\sigma_r{}^1]$$

where

σ_r - stress in the region of the hole in a direction perpendicular to that of the loading

σ_θ - stress in the region of the hole in a direction parallel to that of loading

σ - nominal stress on the plate

a - radius of the hole

r - distance from the center of the hole to the point of interest

θ - angle measured from a horizontal bisector of the hole to the point of interest

ε_r - strain in the region of the hole perpendicular to the direction of loading

ε_θ - strain in the region of the hole parallel to the direction of loading

E - Young's modulus of elasticity

ν - Poisson's Ratio

Of interest was the area along a line bisecting the hole and perpendicular to the loading direction where $\theta = 0$. The strain equation for this region is

$$\varepsilon_\theta = \frac{\sigma}{2}\frac{1}{E}\left[\frac{a^2}{r^2}(1 - 3\nu) + 3\frac{a^4}{r^4}(1 + \nu) + 2\right].$$

For maximum strain r = a, or

$$\varepsilon_{\theta_{max}} = 3\frac{\sigma}{E} .$$

For the average strain value, that which the gage measures, the strain was integrated over the radial distance from the inner edge of the strain gage to the outer edge and divided by that distance such that

$$\varepsilon_{\theta_{avg}} = \frac{\sigma}{2E(r_2 - r_1)} \int_{r_1}^{r_2} \left[\frac{a^2}{r^2}(1 - 3\nu) + 3\frac{a^4}{r^4}(1 + \nu) + 2\right]dr$$

or

$$\varepsilon_{\theta_{avg}} = \frac{\sigma}{2E(r_2 - r_1)} \left[a^2(3\nu - 1)\left(\frac{r_1 - r_2}{r_1 r_2}\right) - a^4(1 + \nu)x \left(\frac{r_1^3 - r_2^3}{r_1^3 r_2^3}\right) + 2(r_2 - r_1)\right]$$

The physical placement of the strain gage on the sheet provided the following data:

$$r_1 = 1.023 \text{ in.}, \ r_2 = 1.062 \text{ in.}, \ a = 1.0 \text{ in.}$$

From data for 2024 aluminum $E = 10.6 \times 10^6$ lbf/in^2 and $\nu = 0.33$. Substitution of the above into the equations for maximum and average strain provides

$$\varepsilon_{\theta_{max}} = 0.28302 \ \sigma \ \mu\text{in/in}$$

and

$$\varepsilon_{\theta_{avg}} = 0.25401 \ \sigma \ \mu\text{in/in.}$$

Substitution of nominal stress values obtained in the actual tests into the above equations provided values of maximum and average strain to compare with the measured values of strain (Table 8, 9, and 10).

Of the three test series run, the second is considered the most accurate and reliable, with runs 3 and 1 next in accuracy in that order. In the comparison of theoretical and actual average strains in all three runs the measured strain exhibited greater deviation from the theoretical strain at the lower stress level of approximately 2000 lbf/in^2 (Table 11). In the two most reliable runs this deviation was approximately 2.5 percent. As stress increased, deviation decreased until stresses of around 9000 lbf/in^2 were reached. At this point the strain deviation again began to increase,

reaching a maximum of less than 1.5 percent at over 17,000 lbf/in^2. Also noted was the tendency of measured strain to cycle about the theoretical strain. At low stresses the theoretical exceeded the measured strain. With increasing stress, measured strain increased, equaled theoretical at approximately 9000 lbf/in^2, then exceeded theoretical strain up to the maximum stress reached in each test.

The deviation of the measured strain from the theoretical strain was considered small and well within the accuracy of the entire material testing system, including the strain gages themselves, and therefore was considered adequate for the purpose of future tests.

The results of the maximum strain data comparisons were somewhat less desirable. In all runs, measured strain was greater than theoretical strain, and deviation continued to increase up to a maximum of approximately 5.25 percent. This greater deviation in the maximum strain tests than in the average strain tests was considered to be due to the placement of the strain gage on the curved, inside edge of the hole. Initial curvature of the strain gage was unavoidable due to its location, and the extension experienced by it was not entirely in the plane of the strain gage, as required for accurate strain reproduction. The trend of the deviation indicates that at higher stress levels than the levels encountered here, the deviation would be accordingly higher.

The increasing trend of the actual measured strain's deviation from the theoretical, and the close correlation of the average strain measured in the test with that calculated by theory, led to the decision to instrument plate specimens for this investigation for average strain data output rather than for maximum strain reproduction.

D. CYCLIC LOADING TESTS

The plate specimens were tested in the MTS Corporation closed-loop, servo-controlled testing system used in the uniaxial specimen tests. The same function generator and analog computer were used in the plate tests. The functions used for strain control of the system were identical to those used in the uniaxial specimen single and dual amplitude cyclic loading tests. Output voltages representing load and strain were recorded on the Hewlett-Packard X-Y recorder and a Varian Corporation eight channel strip recorder. The X-Y recorder was used to record voltage outputs of nominal loads and local strain for test monitoring purposes only, and was not required for actual data analysis. The Varian recorder was calibrated to record one voltage input across two channels, thus doubling the resolution. This was done for six channels to provide more accurate recording of local strain data on two of the doubled channels, and nominal strain data on the third. Nominal load output voltages were recorded on one single channel strip.

Two plates with central holes (Figs. 1 and 2) were constructed from the same master sheet of 7075 T-6 aluminum. Care was taken to ensure that no stress raisers, such as scratches or notches, other than the hole itself were introduced. The cross-sectional area of each plate was 1.080 in^2. Strain gages were mounted at points (A), (B), and (C), as depicted in Figure 2. Strain gages at points (A) and (B) provided local strain at the point of highest stress in the plate and the strain gage at (C) provided nominal strain in the plate. The two local strain gages, one on either side of the hole at the point of maximum stress, were utilized to ensure that the data recorded were representative of a plate in uniaxial tension and not subject to undesirable loading such as shear introduced by improper clamping.

Prior to each test all strain gages on the specimen were zeroed and calibrated with the specimen free at one end. After attachment of the free end to the system's load cell, the strain gages were zeroed under load control and the load output voltage adjusted to zero to ensure zero load at zero strain. Recorders were calibrated prior to each test with a known voltage input to ensure accurate reproduction of voltage inputs from the test system.

1. Single Amplitude Cyclic Loading Test

Nominal stress and strain and local strain data from a plate with a hole under single amplitude cyclic loading were required for evaluation of the accuracy of Neuber's method, and for construction of monotonic local stress vs.

nominal strain curves for comparison with the curves obtained from a plate under a different loading history, and for later use in stress relaxation behavior studies.

The haversine function produced by the function generator in the MTS system and used in the uniaxial specimen test was employed in this test on the plate. The system was driven under strain control to a maximum amplitude of 7.3 VDC of the 10.0 VDC available. This voltage corresponded to 11167 μin/in strain in the specimen, according to strain gage (1) used as a control reference by the system; and to 11696 μin/in strain in strain gage (2), mounted opposite the reference strain gage and used for data consistency comparisons. The specimen was cycled 91 times to the maximum stress value.

The MTS system supplied one local strain and the nominal load voltage outputs to an X-Y recorder for test monitoring purposes. Voltage outputs for local strain, nominal strain, and nominal load were supplied to the Varian recorder for later data reduction.

2. Single Amplitude Cyclic Loading Test Results

The Varian recorder provided voltage representations of nominal load, nominal strain, and local strain from two gages. Nominal stress was obtained by dividing the nominal load by the cross-sectional area of the plate at the clamped ends. Nominal stress and local and nominal strains were computed for numerous points on the initial loading cycle Table 12).

A comparison of stress concentration factors calculated using Neuber's equation,

$$K_t^2 = \frac{\sigma\varepsilon}{Se} ,$$

with the theoretical stress concentration factor calculated for the plate with a central hole was made to evaluate Neuber's theory.

The theoretical stress concentration factor was calculated according to

$$K_t = \frac{3W}{W + D}$$

(Ref. 18), where W was defined as the width of the plate and D was defined as the diameter of the hole. From Figure 2, W = 12.0 in. and D = 2.0 in., therefore the theoretical stress concentration factor was calculated to be $K_t = 2.57$.

The stress and strain data taken from the initial loading cycle were used to calculate stress concentration factors for the plate to evaluate Neuber's equation. Two values of local stress due to material variations were obtained with each strain value from the local strain gages by entering the monotonic stress-strain curves constructed from: (1) the cyclic stress-strain test, and (2) the single amplitude cyclic loading test on the uniaxial specimens. With local and nominal stresses and strains known, the stress concentration factors could be calculated according to

$$K_t^2 = \frac{\sigma\varepsilon}{Se} .$$

This was done at seventeen points of local strain for both local strain gages and the two monotonic stress-strain curves mentioned (Table 13). The results were averaged such that $K_t = 2.59$ for strain gage (1) and $K_t = 2.67$ for strain gage (2) from the single amplitude cyclic loading test monotonic stress-strain curve, and $K_t = 2.61$ for strain gage (1) and $K_t = 2.68$ for strain gage (2) from the monotonic stress-strain curve constructed in the cyclic stress-strain curve test on the uniaxial specimen.

The maximum deviation of the stress concentration factors calculated from Neuber's theory was 4.10 percent. The average of the four values was $K_t = 2.64$, within 2.56 percent of the theoretical value. The close correlation of the experimental stress concentration factors with the theoretical value indicates that Neuber's relationship is valid as a basis for calculating local stress.

Noting the apparent validity of Neuber's equation, data points were calculated for construction of monotonic local stress vs. nominal strain curves, based on Neuber's method, from the viewpoint of the analyst who has knowledge of modulus of elasticity, stress concentration factor, and nominal strain only (ε is unknown). The stress concentration factors calculated from both local strain gages, the several moduli of elasticity, and nominal stress were used to obtain four local stress vs. nominal strain relationships for comparison. Neuber's method was applied, as previously outlined,

to obtain local stress which was then plotted against the corresponding local strain (Fig. 19 and Table 14).

To provide a basis for comparison of the local stress vs. nominal strain from the two sets of data, two curves were constructed: one based upon the average value of the stress concentration factors, $K_t = 2.64$, and the average value of the three moduli of elasticity, $E = 10.29 \times 10^6$ lbf/in^2, and the other based upon the theoretical value of $K_t = 2.57$ and the published value of modulus of elasticity, $E = 10.3 \times 10^6$ lbf/in^2. The average curve, (A), in Figure 19, although slightly above, correlates well with the theoretical curve, (B). The scatter of all data points about these curves is quite low.

The maximum variation between the two sets of data points was 38.46 percent for strain gage (1) and 37.93 percent for strain gage (2), both at the lowest nominal strain (Table 14). The average variation for all points was 6.03 percent and 6.14 percent respectively, but omission of the initial data point with maximum variation on each test reduced this average to 4.00 percent and 4.15 percent, respectively.

The low scatter of the data points about the theoretical and average curves, as well as the relatively low average variation between the points based on the two sets of data, indicated either the average or the published material properties may be used to construct local stress vs. nominal strain curves for practical use.

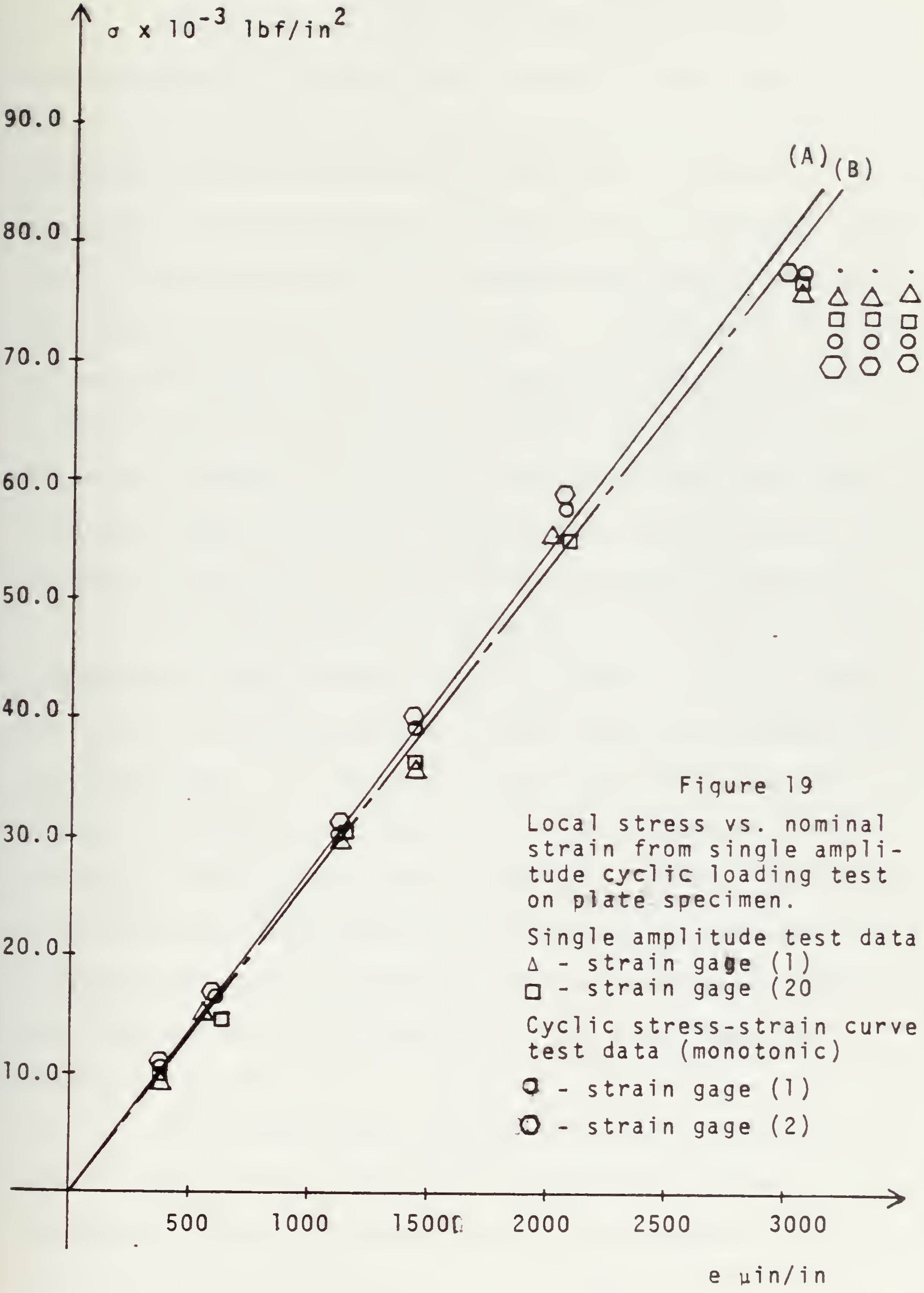

Figure 19

Local stress vs. nominal strain from single amplitude cyclic loading test on plate specimen.

3. Dual Amplitude Cyclic Loading Test

Having established a data base for a simple cyclic loading history of a plate with a hole in the single amplitude cyclic loading test, stress and strain data from a different loading situation were desired. In order to establish a sound data base on more realistic loading situations, a plate specimen with a central hole was subjected to a dual amplitude cyclic loading test. This simple step toward the more realistic situation of random cycling was expected to provide a second evaluation of Neuber's equation, local stress vs. nominal strain curves for comparison with those of the single amplitude cyclic loading test, and additional data for use in the study of local stress relaxation behavior.

The dual amplitude function provided by the analog computer for strain control of the system in the dual amplitude cyclic loading uniaxial specimen test was repeated in this plate test. As in the previous test the system was driven to a maximum amplitude of 7.0 VDC of the 10.0 VDC available. This voltage corresponded to 10708 μin/in strain in the material, according to strain gage (1) used as a reference to control the system; and to 11178 μin/in strain according to local strain gage (2) used as a comparison against the first.

In this test the initial conditions to the analog computer were set to zero prior to the start of the test run. The plate specimen was brought up to a maximum amplitude strain in the first cycle by manual input of the initial

conditions to full value. At the maximum amplitude the analog computer was activated and allowed to run for 114 cycles before test termination.

The system supplied one local strain and the nominal load voltage outputs to an X-Y recorder for monitoring purposes during the test run. Voltage outputs representing both local strains, the nominal load, and the nominal strain were supplied to the Varian recorder for reproduction.

4. Dual Amplitude Cyclic Loading Test Results

As in the single amplitude cyclic loading plate test, nominal load, nominal strain, and two local strains were recorded. Nominal stress was calculated by dividing nominal load by the cross-sectional area of the plate at the clamped end. A second evaluation of Neuber's equation was made by comparison of stress concentration factors calculated from experimental data with the theoretical value for the plate configuration, $K_t = 2.57$.

Stress concentration factors for the plate were first calculated using stress and strain data from the initial loading cycle (Table 15). Local strains were used to obtain local stresses directly from the monotonic stress-strain curves developed from (1) the cyclic stress-strain test and (2) the dual amplitude cyclic loading test on uniaxial specimens. The known values of local stress and strain and nominal stress and nominal strain for fifteen points on the initial loading cycle were used in

$$K_t^2 = \frac{\sigma \varepsilon}{Se}$$

to obtain stress concentration factors for averaging (Table 16). The stress concentration factors thus obtained were $K_t = 2.62$ for strain gage (1) and $K_t = 2.67$ for strain gage (2) based on monotonic stress-strain data from the cyclic stress-strain test, and $K_t = 2.61$ for strain gage (1) and $K_t = 2.65$ for strain gage (2) for data based on the single amplitude cyclic loading test.

The maximum variation of the stress concentration factors calculated by Neuber's theory was 3.75 percent. The average of the four values was $K_t = 2.64$, within 2.56 percent of the theoretical and identical to the average K_t found in the single amplitude cyclic loading test. The conclusion made from the data of the single amplitude cyclic loading test, that Neuber's theory is valid as a basis for calculating local stress, was reinforced by the close correlation of experimental stress concentration factors with the theoretical in this test.

Local stress vs. nominal strain curves were constructed for comparison with those obtained in the previous test. The stress concentration factors were calculated using data from both local strain gages and two moduli of elasticity: one from the dual amplitude cyclic test, and one from the monotonic stress-strain curve of the cyclic stress-strain test, and nominal strain data from this test. The Neuber method was applied to these data to obtain local stress which was plotted against the corresponding nominal strain (Fig. 20

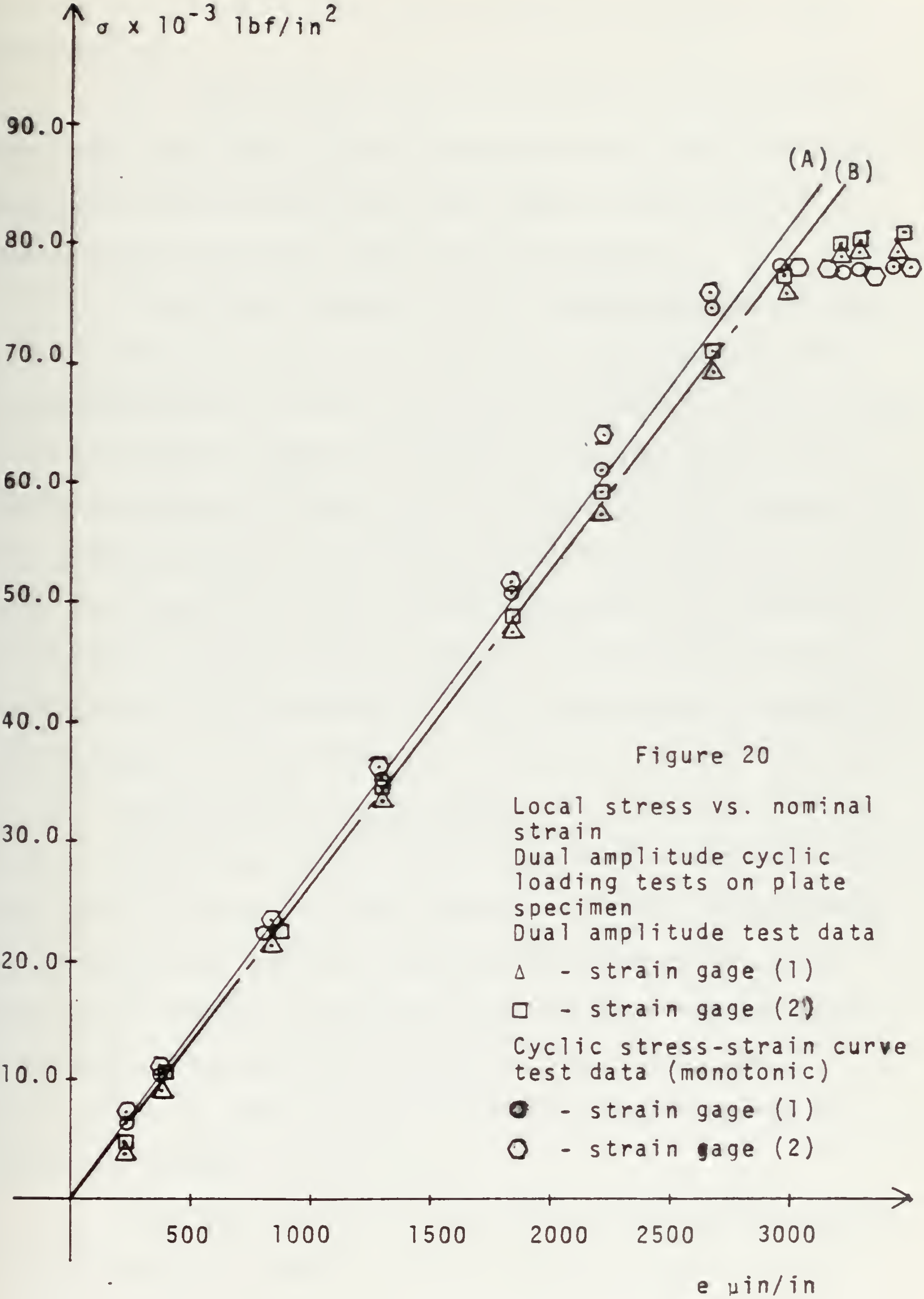

Figure 20

Local stress vs. nominal strain
Dual amplitude cyclic loading tests on plate specimen
Dual amplitude test data

△ - strain gage (1)
□ - strain gage (2)

Cyclic stress-strain curve test data (monotonic)

● - strain gage (1)
⬡ - strain gage (2)

and Table 17) to give four local stress vs. nominal strain relationships.

The theoretical and average curves constructed in the single amplitude cyclic loading test were applied to the data points of this test also and, again, a low scatter of points about the curves (A) and (B) was noted.

A variation between curves constructed on one data base with those of the other data base was noted. Maximum variation between the two sets of data points was 11.94 percent for strain gage (1) and 13.24 percent for strain gage (2), with the average variation for all points of 6.32 percent and 7.71 percent, respectively (Table 17). Due to the low scatter about the theoretical and average curves and the relatively low variation between the two sets, a curve constructed on the basis of either averaged or published material properties would be good for practical use.

5. Discussion of Test Results

The primary objective of the single and dual amplitude cyclic loading tests on plates with central holes were: (1) evaluation of Neuber's relationship, for validity as a basis for a method to calculate local stress from knowledge of nominal strain and material properties alone; and (2) construction of local stress vs. nominal strain curves for comparison between the two tests.

The calculation of the stress concentration factors for evaluation of Neuber's relationship, and the construction of the monotonic local stress vs. nominal strain curves, were

carried out using two sets of stress and strain data for each plate test, the first set being the uniaxial specimen test data corresponding to the particular loading test being applied to the plate, and the second set being based on the monotonic stress-strain curve obtained in the cyclic stress-strain curve test on the uniaxial specimen. The latter data base provided a commonality to the calculations made for the two different plate tests. As would be expected from the close correlation of the stress-strain curves obtained in the uniaxial specimen single and dual amplitude cyclic loading tests, the stress concentration factor calculated in one plate test was approximately equal to that calculated in the other test for a particular strain gage. As further evidence of the consistency of the basic data used in the two tests, the stress concentration factors calculated in each test, based on the monotonic stress-strain curve from the cyclic stress-strain curve test on a uniaxial specimen, were approximately equal from test to test for a particular strain gage. Finally, the maximum variation between any two of the eight stress concentration factors calculated for both tests was 3.63 percent, indicating that the stress concentration factor was essentially consistent from test to test. The average value of all eight factors was $K_t = 2.64$, within 2.56 percent of the theoretical value.

The high correlation of the stress concentration factors obtained experimentally from both tests with the

theoretical value calculated from plate dimensions indicated that Neuber's theory is a valid basis for computation of local stress using only nominal strain.

The low scatter of the local stress vs. nominal strain data points about the theoretical and average curves in both tests, and the relatively low variation between sets of data points within a test, led to the conclusion that a single local stress vs. nominal strain curve based on either average or theoretical data would provide an accurate, practical relationship for determining monotonic local stress at a stress concentration in a structure with only nominal strain and the readily available material property.

E. STRESS RELAXATION BEHAVIOR

1. Introduction and Theory

The stress relaxation behavior of the plate specimens under two different conditions of loading was required for comparison with the behavior of the uniaxial specimens in order to determine the effects, if any, of geometry on the behavior.

Local strain and nominal stress and strain data were obtained from the unloading portion of the stress-strain curve, and from the point of maximum strain on each cycle of the single and dual amplitude cyclic loading tests on plates. The calculation of local stress from these data was required.

The method used to calculate the local stress for the monotonic local stress vs. nominal strain relationships was expanded upon to obtain local stress for relaxation

behavior under cyclic loading conditions, where stress concentration factors could differ from those of the monotonic case. After initial tensile yielding, the stress-strain behavior shifts to the right on the stress-strain curve (Fig. 21), and further cycling is along curve (A-B). This can be thought of as loading from a new origin. Designating quantities which originate from there with a subscript, u, for unloading, and noting that the modulus of elasticity along curve (A-B) is approximately equal to that along curve (O-A), the following quantities are defined:

σ_m - initial maximum local stress in the material

ε_m - initial maximum local strain in the material

σ_u - difference in initial maximum local stress and maximum local stress on a given cycle

ε_u - difference in initial maximum local strain and maximum local strain in a given cycle

S_m - initial maximum nominal stress

S_u - difference in initial maximum nominal stress and maximum nominal stress in a given cycle

K_{tu} - stress concentration factor associated with curve A-B

From these definitions and Figure 21 several general equations can be set forth:

$$\sigma_u = E\,\varepsilon_u$$

$$\sigma_u = K_{tu}S_u$$

$$\varepsilon_u = \varepsilon_m - \varepsilon$$

$$\sigma_u = \sigma_m - \sigma$$

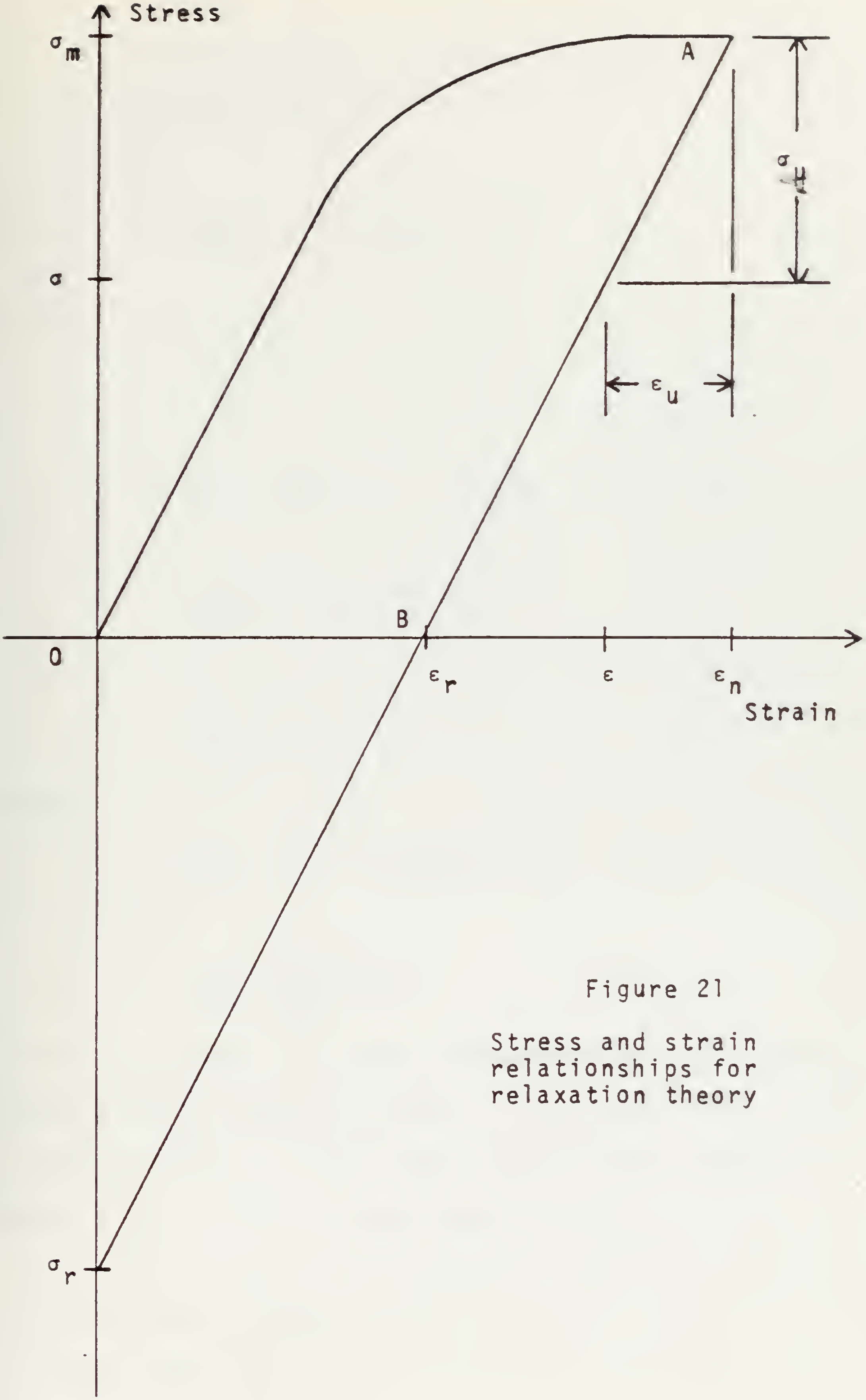

Figure 21

Stress and strain relationships for relaxation theory

Then

$$E\varepsilon_u = K_{tu}S_u$$

or

$$E[\varepsilon_m - \varepsilon] = K_{tu}S_u$$

If

$$\sigma_u = \sigma_m - \sigma$$

and

$$\sigma_u = K_{tu}S_u, \ \sigma_m = K_{tu}S_m, \text{ and } \sigma = K_{tu}S$$

then

$$K_{tu}S_u = K_{tu}S_m - K_{tu}S$$

or

$$S_u = S_m - S$$

Therefore

$$E[\varepsilon_m - \varepsilon] = K_{tu}[S_m - S]$$

or

$$K_{tu} = \frac{\varepsilon_m - \varepsilon}{S_m - S} E .$$

Using this equation the stress concentration factor can be obtained from the measured nominal stress and local strain data from curve A-B. The stress concentration factor is assumed to be constant on subsequent cycles.

Once a stress concentration factor for the curve A-B is obtained, an equation for the local stress at the point of maximum strain in a given cycle may be derived. From the above equations

$$\sigma = \sigma_m - \sigma_u$$

can be written. Then

$$\sigma = \sigma_m - K_{tu}S_u$$

and

$$\sigma = \sigma_m - K_{tu}[S_m - S]$$

follows. For relaxation tests, the nominal stress, S, is a function of the cycle number, N, such that

$$\sigma = \sigma_m - K_{tu}\ [S_m - S(N)]\ .$$

Stress relaxation appears to occur only after the material is yielded; therefore, the maximum local stress, σ_m, will be assumed to be the yield stress of the material. Thus the local stress at the point of maximum strain in a given cycle can be determined as a function of initial maximum local stress, stress concentration factor, initial maximum nominal stress, and the maximum nominal stress of a given cycle.

This method eliminates the requirement for a cyclic stress-strain curve in local stress calculations. Consideration of Figure 21 indicates that after initial yield the specimen does not follow the monotonic nor the cyclic stress-strain curves as constructed from the uniaxial specimen tests, but rather follows one which is shifted to the right and which is not identical to one passing through the origin of the stress-strain coordinates.

Utilizing the above procedure, a satisfactory calculation can be made of local stress at the hole to provide data for the study of the effects of geometry on local stress relaxation behavior. Thus, with local stress available as a function of the cycle number, N, a determination of stress relaxation behavior could be made.

2. Single Amplitude Cyclic Loading Test Results

The stress and strain data obtained from eleven points on the initial unloading portion of the stress-strain curve of the single amplitude cyclic loading test on a plate (Table 18) were used to calculate stress concentration factors by the method previously developed. Moduli of elasticity of $E = 10.67 \times 10^6$ lbf/in^2 from the monotonic stress-strain curve obtained in the cyclic stress-strain curve test, and $E = 10.0 \times 10^6$ lbf/in^2 from the single amplitude cyclic loading test on uniaxial specimens, were used. Local strains from both strain gages were also used to provide four stress concentration factors for comparison (Table 19). The values thus calculated were averaged to produce $K_t = 2.85$ for strain gage (1) and $K_t = 2.94$ for strain gage (2), using data from the monotonic stress-strain curve obtained in the uniaxial specimen cyclic stress-strain curve test; and $K_t = 2.66$ for strain gage (1) and K_t 2.76 for strain gage (2), from data obtained in the uniaxial specimen single amplitude cyclic loading test.

Due to the significant variation of the stress concentration factors from the theoretical value, $K_t = 2.57$, and from each other, a more classical method of calculation of stress concentration factors was used to evaluate the results. From the previous development

$$\sigma(N) = \sigma_m - \sigma_u$$

$$\varepsilon(N) = \varepsilon_m - \varepsilon_u$$

and

$$\sigma_u = E\varepsilon_u$$

were obtained and the equation

$$\sigma_u = \sigma_m - \sigma(N) = E\varepsilon_u$$

or

$$\sigma(N) - \sigma_m = - E[\varepsilon_m - \varepsilon(N)]$$

could be written. Then,

$$\sigma(N) = \sigma_m - E[\varepsilon_m - \varepsilon(N)].$$

In order for $K_t = \frac{\sigma}{S}$ to be valid on the unloading portion of the curve, residual stress, σ_r, must be accounted for such that

$$K_t = \frac{\sigma(N) - \sigma_r}{S(N)}$$

or

$$K_t = \frac{\sigma_m - E[\varepsilon_m - \varepsilon(N)] - \sigma_r}{S(N)}$$

where $\sigma_r = \sigma_m - E[\varepsilon_m - \varepsilon_r]$ and ε_r is the value of residual strain when nominal stress is zero. The average values calculated by this method (Table 20) were only slightly higher (1%) than those calculated by the orignal method in every case, lending validity to the first calculations. Subsequent data reduction was made using the first stress concentration factors obtained.

Because of the wide variation in stress concentration factors, the calculation of local stresses for the relaxation behavior study was done using all the factors obtained, in order to determine what effects the differences would have in this area.

To calculate local stress for determination of the local stress relaxation behavior, the equation

$$\sigma = \sigma_m - K_t[S_m - S(N)]$$

was applied to the maximum nominal stress in a given cycle. The nominal stress was computed from the recorder plot of output voltage for the initial cycle, to obtain S and σ_m, and for every fifth cycle throughout the test run (Table 21). The stress concentration factors found using the two moduli of elasticity and data from the two local strain gages were applied to the equation to obtain four values of local stress (Fig. 22 and 23 and Table 22) for a given cycle number, N. As in the uniaxial specimen tests, a least squares exponential curve fit routine was applied to the data to determine equations of the form $\sigma = \sigma_0 e^{-bN}$, describing the local stress

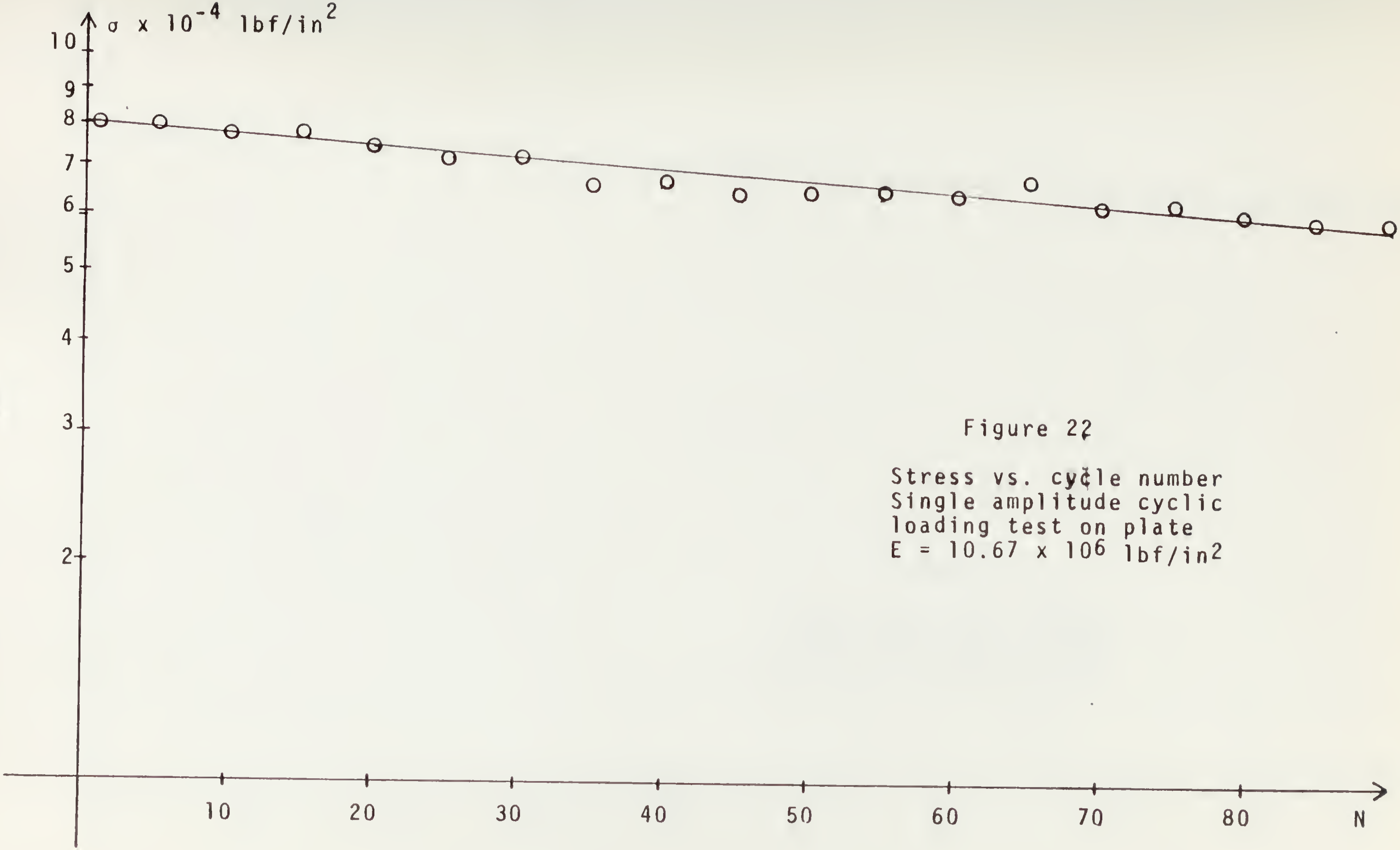

Figure 22

Stress vs. cycle number
Single amplitude cyclic
loading test on plate
$E = 10.67 \times 10^6$ lbf/in^2

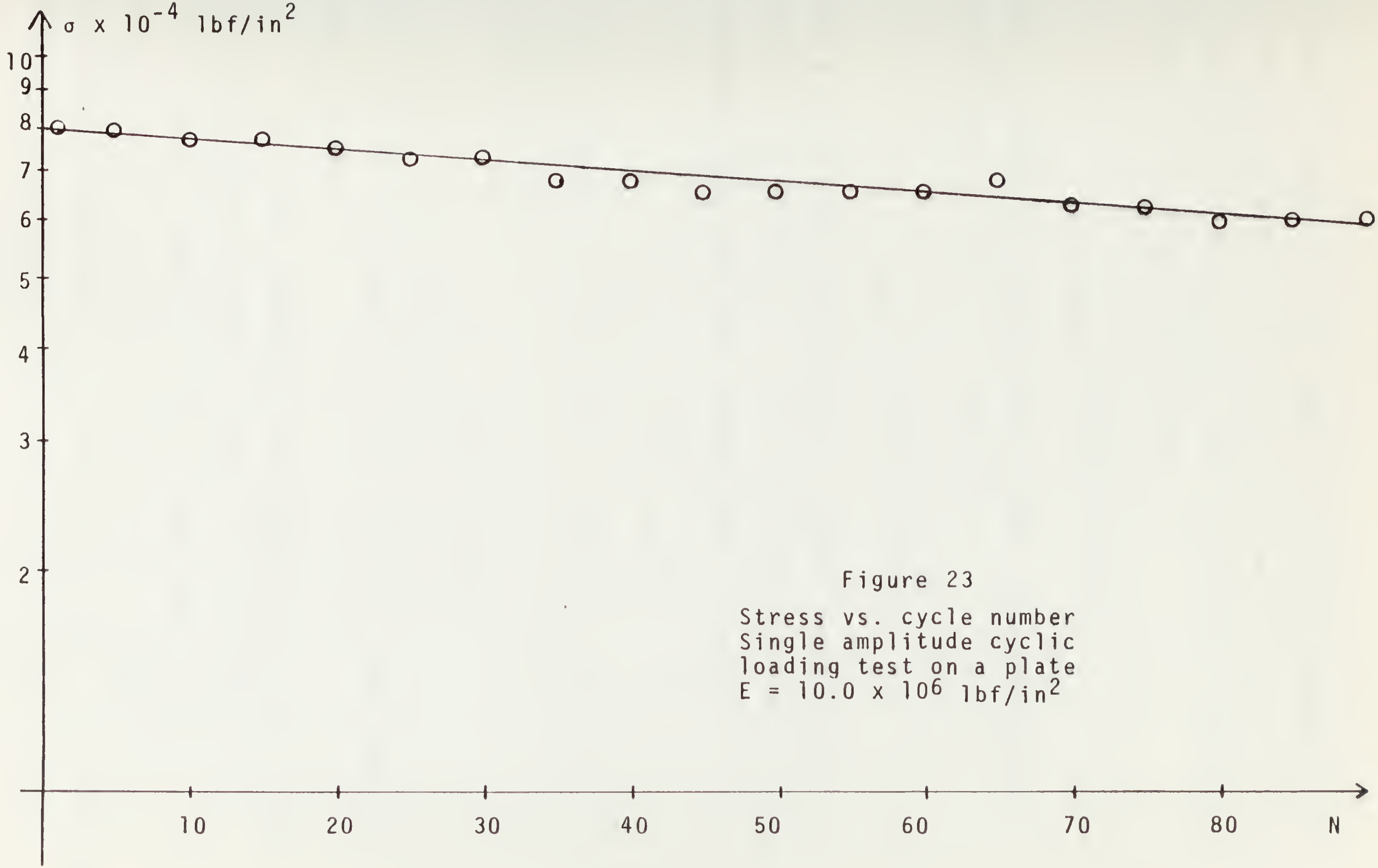

Figure 23

Stress vs. cycle number
Single amplitude cyclic
loading test on a plate
$E = 10.0 \times 10^6$ lbf/in^2

relaxation behavior. All four sets of data were used to provide a comparison. For data based on the monotonic stress-strain curve obtained from the uniaxial specimen cyclic stress-strain curve test:

$$\sigma = 79220\ 3^{-(3.427 \times 10^{-3})N}$$

with a correlation coefficient of 0.9650 , was obtained for strain gage (1) with $K_t = 2.85$; and

$$\sigma = 79470\ e^{-(3.752 \times 10^{-3})N}$$

with a correlation coefficient of 0.9650, was obtained for strain page (2) with $K_t = 2.95$. Data based on the uniaxial specimen single amplitude loading test produced

$$\sigma = 79470\ e^{-(3.324 \times 10^{-3})N}$$

with a correlation coefficient of 0.964 for strain gage (1) with $K_t = 2.66$ and

$$\sigma = 79470\ e^{-(3.470 \times 10^{-3})N}$$

with a correlation coefficient of 0.9650 for strain gage (2) with $K_t = 2.76$.

The four equations thus obtained for local stress relaxation behavior exhibit little or no variation in the initial stress; however, there is a maximum variation of 7.52 percent between the stress relaxation rate parameters for a single strain gage but of different data bases. The variation of stress concentration factors was considered the cause of

this result. Because the data used to calculate the stress relaxation behavior equations were from equally valid tests, no further conclusions were drawn at this point as to the accuracy of one equation over the other.

3. Dual Amplitude Cyclic Loading Test Results

The stress and strain data taken from six points on the initial unloading portion of the stress-strain curve of the dual amplitude cyclic loading test on a plate (Table 23) were used to calculate stress concentration factors by the previously outlined method.

The moduli of elasticity of $E = 10.67 \times 10^6$ lbf/in^2, from the monotonic stress-strain curve obtained in the cyclic stress-strain curve test, and $E = 10.19 \times 10^6$ lbf/in^2, from the dual amplitude loading test on uniaxial specimens were used. Local strains from both strain gages were also used (Table 24). Again, the values of stress concentration factors calculated for individual points along the stress-strain curve were averaged. Stress concentration factors thus obtained were $K_t = 3.09$ for strain gage (1), and $K_t = 3.17$ for strain gage (2), based on data from the monotonic stress-strain curve of the cyclic stress-strain curve test on the uniaxial specimen test; and $K_t = 2.95$ for strain gage (1), and $K_t = 3.03$ for strain gage (2), based on the uniaxial specimen dual amplitude loading test.

As in the single amplitude cyclic loading test, significant variation of the calculated stress concentration factors from the theoretical value, $K_t = 2.57$, and between

each other, was noted. The classical method previously described was applied to the data of this test (Table 25). The values obtained by this method were also varied, but considerably lower and much closer to the theoretical value of $K_t = 2.57$. Because the results of the single amplitude cyclic loading test exhibited close correlation between K_t values calculated by both methods, and the opposite was found in this test, additional tests were indicated prior to forming a definite conclusion as to the actual value of stress concentration factor on the unloading portion of the stress-strain curve.

In the interests of uniformity of method, the first set of stress concentration factors obtained was used in the calculation of the stress relaxation behavior equations, as was done in the single amplitude cyclic loading test. Due to the variation within this set, all values were used in subsequent calculations.

Local stresses for the determination of local stress relaxation behavior were calculated according to

$$\sigma = \sigma_m - K_t \, [S_m - S(N)]$$

Because high stress cycles were alternated with low stress cycles in this test, two sets of stress relaxation behavior data were obtained. Maximum nominal stress and local strain were computed for the peak of the initial cycle to provide S_m and σ_m for both high and low stress calculations and then for every fourth cycle thereafter on both high and low peak

local strain amplitudes (Table 26). The stress concentration factors found using two moduli of elasticity and data from two local strain gages were applied to the equation to obtain four values of local stress for each cycle number, N (Fig. 24 and 25 and Tables 27 and 21).

To obtain an equation of the form $\sigma = \sigma_0 e^{-bN}$ describing the local stress relaxation behavior of the high stress data, the least squares exponential curve fit routine used in the other uniaxial and plate specimen tests was applied to the data. For data based on the monotonic stress-strain curve obtained in the uniaxial specimen cyclic stress-strain curve test

$$\sigma = 78080\ e^{-(2.593 \times 10^{-3})n}$$

was calculated for local strain gage (1), based on twenty-nine data points with a correlation coefficient of 0.947; and

$$\sigma = 78100\ e^{-(2.671 \times 10^{-3})N}$$

was calculated for strain gage (2), based on twenty-nine data points with a correlation coefficient of 0.947. For data based on the monotonic stress-strain curve obtained in the uniaxial specimen dual amplitude loading test

$$\sigma = 78060\ e^{-(2.457 \times 10^{-3})N}$$

was calculated for strain gage (1), based on twenty-nine points with a correlation coefficient of 0.947; and

$$\sigma = 78070\ e^{-(2.534 \times 10^{-3})N}$$

was calculated for strain gage (2), based on twenty-nine points with a correlation coefficient of 0.947.

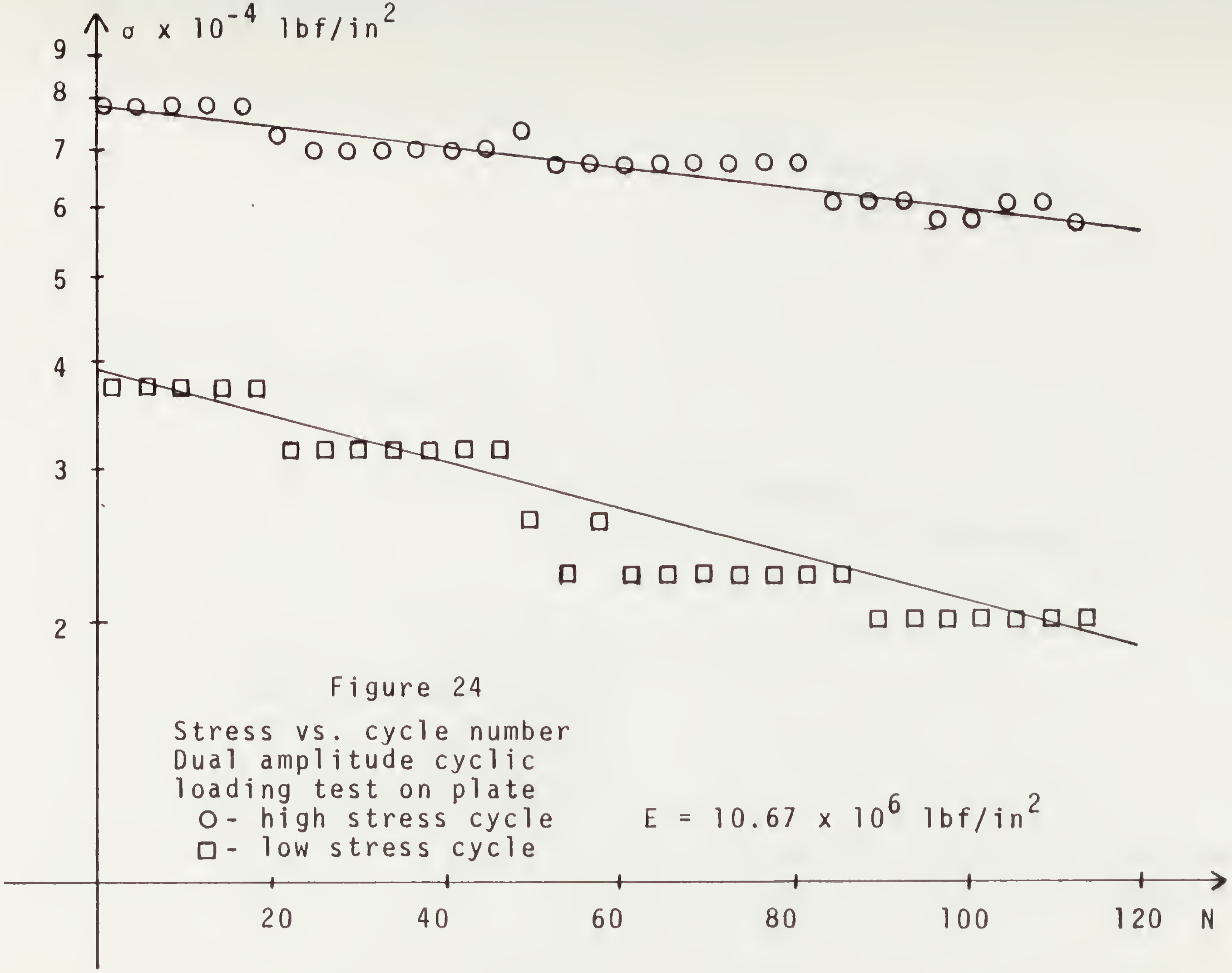

Figure 24

Stress vs. cycle number
Dual amplitude cyclic
loading test on plate
○ - high stress cycle
☐ - low stress cycle

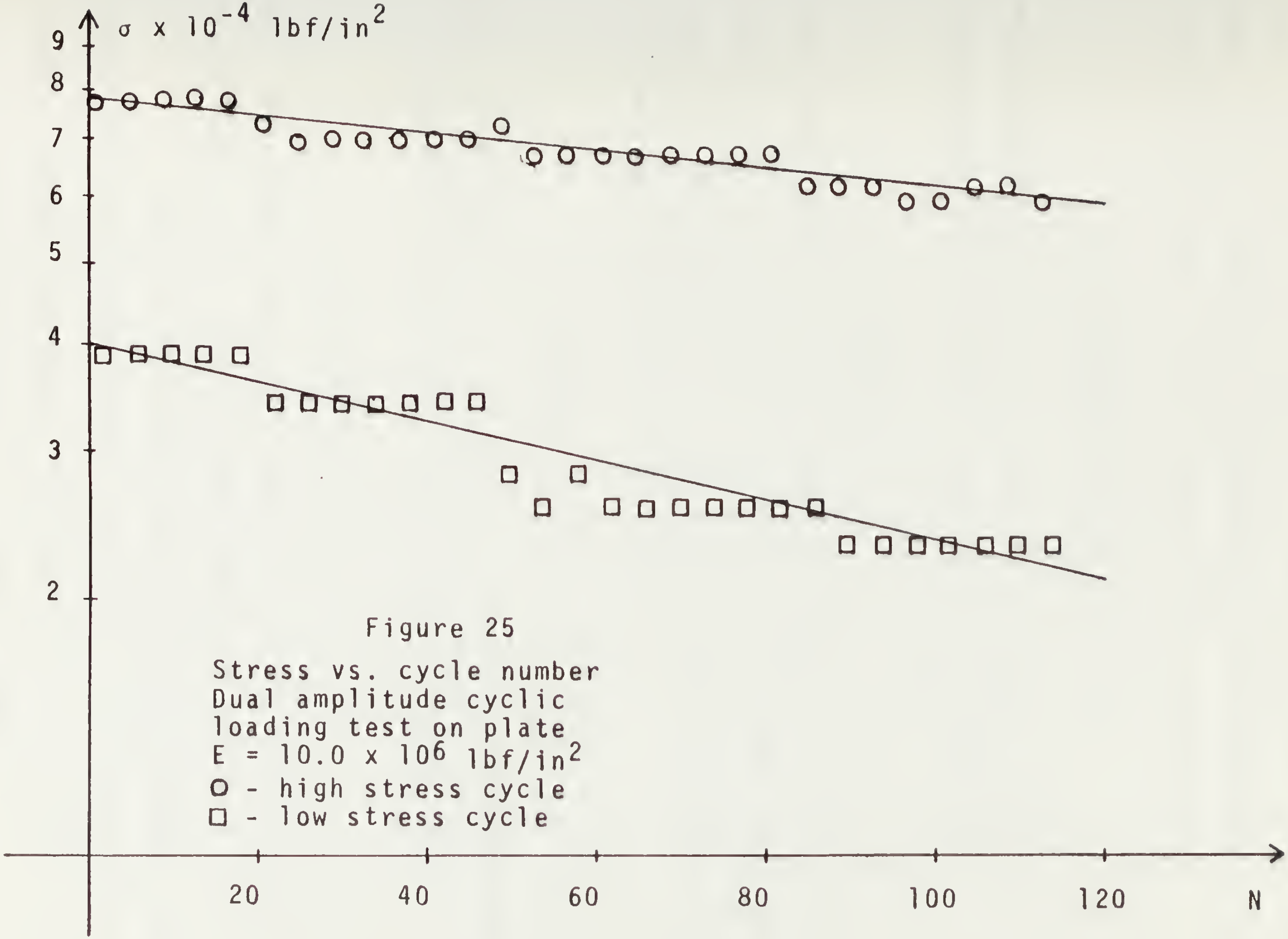

Figure 25

Stress vs. cycle number
Dual amplitude cyclic
loading test on plate
$E = 10.0 \times 10^6$ lbf/in^2
○ - high stress cycle
□ - low stress cycle

The least squares exponential curve fit routine was also applied to the data for the low stress cycles to obtain the low local stress relaxation behavior. For data based on the monotonic stress-strain curve obtained in the uniaxial specimen cyclic stress-strain curve test

$$\sigma = 39030\ e^{-(6.350 \times 10^{-3})N}$$

was calculated for strain gage (1), based on twenty-nine points with a correlation coefficient of 0.960 and

$$\sigma = 38120\ e^{-(6.843 \times 10^{-3})N}$$

was calculated for strain gage (2), based on twenty-nine points with a correlation coefficient of 0.961. For data based on the monotonic stress-strain curve from the uniaxial specimen dual amplitude loading test

$$\sigma = 40650\ e^{-(5.594 \times 10^{-3})N}$$

was calcualted for strain gage (1), based on twenty-nine points with a correlation coefficient of 0.959 and

$$\sigma = 39720\ e^{-(6.010 \times 10^{-3})N}$$

was calculated for strain gage (2), based on twenty-nine points with a correlation coefficient of 0.960.

The four equations obtained for the stress relaxation behavior of the high stress cycles show excellent correlation between initial stresses. Maximum variation in the relaxation rate parameter was found to be 5.24 percent.

The four equations obtained for the low stress cycles exhibited greater variation in the initial stresses, where a maximum variation of 4.03 percent was found. Maximum variation between the relaxation rate parameters was found to be 12.17 percent.

The variations noted in the stress relaxation behavior equations were considered due, in part, to the variations in stress concentration factors used in the calculations. No further conclusions were drawn due to the equally valid tests from which the data bases were drawn.

4. Discussion of Test Results

The stress concentration factors calculated for local stress computation in the study of stress relaxation behavior were found to be significantly greater than those calculated for the construction of local stress vs. nominal strain curves and the theoretical value computed from plate geometry. An attempt to verify the validity of the stress concentration factors based on data from the unloading portion of the stress-strain curve, by comparison with those calculated by a more classical method, provided two divergent results in two tests, and no conclusion could be offered as to the validity of one stress concentration factor over another at this point. Further tests are warranted to resolve this inconsistency.

Because of the wide variation in stress concentration factors, the calculation of local stresses for the relaxation behavior study was done using all factors obtained

in order to determine what effects the differences would have in this area. The local stress relaxation behavior described by equations of the form

$$\sigma = \sigma_0 e^{-bN}$$

can best be compared by considering Table 29, where the parameters σ_0 and b are listed according to test and data source, and Figure 26, where these parameters are plotted against each other, along with those values obtained in the uniaxial specimen tests under single and dual amplitude cylic loading. Of particular interest is the symmetric grouping of the high stress data points, with respect to the relaxation rate parameter, b, based on plate tests around the points for the uniaxial specimen tests' data points. The average relaxation rate parameter for all ten data points is 3.06, with single amplitude plate test values tending to be higher, dual amplitude plate test values somewhat lower. Although only two plate tests were run, the four values for each plate test, differing due to data base used in the calculations, appear to indicate that the local high stress relaxation rate tends to follow that of the uniaxial specimen rate. The local low stress and uniaxial low stress relaxation parameters are widely scattered and will require additional data to delineate the correct behavior description.

The accuracy of the stress relaxation behavior noted in this study is subject to the variation of the calculated stress concentration factors. This effect would be equally

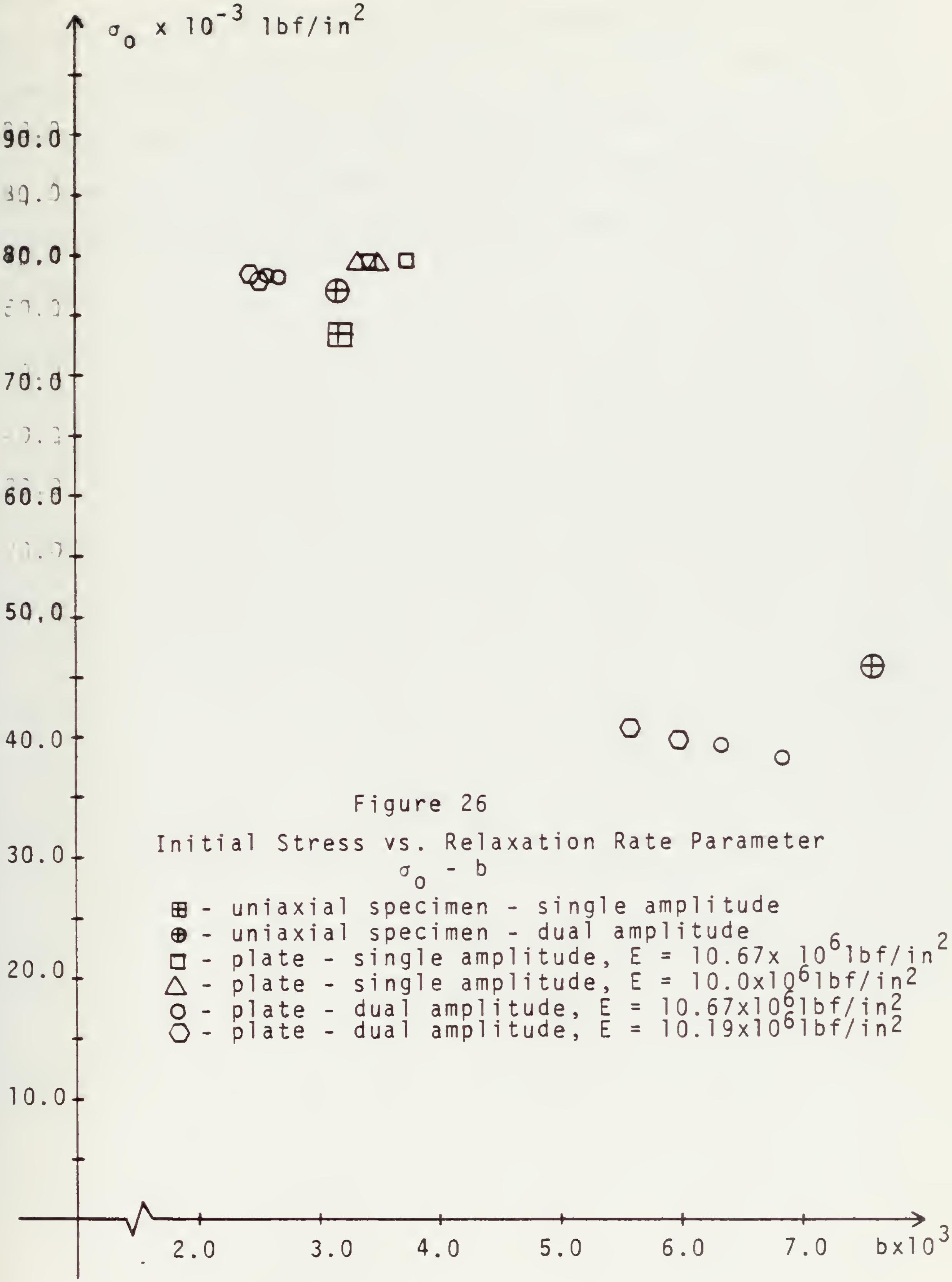

Figure 26

Initial Stress vs. Relaxation Rate Parameter

σ_o - b

⊞ - uniaxial specimen - single amplitude
⊕ - uniaxial specimen - dual amplitude
□ - plate - single amplitude, $E = 10.67 \times 10^6$ lbf/in^2
△ - plate - single amplitude, $E = 10.0 \times 10^6$ lbf/in^2
○ - plate - dual amplitude, $E = 10.67 \times 10^6$ lbf/in^2
⬡ - plate - dual amplitude, $E = 10.19 \times 10^6$ lbf/in^2

applied to both single and dual amplitude cyclic loading test results, and therefore would not affect the relationship between the data points of the two on the initial stress vs. relaxation rate parameter curve significantly (Fig. 26). Thus, the conclusions drawn on relaxation behavior were considered to be qualitatively, if not quantitatively, accurate.

IV. CONCLUSIONS ON TEST RESULTS

The major areas of interest in the tests on uniaxial and plate specimens were: (1) determining whether Neuber's relationship, $K_t^2 = \frac{\sigma\varepsilon}{Se}$, would provide an accurate, practical method of calculating local stress, with knowledge of the material properties and nominal strain alone, in a structure subject to stress concentrations, (2) determining whether the local stress in the specimen follows the stress relaxation behavior of the uniaxial specimen; and (3) determining whether the type of loading applied to both uniaxial and plate specimens alters the stress relaxation behavior.

Neuber's theory proved to be a valid basis on which to establish a method of calculating local stress at a stress concentration in a structure based on knowledge of nominal strain and material properties alone. Because Neuber's method provides only the initial monotonic local stress in the structure, the stress relaxation behavior must be known to utilize the method in practical fatigue life determination.

In the area of stress relaxation behavior, further study of the calculation of stress concentration factors is warranted. The values calculated for the unloading portion of the stress-strain curve ranged from $K_t = 2.66$ to $K_t = 3.17$, significantly different than the corresponding stress concentration factors calulated on the initial loading cycle of the same curve, and varying greatly among themselves.

Additional tests are recommended to determine whether the stress concentration factor does vary from the loading to unloading portions of the curve, and whether a consistent factor can be obtained for the unloading segment. However, because a number of stress concentration factors were calculated and used to determine stress relaxation behavior, it is felt that essentially valid conclusions can be drawn regarding relaxation behavior without detrimental influence due to possibly incorrect values of stress concentration factors.

A comparison of stress relaxation behavior obtained in the uniaxial and plate specimen tests indicated that, when the material is cycled repeatedly into the yield stress range, the relaxation rate tends to be low, in the area of $b = 3.00 \times 10^{-3}$ (Fig. 26), regardless of the loading situation of the geometric configuration. Due to the scatter realized in the low stress relaxation behavior data, no conclusion could be drawn in this area other than the fact that relaxation rate parameters are significantly higher than those of the high stress behaviors. Additionally, it appeared that the type of loading situation had some influence on the high stress relaxation rates found in the plate tests. This was not the case in the uniaxial specimens, which would indicate that some combined influences of geometric effects and loading history were present in the plates with regard to stress relaxation behavior. Further tests are necessary to establish the stress relaxation behavior throughout the range of stress

from high to low values. These tests would hopefully reveal a relationship between initial stress and relaxation rate which would reduce the present form of the equation.

$$\sigma = \sigma_o e^{-bN}$$

to a form involving relaxation rate, b, as a function of initial stress, σ_o, or

$$\sigma = \sigma_o e^{-a(\sigma_o)N}$$

thus facilitating the calculation of local stress at a given cycle. The establishment of a valid stress relaxation behavior equation is necessary in order to extend the use of Neuber's method to practical situations where structures do, in fact, cycle repeatedly. The local stress-nominal strain relationships are valid only for the initial cycle, after which stress relaxation behavior must be applied to obtain accurate knowledge of local stress for fatigue life studies.

In general, the conclusions were that the initial local stress in a structure subject to geometric effects can be obtain readily and accurately by applying Neuber's method; and that once the initial local stress is known, a stress relaxation behavior equation of the form

$$\sigma = \sigma_o e^{-bN}$$

can be applied to obtain local stresses at given cycles for studies involving fatigue life estimation in aircraft structures.

APPENDIX A - TABULAR DATA

TABLE 1

Strain data and percent bending moment from alignment evaluation on MTS test system's load cell.

Strain Gage 1	Strain Gage 2	Strain Gage 3	Strain Gage 4	Maximum Strain	Average Strain	Percent Bending Moment
0	0	0	0	0	0	0
939	983	966	920	983	952	3.26
1404	1479	1458	1385	1479	1431.5	3.32
1780	1875	1849	1757	1875	1815.25	3.29
1399	1481	1455	1380	1481	1428.75	3.66
928	990	965	909	990	948.00	4.43
- 979	- 931	- 920	- 959	- 979	- 947.25	3.35
-1452	-1404	-1381	-1417	-1452	-1413.50	2.72
-1828	-1781	-1749	-1785	-1828	-1785.75	2.37
-1450	-1390	-1384	-1431	-1450	-1413.75	2.56
- 972	- 910	- 925	- 974	- 974	- 945.25	3.04

Percent bending moment calculated according to:

$$\% \text{ Bending} = \frac{\text{max} - \text{avg}}{\text{avg}} \times 100$$

Strain gages were calibrated such that
1.0 VDC = 1000 μin/in

TABLE 2

Cyclic stress and strain data from cyclic stress-strain curve test on a uniaxial specimen.

TENSILE LOADS

Cycle	Load Volts	Strain Volts	Stress lbf/in^2	Strain μin/in
1	7.80	7.40	78000	11339
2	7.75	7.05	77500	10802
3	7.60	6.80	76000	10419
4	7.50	6.50	75000	9960
5	7.30	6.00	73000	9193
6	7.00	5.30	70000	8121
7	6.40	4.50	64000	6895
8	5.30	3.55	53000	5439
9	3.90	2.50	39000	3831

COMPRESSIVE LOADS

Cycle	Load Volts	Strain Volts	Stress lbf/in^2	Strain μin/in
1	-7.90	-7.35	-79000	-11262
2	-7.90	-7.25	-79000	-11109
3	-7.85	-7.00	-78500	-10726
4	-7.80	-6.55	-78000	-10036
5	-7.60	-5.95	-76000	- 9117
6	-7.20	-5.20	-72000	- 7968
7	-6.30	-4.30	-63000	- 6589
8	-5.00	-3.35	-50000	- 5133

CALIBRATION

Load: 1.0 VDC = 10,000 lbf

Strain: 1.0 VDC = 153223 μin/in

Stress: 1.0 VDC = 10,000 lbf/in^2

TABLE 3

Monotonic stress and strain data from cyclic stress-strain curve test on a uniaxial specimen.

Load Volts	Strain Volts	Stress lbf/in^2	Strain μin/in
1.00	0.60	10000	919
2.00	1.20	20000	1839
3.00	1.85	30000	2835
4.00	2.5	40000	3831
5.00	3.10	50000	4750
6.00	3.80	60000	5822
7.00	4.20	70000	6435
7.80	5.20	78000	7968
7.80	7.40	78000	11339

CALIBRATION

Load: 1.0 VDC = 10,000 lbf

Strain: 1.0 VDC = 1532.23 μin/in

Stress: 1.0 VDC = 10,000 lbf/in^2

TABLE 4

Monotonic stress and strain data from single amplitude cyclic loading test on a uniaxial specimen.

Load Volts	Strain Volts	Stress lbf/in^2	Strain $\mu in/in$	Stress x Strain lbf/in^2
0.00	0.00	0.00	0.00	0.00
0.50	0.40	5000	612	3.062
1.00	0.70	10000	1071	10.71
1.50	1.10	15000	1683	25.25
2.00	1.35	20000	2065	41.30
2.50	1.65	25000	2524	63.10
3.00	2.00	30000	3060	91.80
3.50	2.30	35000	3518	123.13
4.00	2.60	40000	3977	159.08
4.50	2.95	45000	4513	203.09
5.00	3.25	50000	4972	248.60
5.50	3.58	55000	5477	301.24
6.00	3.90	60000	5966	357.96
6.50	4.25	65000	6501	422.57
7.00	4.60	70000	7037	492.59
7.20	4.75	72000	7266	523.15
7.40	4.90	74000	7496	554.70
7.50	5.00	75000	7649	573.68
7.60	5.10	76000	7802	592.95
7.70	5.30	77000	8108	624.32
7.80	5.40	78000	8261	644.36
7.90	6.00	79000	9179	725.14
8.00	6.60	80000	10096	807.68
8.00	7.30	80000	11167	893.36

CALIBRATION

Load: 1.0 VDC = 10,000 lbf

Strain: 1.0 VDC = 1529.76 $\mu in/in$

Stress: 1.0 VDC = 10,000 lbf/in^2

TABLE 5

Stress and cycle number data from single amplitude cyclic loading test on a uniaxial specimen.

Cycle	Load Volts	Stress lbf/in^2	Cycle	Load Volts	Stress lbf/in^2
1	8.00	80000	45	6.30	63000
2	7.85	78500	46	6.30	63000
3	7.80	78000	47	6.30	63000
4	7.75	77500	48	6.25	62500
5	7.70	77000	49	6.25	62500
6	7.65	76500	50	6.20	62000
7	7.60	76000	51	6.20	62000
8	7.60	76000	52	6.15	61500
9	7.55	75500	53	6.10	61000
10	7.50	75000	54	6.05	60500
11	7.50	75000	55	6.05	60500
12	7.45	74500	56	6.00	60000
13	7.40	74000	57	6.00	60000
14	7.40	74000	58	6.00	60000
15	7.35	73500	59	5.95	59000
16	7.30	73000	60	5.90	59000
17	7.25	72500	61	5.90	59000
18	7.20	72000	62	5.90	59000
19	7.15	71500	63	5.85	58500
20	7.10	71000	64	5.85	58500
21	7.10	71000	65	5.80	58000
22	7.05	70500	66	5.80	58000
23	7.05	70500	67	5.80	58000
24	7.00	70000	68	5.75	57500
25	6.95	69500	69	5.70	57000
26	6.90	69000	70	5.70	57000
27	6.90	69000	71	5.70	57000
28	6.85	68500	72	5.65	56500
29	6.80	68000	73	5.65	56500
30	6.80	68000	74	5.60	56000
31	6.75	67500	75	5.60	56000
32	6.70	67000	76	5.60	56000
33	6.70	67000	77	5.55	55500
34	6.65	66500	78	5.55	55500
35	6.60	66000	79	5.50	55000
36	6.60	66000	80	5.50	55000
37	6.55	65500	81	5.50	55000
38	6.50	65000	82	5.45	54500
39	6.50	65000	83	5.45	54500
40	6.45	64500	84	5.40	54000
41	6.40	64000	85	5.40	54000
42	6.40	64000	86	5.40	54000
43	6.40	64000	87	5.40	54000
44	6.35	63500	88	5.35	53500

Cycle	Load Volts	Stress lbf/in^2	Cycle	Load Volts	Stress lbf/in^2
89	5.35	53500	140	4.60	46000
90	5.30	53000	141	4.60	46000
91	5.30	53000	142	4.60	46000
92	5.30	53000	143	4.60	46000
93	5.30	53000	144	4.60	46000
94	5.30	53000	145	4.55	45500
95	5.25	52500	146	4.55	45500
96	5.25	52500	147	4.55	45000
97	5.20	52000	148	4.50	45000
98	5.20	52000	149	4.50	45000
99	5.20	52000	150	4.50	45000
100	5.20	52000	151	4.50	45000
101	5.15	51500	152	4.50	45000
102	5.15	51500	153	4.50	45000
103	5.10	51000	154	4.45	44500
104	5.10	51000	155	4.45	44500
105	5.10	51000	156	4.40	44000
106	5.10	51000	157	4.40	44000
107	5.05	50500	158	4.40	44000
108	5.05	50500	159	4.40	44000
109	5.00	50000	160	4.40	44000
110	5.00	50000	161	4.35	43500
111	5.00	50000	162	4.35	43500
112	5.00	50000	163		
113	5.00	50000	164		
114	4.95	49500	165		
115	4.95	49500	166		
116	4.95	49500	167		
117	4.90	49000	168		
118	4.90	49000	169		
119	4.90	49000	170		
120	4.90	49000	171		
121	4.85	48500	172		
122	4.85	48500	173		
123	4.85	48500	174		
124	4.80	48000	175		
125	4.80	48000	176		
126	4.80	48000	177	4.15	41500
127	4.80	48000	178	4.15	41500
128	4.75	47500	179	4.10	41000
129	4.75	47500	180	4.10	41000
130	4.75	47500	181	4.10	41000
131	4.75	47500	182	4.05	40500
132	4.70	47000	183	4.05	40500
133	4.70	47000	184	4.05	40500
134	4.70	47000	185	4.00	40000
135	4.70	47000	186	4.00	40000
136	4.65	46500	187	4.00	40000
137	4.65	46500	188	4.00	40000
138	4.65	46500	189	4.00	40000
139	4.60	46000	190	4.00	40000

Cycle	Load Volts	Stress lbf/in^2	Cycle	Load Volts	Stress lbf/in^2
191	4.00	40000	234	3.60	36000
192	3.95	39500	235	3.55	35500
193	3.95	39500	236	3.55	35500
194	3.95	39500	237	3.55	35500
195	3.90	39000	238	3.55	35500
196	3.90	39000	239	3.55	35500
197	3.90	39000	240	3.50	35000
198	3.90	39000	241	3.50	35000
199	3.90	39000	242	3.50	35000
200	3.85	38500	243	3.50	35000
201	3.85	38500	244	3.50	35000
202	3.85	38500	245	3.50	35000
203	3.80	38000	246	3.45	34500
204	3.80	38000	247	3.45	34500
205	3.80	38000	248	3.45	34500
206	3.80	38000	249	3.45	34500
207	3.80	38000	250	3.40	34000
208	3.80	38000	251	3.40	34000
209	3.75	37500	252	3.40	34000
210	3.75	37500	253	3.40	34000
211	3.75	37500	254	3.35	33500
212	3.75	37500	255	3.35	33500
213	3.75	37500	256	3.30	33000
214	3.75	37500	257	3.30	33000
215	3.75	37500	258	3.30	33000
216	3.70	37000	259	3.25	32500
217	3.70	37000	260	3.20	32000
218	3.70	37000	261	3.20	32000
219	3.70	37000	262	3.20	32000
220	3.70	37000	263	3.15	31500
221	3.70	37000	264	3.10	31000
222	3.70	37000	265	3.10	31000
223	3.70	37000	266	3.05	30500
224	3.70	37000	267	3.00	30000
225	3.65	36500	268	3.00	30000
226	3.65	36500	269	2.85	28500
227	3.65	36500	270	2.65	26500
228	3.60	36000	271	2.50	25000
229	3.60	36000	272	2.40	24000
230	3.60	36000	273	2.40	24000
231	3.60	36000	274	2.35	23500
232	3.60	36000	275	2.30	23000
233	3.60	36000			

CALIBRATION

Load: 1.0 VDC = 10,000 lbf

Stress: 1.0 VDC = 10,000 lbf/in^2

TABLE 6

Monotonic stress and strain data from dual amplitude cyclic loading test on a uniaxial specimen.

Load Volts	Strain Volts	Stress lbf/in^2	Strain μin/in	Stress x Strain lbf/in^2
0	0	0	0	0
0.50	0.30	5000	459	2.295
1.00	0.60	10000	918	9.180
1.50	0.90	15000	1377	20.655
2.00	1.25	20000	1912	38.240
2.50	1.55	25000	2371	59.275
3.00	1.90	30000	2907	87.210
3.50	2.20	35000	3365	117.78
4.00	2.55	40000	3901	156.04
4.50	2.90	45000	4436	199.62
5.00	3.20	50000	4895	244.75
5.50	3.55	55000	5431	298.71
6.00	3.90	60000	5966	357.96
6.50	4.30	65000	6578	427.57
6.60	4.40	66000	6731	444.25
6.70	4.55	67000	6960	466.32
6.80	4.60	68000	7037	478.52
6.90	4.70	69000	7190	496.11
7.00	4.80	70000	7343	514.01
7.10	5.00	71000	7649	543.08
7.20	5.05	72000	7729	556.49
7.30	5.25	73000	8031	586.26
7.40	5.40	74000	8261	611.31
7.50	5.50	75000	8414	631.05
7.60	5.60	76000	8567	651.09
7.70	5.80	77000	8873	683.22
7.80	6.00	78000	9179	715.96
7.80	6.20	78000	9485	739.83
7.80	7.10	78000	10861	847.16

CALIBRATION

Load: 1.0 VDC = 10,000 lbf

Strain: 1.0 VDC = 1532.23 μin/in

Stress: 1.0 VDC = 10,000 lbf/in^2

TABLE 7

Stress and cyclic number data from dual amplitude cyclic loading test on a uniaxial specimen test.

Cycle	Load Volts	Stress lbf/in^2	Cycle	Load Volts	Stress lbf/in^2
1	7.80	78000	47	6.60	66000
2	4.60	46000	48	3.20	32000
3	7.65	765000	49	6.60	66000
4	4.40	44000	50	3.15	31500
5	7.60	76000	51	6.55	66500
6	4.30	43000	52	3.10	31000
7	7.50	75000	53	6.50	65000
8	4.20	42000	54	3.05	30500
9	7.45	74500	55	6.45	64500
10	4.15	41500	56	3.05	30500
11	7.40	74000	57	6.40	64000
12	4.05	40500	58	3.00	30000
13	7.40	74000	59	6.40	64000
14	4.00	40000	60	2.95	29500
15	7.30	73000	61	6.35	63500
16	3.95	39500	62	2.90	29000
17	7.30	73000	63	6.30	63000
18	3.90	39000	64	2.85	28500
19	7.25	72500	65	6.25	62500
20	3.85	38500	66	2.85	28500
21	7.20	72000	67	6.20	62000
22	3.80	38000	68	2.80	28000
23	7.15	71500	69	6.20	62000
24	3.75	37500	70	2.75	27500
25	7.10	71000	71	6.15	61500
26	3.70	37000	72	2.70	27000
27	7.05	70500	73	6.10	61000
28	3.65	36500	74	2.65	26500
29	7.00	70000	75	6.05	60500
30	3.60	36000	76	2.60	26000
31	7.00	70000	77	6.00	60000
32	3.55	35500	78	2.60	26000
33	6.95	69500	79	6.00	60000
34	3.50	35000	80	2.55	25500
35	6.90	69000	81	5.95	59500
36	3.45	34500	82	2.45	24500
37	6.85	68500	83	5.90	59000
38	3.40	34000	84	2.45	24500
39	6.80	68000	85	5.85	58500
40	3.35	33500	86	2.40	24000
41	6.75	67500	87	5.80	58000
42	3.30	33000	88	2.35	23500
43	6.70	67000	89	5.80	58000
44	3.30	33000	90	2.30	23000
45	6.65	66500	91	5.75	57500
46	3.25	32500	92	2.30	23000

Cycle	Load Volts	Stress lbf/in^2	Cycle	Load Volts	Stress lbf/in^2
93	5.70	57000	117	5.30	53000
94	2.25	22500	118	1.85	18500
95	5.70	57000	119	5.25	52500
96	2.25	22500	120	1.80	18000
97	5.65	56500	121	5.20	52000
98	2.20	22000	122	1.80	18000
99	5.60	56000	123	5.20	52000
100	2.20	22000	124	1.75	17500
101	5.60	56000	125	5.20	52000
102	2.15	21500	126	1.75	17500
103	5.60	56000	127	5.15	51500
104	2.10	21000	128	1.70	17000
105	5.50	55000	129	5.10	51000
106	2.05	20500	130	1.65	16500
107	5.50	55000	131	5.10	51000
108	2.00	20000	132	1.65	16500
109	5.45	54500	133	5.05	50500
110	2.00	20000	134	1.60	16000
111	5.40	54000	135	5.05	50500
112	2.00	20000	136	1.60	16000
113	5.40	54000	137	5.00	50000
114	1.95	19500	138	1.55	15500
115	5.35	53500	139	5.00	50000
116	1.90	19000	140	1.50	15000

CALIBRATION

Load: 1.0 VDC = 10,000 lbf

Stress: 1.0 VDC = 10,000 lbf/in^2

TABLE 8

Stress and strain data from strain gage placement tests and comparison of experimental and theoretical strains, maximum and average. Run number 1

Load Volts	Average Strain Volts	Maximum Strain Volts	Stress lbf/in^2	Exp. Avg. Strain μin/in	Theo. Avg Strain μin/in	Exp. Max. Strain μin/in	Theo. Max. Strain μin/in
1.054	2.018	2.195	1996	496	507	587	565
2.000	2.479	2.725	3788	957	962	1117	1072
2.993	2.957	3.278	5669	1435	1440	1670	1604
4.021	3.459	3.853	7615	1937	1934	2245	2155
5.021	3.948	4.413	9509	2426	2416	2805	2691
6.011	4.435	4.971	11384	2913	2892	3363	3222
7.004	4.924	5.532	13265	3402	3369	3924	3754
7.998	5.417	6.096	15148	3895	3848	4488	4287
9.014	5.923	6.680	17072	4401	4336	5072	4832
8.017	5.423	6.099	15184	3901	3857	4491	4297
7.006	4.917	5.518	13269	3395	3370	3910	3755
6.032	4.433	4.956	11424	2911	2902	3348	3233
5.018	3.934	4.383	9504	2412	2414	2775	2690
4.018	3.441	3.816	7610	1919	1933	2208	2154
3.008	2.949	3.250	5697	1427	1447	1642	1612
2.004	2.462	2.687	3795	940	964	1079	1074
1.008	1.982	2.130	1909	460	485	522	540

CALIBRATION

Load: 1.0 VDC = 10,000 lbf

Strain: 1.0 VDC = 245.76 μin/in

Stress: 1.0 VDC = 1893.74 lbf/in^2

TABLE 9

Stress and strain data from strain gage placement tests and comparison of experimental and theoretical strains, maximum and average. Run number 2

Load Volts	Average Strain Volts	Maximum Strain Volts	Stress lbf/in^2	Exp. Avg. Strain μin/in	Theo. Avg Strain μin/in	Exp. Max. Strain μin/in	Theo. Max. Strain μin/in
1.013	2.011	2.135	1919	477	487	564	543
1.998	2.486	2.691	3784	952	961	1120	1071
3.018	2.978	3.264	5716	1444	1452	1693	1618
4.010	3.464	3.823	7595	1930	1929	2252	2149
5.010	3.952	4.387	9489	2418	2410	2816	2685
6.015	4.444	4.953	11392	2910	2894	3382	3224
7.014	4.936	5.519	13284	3402	3374	3948	3760
8.040	5.445	6.099	15227	3911	3868	4528	4310
9.001	5.921	6.647	17047	4387	4330	5076	4825
8.023	5.435	6.083	15195	3901	3860	4512	4301
7.026	4.942	5.514	13307	3408	3380	3943	3766
6.015	4.442	4.936	11392	2908	2894	3365	3224
5.025	3.954	4.372	9517	2420	2417	2801	2694
4.015	3.458	3.802	7604	1924	1932	2231	2152
3.012	2.970	3.238	5705	1436	1449	1667	1615
2.008	2.483	2.677	3803	949	966	1106	1076
1.021	2.011	2.128	1934	477	491	557	547

CALIBRATION

Load: 1.0 VDC = 10,000 lbf

Strain: 1.0 VDC = 245.76 μin/in

Stress: 1.0 VDC = 1893.74 lbf/in^2

TABLE 10

Stress and strain data from strain gage placement tests and comparison of experimental and theoretical strains, maximum and average. Run number 3

Load Volts	Average Strain Volts	Maximum Strain Volts	Stress lbf/in^2	Exp. Avg. Strain μin/in	Theo. Avg. Strain μin/in	Exp. Max. Strain μin/in	Theo. Max. Strain μin/in
1.011	1.990	1.752	1915	474	486	559	542
2.015	2.474	2.317	3816	958	969	1124	1080
3.023	2.962	2.885	5725	1446	1454	1692	1620
4.035	3.455	3.455	7642	1939	1941	2262	2163
5.023	3.937	4.013	9513	2421	2416	2820	2692
6.033	4.433	4.583	11426	2917	2902	3390	3234
7.020	4.919	5.143	13295	3403	3377	3950	3763
8.017	5.412	5.708	15184	3896	3857	4515	4297
9.023	5.911	6.283	17089	4395	4341	5090	4837
8.032	5.418	5.707	15212	3902	3864	4514	4305
7.021	4.919	5.132	13297	3403	3378	3939	3763
6.017	4.423	4.557	11396	3907	2895	3364	3225
5.037	3.939	4.000	9540	2423	2423	2807	2670
4.014	3.439	3.424	7602	1923	1931	2231	2152
3.028	2.959	2.867	5735	1443	1457	1674	1623
2.006	2.465	2.297	3799	949	965	1104	1075
1.014	1.991	1.746	1920	475	488	553	544

CALIBRATION

Load: 1.0 VDC = 10,000 lbf

Strain: 1.0 VDC = 245.76 μin/in

Stress: 1.0 VDC = 1893.74 lbf/in^2

TABLE 11

Percent differences in experimental and theoretical strain valves from strain gage placement tests.

Run No. 1			Run No. 2			Run No. 3		
Stress lbf/in^2	Avg. Strain Diff. percent	Max. Strain Diff. percent	Stress lbf/in^2	Avg. Strain Diff. percent	Max. Strain Diff. percent	Stress lbf/in^2	Avg. Strain Diff. percent	Max. Strain Diff. percent
1966	2.18	3.90	1919	2.12	3.87	1915	2.54	3.15
3788	0.54	4.19	3784	0.96	4.58	3816	1.17	4.07
5669	0.34	4.09	5716	0.54	4.65	5725	0.57	4.42
7616	0.13	4.16	7595	0.05	4.77	7642	0.11	4.58
9509	0.43	4.22	9489	0.32	4.86	9513	0.19	4.74
11384	0.73	4.38	11392	0.56	4.89	11426	0.50	4.83
13265	0.97	4.52	13284	0.82	5.01	13295	0.76	4.97
15148	1.23	4.69	15227	1.11	5.07	15184	1.02	5.07
17072	1.49	4.97	17047	1.31	5.21	17089	1.25	5.24
15184	1.15	4.51	15195	1.07	4.92	15212	0.98	4.85
13269	0.73	4.12	13307	0.83	4.70	13297	0.75	4.67
11424	0.31	3.55	11392	0.49	4.37	11396	0.43	4.30
9504	0.09	3.17	9517	0.11	3.99	9540	0.01	3.96
7610	0.72	2.52	7604	0.39	3.66	7602	0.42	3.69
5697	1.39	1.84	5705	0.90	3.25	5735	0.94	3.14
3795	2.50	0.45	3803	1.76	2.76	3799	1.66	2.67
1909	5.14	3.39	1934	2.89	1.78	1920	2.63	1.74

$$\text{Percent difference} = 1 - \frac{\text{avg x 100}}{\text{max}}$$

TABLE 12

Monotonic stress and strain data from single amplitude cyclic loading test on a plate.

Nominal Load Volts	Nominal Stress Volts	Local Strain (1) Volts	Local Strain (2) Volts	Nominal Stress lbf/in^2	Nominal Strain μin/in	Local Strain (1) μin/in	Local Strain (2) μin/in
0.048	0.019	0.006	0.001	444	29	9	2
0.10	0.15	0.250	0.250	926	229	382	401
0.30	0.25	0.650	0.650	2778	381	994	1041
0.70	0.55	1.250	1.250	6481	839	1912	2003
1.40	0.85	2.05	1.95	12963	1296	3136	3124
2.00	1.20	3.00	2.85	18519	1830	4589	4566
2.40	1.45	3.75	3.65	22222	2211	5737	5848
3.00	1.75	4.65	4.55	27778	2668	7113	7290
3.40	1.95	5.00	5.00	31481	2973	7649	8011
3.40	2.10	5.45	5.50	31481	3202	8337	8812
3.60	2.10	5.85	5.85	33333	3202	8949	9373
3.60	2.15	6.15	6.25	33333	3278	9408	10014
3.80	2.25	6.50	6.55	35185	3431	9943	10495
3.80	2.25	6.75	6.85	35185	3431	10326	10975
4.00	2.25	6.95	7.05	37037	3431	10632	11296
4.00	2.35	7.15	7.25	37037	3583	10938	11616
4.00	2.35	7.25	7.35	37037	3583	11091	11776
4.00	2.35	7.35	7.45	37037	3583	11244	11937

CALIBRATION

Load: 1.0 VDC=10,000 lbf
Strain: 1.0 VDC=1532.23 μin/in
Stress: 1.0 VDC=9259.26 lbf/in^2

TABLE 13

Data for calculation of average stress concentration factors for monotonic local stress vs. nominal strain curves at single amplitude cyclic loading test on a plate.

Strain Gage (1)

			SAL Data		Mono. Data	
Nominal Stress lbf/in^2	Nominal Strain μin/in	Local Strain μin/in	Local Stress lbf/in^2	K_t	Local Stress lbf/in^2	K_t
444	29	9	0	0	0	0
926	229	382	4000	2.68	4000	2.68
2778	381	994	9750	3.03	10000	3.06
6481	839	1912	19000	2.58	20500	2.68
12936	1296	3136	31000	2.41	32750	2.47
18519	1830	4589	45000	2.47	49000	2.58
22222	2211	5737	56500	2.57	60000	2.65
27778	2668	7113	70500	2.60	74000	2.67
31481	2973	7649	74750	2.47	76500	2.50
31481	3202	8337	77500	2.53	78000	2.54
33333	3202	8949	79000	2.57	78000	2.56
33333	3278	9408	79500	2.62	78000	2.59
35185	3431	9943	80000	2.57	78000	2.53
35185	3431	10326	80000	2.62	78000	2.58
37037	3431	10632	80000	2.59	78000	2.55
37037	3583	10938	80000	2.57	78000	2.54
37037	3583	11091	80000	2.59	78000	2.55
37037	3583	11244	80000	2.60	78000	2.57
		AVERAGE K_t		2.59		2.61

Strain Gage (2)

444	29	2	0	0	0	0
926	229	401	4000	2.75	4000	2.75
2778	381	1041	10500	3.21	11000	3.29
6481	839	2003	19750	2.70	21000	2.78
12936	1296	3124	31000	2.40	33000	2.48
18519	1830	4566	44750	2.46	47750	2.54
22222	2211	5848	57750	2.62	61250	2.70
27778	2668	7290	72000	2.66	75000	2.72
31481	2973	8011	76500	2.56	77000	2.57
31481	3202	8812	79000	2.63	78000	2.61
33333	3202	9373	79500	2.64	78000	2.62
33333	3278	10014	80000	2.71	78000	2.67

Table 13 (Cont'd)

Strain Gage (2)

Nominal Stress lbf/in^2	Nominal Strain μin/in	Local Strain μin/in	SAL Data Local Stress lbf/in^2	SAL Data K_t	Mono. Data Local Stress lbf/in^2	Mono. Data K_t
35185	3431	10495	80000	2.64	78000	2.60
35185	3431	10975	80000	2.70	78000	2.66
37037	3431	11296	80000	2.67	78000	2.63
37037	3583	11616	80000	2.65	78000	2.61
37037	3583	11776	80000	2.66	78000	2.63
37037	3583	11937	80000	2.68	78000	2.65
	AVERAGE K_t			2.67		2.68

SAL - Single amplitude cyclic loading test data

Mono. - Monotonic stress-strain data from cyclic stress-strain curve test.

TABLE 14

Stress and strain data for construction of local stress vs. nominal strain curves of single amplitude cyclic loading test on a plate and percent variation between stresses calculated from one strain gage and two data bases.

Single Amplitude Cyclic Leading Test Data

Nominal Strain μin/in	Stress x Strain lbf/in^2	Local Stress (1) lbf/in^2	Stress x Strain	Local Stress (2) lbf/in^2	Percent Variation Strain gage (1)
29	0.0564	0	0.05995	0	0
229	3.518	4000	3.7385	4500	38.46
381	9.738	9250	10.348	9500	11.90
839	47.22	21500	50.182	22000	4.44
1296	112.67	33500	119.74	34500	4.29
1830	224.65	47500	238.74	48750	6.40
2211	327.93	57500	348.50	59250	7.63
2668	477.50	69250	507.45	71000	7.36
2973	592.91	76000	630.10	77500	2.56
3202	687.77	79000	730.91	79750	1.27
3202	687.77	79000	730.91	79750	1.27
3278	720.80	79500	766.02	80000	1.89
3431	789.66	80000	839.20	80000	2.50
3431	789.66	80000	839.20	80000	2.50
3431	789.66	80000	839.20	80000	2.50
3583	861.18	80000	915.20	80000	2.50
3583	861.18	80000	915.20	80000	2.50
3583	861.18	80000	915.20	80000	2.50
					6.03
					(4.00)

Table 14 (Cont'd)

Monotonic data from cyclic stress-strain curve test

Nominal Strain μin/in	Stress x Strain lbf/in^2	Local Stress (1) lbf/in^2	Stress x Strain	Local Stress (2) lbf/in^2	Percent Variation Strain gage (2)
29	0.0611	0	0.0644	0	0
229	3.8117	6500	4.0189	7250	37.93
381	10.551	10500	11.125	11000	13.64
839	51.165	22500	53.946	23250	5.38
1296	122.08	35000	128.72	36000	4.17
1830	243.42	50750	256.65	52250	6.70
2211	355.32	62250	374.64	64000	7.42
2668	517.39	74750	545.51	76000	6.58
2973	642.44	78000	677.37	78000	0.64
3202	745.23	78000	785.74	78000	2.19
3202	745.23	78000	785.74	78000	2.19
3278	781.02	78000	823.48	78000	2.50
3431	855.63	78000	902.14	78000	2.50
3431	855.63	78000	902.14	78000	2.50
3431	855.63	78000	902.14	78000	2.50
3583	933.12	78000	983.85	78000	2.50
3583	933.12	78000	983.85	78000	2.50
3583	933.12	78000	983.85	78000	2.50
					6.14
					(4.15)

TABLE 15

Monotonic stress and strain data from dual amplitude cyclic loading test on a plate.

Nominal Load Volts	Nominal Strain Volts	Local Strain (1) Volts	Local Strain (2) Volts	Nominal Stress lbf/in^2	Nominal Strain $\mu in/in$	Local Strain (1) $\mu in/in$	Local Strain (2) $\mu in/in$
0.00	0.10	0.20	0.20	0	152	306	319
0.20	0.25	0.55	0.55	1852	381	841	878
0.70	0.40	1.15	1.15	6481	610	1759	1836
1.10	0.75	1.75	1.75	10185	1144	2677	2794
1.50	0.95	2.40	2.35	13889	1449	3671	3753
2.00	1.35	3.35	3.25	18519	2059	5125	5190
3.20	2.00	5.50	5.35	29630	3050	8414	8543
3.50	2.10	5.95	5.80	32407	3202	9102	9262
3.70	2.20	6.50	6.40	34259	3355	9943	10220
3.90	2.20	6.60	6.60	36111	3355	10096	10539
3.90	2.20	6.70	6.60	36111	3355	10249	10539
3.90	2.20	6.80	6.70	36111	3355	10402	10699
3.90	2.35	7.00	6.95	36111	3583	10708	11098
3.90	2.30	7.10	7.00	36111	3507	10861	11178
3.90	2.35	7.15	7.10	36111	3583	10938	11337
3.90	2.30	7.15	7.10	36111	3507	10938	11337

CALIBRATION

Load: 1.0 VDC= 10,000 lbf
Strain: 1.0 VDC= 1532.23 μin/in
Stress: 1.0 VDC= 9259.26 lbf/in^2

TABLE 16

Data for calculation of average stress concentration factors for monotonic local stress vs. nominal strain curves of dual amplitude cyclic loading test on a plate.

Strain Gage (1)

Nominal Stress lbf/in^2	Nominal Strain μin/in	Local Strain μin/in	DAL Data Local Stress lbf/in^2	K_t	Mono. Data Local Stress lbf/in^2	K_t
0	152	306	3500	0	3250	0
1852	381	841	9000	3.28	8750	3.23
6481	610	1759	13000	2.83	13500	2.87
10185	1144	2677	27500	2.51	23000	2.54
13889	1449	3671	37500	2.62	38500	2.65
18519	2059	5125	52500	2.66	53750	2.69
29630	3050	8414	75500	2.65	77750	2.69
32407	3202	9102	77750	2.61	78000	2.62
34259	3355	9943	78000	2.60	78000	2.60
36111	3355	10096	78000	2.55	78000	2.55
36111	3355	10249	78000	2.57	78000	2.57
36111	3355	10402	78000	2.59	78000	2.59
36111	3583	10708	78000	2.54	78000	2.54
36111	3507	10861	78000	2.59	78000	2.59
36111	3583	10938	78000	2.57	78000	2.57
36111	3507	10938	78000	2.60	78000	2.60
		AVERAGE K_t		2.61		2.62

Strain Gage (2)

0	152	319	3500	0	3250	0
1852	381	878	9250	3.39	9250	3.39
6481	610	1836	19000	2.97	19250	2.99
10185	1144	2794	28500	2.61	29000	2.64
13889	1449	3753	38500	2.68	39500	2.71
18519	2059	5190	52750	2.68	54250	2.72
29630	3050	8543	76000	2.68	78000	2.72
32407	3202	9262	78000	2.64	78000	2.64
34259	3355	10220	78000	2.63	78000	2.63
36111	3355	10539	78000	2.60	78000	2.60
36111	3355	10539	78000	2.60	78000	2.60
36111	3355	10699	78000	2.62	78000	2.62
36111	3583	11098	78000	2.59	78000	2.59
36111	3507	11178	78000	2.62	78000	2.62
36111	3583	11337	78000	2.61	78000	2.61
36111	3507	11337	78000	2.64	78000	2.64
		AVERAGE K_t		2.66		2.67

DAL - Dual amplitude cyclic loading test data

Mono. - Monotonic stress-strain data from cyclic stress-strain curve test.

TABLE 17

Stress and strain data for construction of local stress vs. nominal strain curves of dual amplitude cyclic loading test on a plate and percent variation between stresses calculated from one strain gage and two data bases.

Dual amplitude cyclic loading test data

Nominal Strain μin/in	Stress x Strain lbf/in^2	Local Stress (1) lbf/in	Stress x Strain lbf/in^2	Local Stress (2) lbf/in^2	Percent Variation Strain gage (1)
381	10.076	9500	10.466	9750	11.63
610	25.829	14750	26.829	14750	11.94
1144	90.846	29750	94.360	30250	3.25
1449	145.74	35750	151.38	36500	9.49
2059	294.28	55000	305.67	55000	4.76
3050	635.74	76000	670.71	76750	2.56
3202	711.70	77500	739.23	78000	0.64
3355	781.34	78000	811.56	78000	6.32
3355	781.34	78000	811.56	78000	
3355	781.34	78000	811.56	78000	
3355	781.34	78000	811.56	78000	
3583	891.15	78000	925.62	78000	
3507	853.74	78000	886.77	78000	
3583	891.15	78000	925.62	78000	
3507	853.74	78000	886.77	78000	

Table 17 (Cont'd)

Monotonic data from cyclic stress-strain curve test

Nominal Strain µin/in	Stress x Strain lbf/in^2	Local Stress (1) lbf/in	Stress x Strain lbf/in^2	Local Stress (2) lbf/in^2	Percent Variation Strain gage (2)
381	10.632	10750	11.042	11000	11.36
610	27.254	16750	28.304	17000	13.24
1144	95.856	30750	99.549	31500	3.97
1449	153.78	39500	159.71	40250	9.32
2059	310.51	57750	322.48	59000	6.78
3050	681.34	78000	707.60	78000	1.60
3202	750.95	78000	779.88	78000	7.71
3355	824.43	78000	856.19	78000	
3355	824.43	78000	856.19	78000	
3355	824.43	78000	856.19	78000	
3355	824.43	78000	856.19	78000	
3583	940.29	78000	976.52	78000	
3507	900.82	78000	935.53	78000	
3583	940.29	78000	976.52	78000	
3507	900.82	78000	935.53	78000	

TABLE 18

Stress and strain data from unloading portion of initial loading cycle from single amplitude cyclic loading test on a plate.

Nominal Load Volts	Local Strain (1) Volts	Local Strain (2) Volts	Nominal Stress lbf/in^2	Local Strain (1) $\mu in/in$	Local Strain (2) $\mu in/in$
4.0	7.35	7.45	37037	11244	11937
4.0	7.25	7.35	37037	11091	11776
3.8	7.00	7.05	35185	10708	11296
3.4	6.45	6.60	31481	9867	10575
3.0	5.75	6.00	27778	8796	9613
2.6	5.00	5.20	24074	7649	8332
2.0	4.05	4.25	18519	6196	6809
1.4	3.20	3.40	12963	4895	5448
0.8	2.35	2.50	7407	3595	4006
0.4	1.55	1.80	3704	2371	2884
0.0	0.90	1.10	0	1377	1762

CALIBRATION

Load: 1.0 VDC= 10,000 lbf
Strain: 1.0 VDC= 1532.23 $\mu in/in$
Stress: 1.0 VDC= 9259.26 lbf/in^2

TABLE 19

Data for calculation of average stress concentration factors for stress relaxation behavior study of single amplitude cyclic loading test on a plate.

Nominal Stress lbf/in^2	Local Strain (1) μin/in	Local Strain (2) μin/in	K_t (1) Mono. Data	K_t (1) SAL Data	K_t (2) Mono. Data	K_t (2) SAL Data
37037	11244	11937	0	0	0	0
37037	11091	11776	0	0	0	0
35185	10708	11296	3.09	2.89	3.69	3.46
31481	9867	10575	2.64	2.48	2.62	2.45
27778	8796	9316	2.82	2.64	2.68	2.51
24074	7649	8332	2.96	2.77	2.97	2.78
18519	6196	6809	2.91	2.73	2.95	2.77
12963	4895	5448	2.81	2.64	2.88	2.70
7407	3595	4006	2.75	2.44	2.86	2.68
3704	2371	2884	2.84	2.66	2.90	2.72
0	1377	1762	2.84	2.66	2.93	2.75
		AVERAGE K_t	2.85	2.66	2.94	2.76

SAL - Single amplitude cyclic loading test data. .
Mono. Monotonic data from cyclic stress-strain curve test.

TABLE 20

Data from alternate calculation of average stress concentration factors for unloading portion of initial loading cycle in single amplitude cyclic loading test on a plate.

Nominal Stress lbf/in^2	Local Strain (1) μin/in	Local Stress (2) μin/in	Mono. Data $K_t(1)$	Mono. Data $K_t(2)$	SAL Data $K_t(1)$	SAL Data $K_t(2)$
37037	11244	11937	2.84	2.93	2.66	2.75
37037	11091	11776	2.89	2.88	2.62	2.70
35185	10708	11296	2.83	2.89	2.65	2.71
31481	9867	10575	2.88	2.99	2.70	2.80
27778	8796	9613	2.85	3.02	2.67	2.83
24074	7649	8332	2.78	2.91	2.61	2.73
18519	6196	6809	2.78	2.91	2.60	2.73
12963	4895	5448	2.90	3.03	2.71	2.84
7407	3595	4006	3.20	3.23	2.99	3.03
3704	2371	2884	2.86	3.23	2.68	3.03
0	1377	1762	0	0	0	0
			2.88	3.00	2.69	2.82

Mono. - Monotonic data from cyclid stress-strain curve test
σ_m = 78,000 lbf/in^2 E= 10.67 x 10^6 lbf/in^2

SAL - Single amplitude cyclic loading test data
σ_m = 80,000 lbf/in^2 E= 10.0 x 10^6 lbf/in^2

TABLE 21

Stress, strain, and cycle number data from single amplitude cyclic loading test on a plate.

Cycle	Nominal Load Volts	Nominal Strain Volts	Local Strain(1) Volts	Local Strain(2) Volts	Nominal Stress lbf/in^2	Nominal Strain μin/in	Local Strain(1) μin/in	Local Strain(2) μin/in
1	4.0	2.40	7.35	7.45	37037	3660	11244	11937
2	4.0	2.40	7.35	7.45	37037	3660	11244	11937
3	4.0	2.40	7.35	7.45	37037	3660	11244	11937
4	4.0	2.30	7.40	7.50	37037	3507	11320	12017
5	4.0	2.30	7.40	7.50	37037	3507	11320	12017
6	3.9	2.30	7.40	7.50	36111	3507	11320	12017
7	3.9	2.30	7.40	7.45	36111	3507	11320	11937
8	3.9	2.30	7.40	7.50	36111	3507	11320	12017
9	3.9	2.30	7.40	7.50	36111	3507	11320	12017
10	3.9	2.30	7.40	7.50	36111	3507	11320	12017
11	3.9	2.30	7.40	7.50	36111	3507	11320	12017
12	3.9	2.30	7.40	7.50	36111	3507	11320	12017
13	3.9	2.30	7.40	7.50	36111	3507	11320	12017
14	3.9	2.30	7.40	7.50	36111	3507	11320	12017
15	3.9	2.30	7.40	7.50	36111	3507	11320	12017
16	3.8	2.30	7.40	7.50	35185	3507	11320	12017
17	3.8	2.30	7.40	7.50	35185	3507	11320	12017
18	3.9	2.30	7.40	7.50	36111	3507	11320	12017
19	3.9	2.30	7.40	7.50	36111	3507	11320	12017
20	3.8	2.20	7.40	7.50	35185	3355	11320	12017
21	3.8	2.20	7.40	7.50	35185	3355	11320	12017
22	3.8	2.20	7.40	7.50	35185	3355	11320	12017
23	3.8	2.20	7.35	7.45	35185	3355	11244	11937

Table 21 (Cont'd)

Cycle	Nominal Load Volts	Nominal Strain Volts	Local Strain(1) Volts	Local Strain(2) Volts	Nominal Stress lbf/in^2	Nominal Strain μin/in	Local Strain(1) μin/in	Local Strain(2) μin/in
24	3.8	2.20	7.35	7.45	35185	3355	11244	11937
25	3.7	2.20	7.35	7.45	34259	3355	11244	11937
26	3.6	2.20	7.35	7.45	34259	3355	11244	11937
27	3.6	2.15	7.35	7.45	34259	3278	11244	11937
28	3.6	2.15	7.35	7.45	34259	3278	11244	11937
29	3.6	2.15	7.35	7.45	34259	3278	11244	11937
30	3.6	2.15	7.35	7.45	34259	3278	11244	11937
31	3.6	2.15	7.35	7.45	34259	3278	11244	11937
32	3.5	2.15	7.35	7.45	32407	3278	11244	11937
33	3.6	2.15	7.35	7.45	34259	3278	11244	11937
34	3.6	2.15	7.35	7.35	34259	3278	11244	11937
35	3.5	2.15	7.35	7.45	32407	3278	11244	11937
36	3.5	2.05	7.35	7.45	32407	3126	11244	11937
37	3.5	2.10	7.35	7.45	32407	3202	11244	11937
38	3.5	2.10	7.35	7.45	32407	3202	11244	11937
39	3.6	2.10	7.35	7.45	34259	3202	11244	11937
40	3.5	2.10	7.35	7.45	32407	3202	11244	11937
41	3.6	2.10	7.40	7.45	34259	3202	11320	11937
42	3.5	2.05	7.35	7.45	32407	3126	11244	11937
43	3.6	2.10	7.35	7.35	34259	3202	11244	11937
44	3.4	2.10	7.35	7.45	31481	3202	11244	11937
45	3.4	2.10	7.35	7.45	31481	3202	11244	11937
46	3.4	2.10	7.35	7.50	31481	3202	11244	12017
47	3.4	2.10	7.35	7.50	31481	3202	11244	12017
48	3.4	2.10	7.40	7.50	31481	3202	11320	12017

Table 21 (Cont'd)

Cycle	Nominal Load Volts	Nominal Strain Volts	Local Strain(1) Volts	Local Strain(2) Volts	Nominal Stress lbf/in^2	Nominal Strain μin/in	Local Strain(1) μin/in	Local Strain(2) μin/in
49	3.4	2.10	7.40	7.50	31481	3202	11320	12017
50	3.4	2.10	7.40	7.50	31481	3202	11320	12017
51	3.4	2.10	7.40	7.50	31481	3202	11320	12017
52	3.4	2.10	7.40	7.50	31481	3202	11320	12017
53	3.4	2.10	7.40	7.50	31481	3202	11320	12017
54	3.4	2.00	7.40	7.50	31481	3050	11320	12017
55	3.4	2.00	7.40	7.50	31481	3050	11320	12017
56	3.5	2.00	7.40	7.50	32407	3050	11320	12017
57	3.5	2.00	7.40	7.50	32407	3050	11320	12017
58	3.5	2.00	7.40	7.50	32407	3050	11320	12017
59	3.5	2.00	7.40	7.50	32407	3050	11320	12017
60	3.4	2.00	7.40	7.50	21481	3050	11320	12017
61	3.4	2.00	7.40	7.50	31481	3050	11320	12017
62	3.5	2.00	7.40	7.50	32407	3050	11320	12017
63	3.4	2.00	7.40	7150	31481	3050	11320	12017
64	3.5	2.00	7.40	7.50	32407	3050	11320	12017
65	3.5	2.00	7.40	7.50	32407	3050	11320	12017
66	3.3	2.00	7.40	7.50	30556	3050	11320	10217
67	3.3	2.00	7.40	7.50	30556	3050	11320	12017
68	3.3	2.00	7.40	7.50	30556	3050	11320	12017
69	3.2	2.00	7.40	7.50	29630	3050	11320	12017
70	3.3	2.00	7.40	7.50	30556	3050	11320	12017
71	3.3	2.00	7.40	7.55	30556	3050	11320	12097
72	3.3	2.00	7.40	7.55	30556	3050	11320	12097
73	3.3	2.00	7.40	7.55	30556	3050	11320	12097

Table 21 (Cont'd)

Cycle	Nominal Load Volts	Nominal Strain Volts	Local Strain(1) Volts	Local Strain(2) Volts	Nominal Stress lbf/in^2	Nominal Strain μin/in	Local Strain(1) μin/in	Local Strain(2) μin/in
74	3.3	2.00	7.40	7.50	30556	3050	11320	12017
75	3.3	1.95	7.40	7.50	30556	2973	11320	12017
76	3.3	1.95	7.40	7.50	30556	2973	11320	12017
77	3.2	1.90	7.40	7.50	29630	2897	11320	12017
78	3.3	1.95	7.40	7.50	30556	2973	11320	12017
79	3.2	1.90	7.40	7.50	29630	2897	11320	12017
80	3.2	1.95	7.40	7.50	29630	2973	11320	12017
81	3.2	1.95	7.40	7.50	29630	2973	11320	12017
82	3.3	1.95	7.40	7.50	30556	2973	11320	12017
83	3.3	1.95	7.40	7.50	30556	2973	11320	12017
84	3.2	1.95	7.40	7.50	29630	2973	11320	12017
85	3.2	1.90	7.40	7.50	29630	2897	11320	12017
86	3.2	1.95	7.40	7.50	29630	2973	11320	12017
87	3.2	1.95	7.40	7.50	29630	2973	11320	12017
88	3.2	1.90	7.40	7.50	29630	2897	11320	12017
89	3.3	1.95	7.40	7.45	30556	2973	11320	11937
90	3.2	1.90	7.40	7.40	29630	2897	11320	11857

CALIBRATION

Load: 1.0 VDC= 10,000 lbf
Strain: Strain Gage (1) 1.0 VDC= 1529.76 μin/in
Strain Gage (2) 1.0 VDC= 1602.23 μin/in
Nominal Strain Gage 1.0 VDC= 1524.83 μin/in
Stress: 1.0 VDC= 9559.26 lbf/in^2

TABLE 22

Data for calculation of local stress for stress relaxation behavior of single amplitude cyclic loading test on a plate.

		Mono. Data		SAL Data	
Cycle	Nominal Stress lbf/in^2	Local Stress(1) lbf/in^2	Local Stress(2) lbf/in^2	Local Stress(1) lbf/in^2	Local Stress(2) lbf/in^2
1	37037	80000	80000	80000	80000
5	37037	80000	80000	80000	80000
10	36111	77361	77268	77537	77444
15	36111	77361	77268	77537	77444
20	35185	74722	74537	75074	74888
25	34259	72083	71805	72611	72333
30	34259	72083	71805	72611	72333
35	32407	66805	66342	67684	67221
40	32407	66805	66342	67684	67221
45	31481	64165	63610	65221	64665
50	31481	64165	63610	65221	64665
55	31481	64165	63610	65221	64665
60	31481	64165	63610	65221	64665
65	32407	66805	66342	67684	67221
70	30556	61529	60881	62761	62112
75	30556	61529	60881	62761	62112
80	29630	58890	58149	60297	59557
85	29630	58890	58149	60297	59557
90	29630	58890	58149	60297	59557

S_m = 37037 lbf/in^2
σ_m = 80,000 lbf/in^2
Mono.-Monotonic data from cyclic stress-strain curve test
$E = 10.67 \times 10^6$ lbf/in^2
SAL - Single amplitude cyclic loading test data
$E = 10.0 \times 10^6$ lbf/in^2

TABLE 23

Stress and strain data from unloading portion of initial loading cycle from dual amplitude cyclic loading test on a plate.

Nominal Load Volts	Local Strain(1) Volts	Local Strain(2) Volts	Nominal Stress lbf/in^2	Local Strain(1) μin/in	Strain(2) μin/in
3.8	7.10	7.10	35185	10861	11337
3.4	6.30	6.30	31481	9637	10060
2.3	4.50	4.50	21296	6884	7186
1.1	2.30	2.50	10185	3518	3992
0.10	1.00	1.10	926	1530	1757
0.0	0.90	0.95	0	1377	1517
-0.60	0.0	0.20	-5556	0	319

CALIBRATION

Load: 1.0 VDC= 10,000 lbf
Strain: 1.0 VDC= 1523.23 μin/in
Stress: 1.0 VDC= 9259.26 lbf/in^2

TABLE 24

Data for calculation of average stress concentration factors for stress relaxation behavior study of dual amplitude cyclic loading test on a plate.

Nominal Stress lbf/in^2	Local Strain (1) $\mu in/in$	Local Strain (2) $\mu in/in$	$K_t(1)$ Mono. Data	$K_t(1)$ DAL Data	$K_t(2)$ Mono. Data	$K_t(2)$ DAL Data
35185	10861	11337	0	0	0	0
31481	9637	10060	3.53	3.37	3.68	3.51
21296	6884	7186	3.06	2.92	3.19	3.05
10185	3518	3992	3.13	2.99	3.13	2.99
926	1530	1757	2.91	2.78	2.98	2.85
0	1377	1517	0	0	0	0
-5556	0	319	2.84	2.72	2.89	2.76
		AVERAGE K_t	3.09	2.95	3.17	3.03

DAL - Dual amplitude cyclic loading test data.

Mono. - Monotonic data from cyclic stress-strain curve test.

TABLE 25

Data from alternate calculation of average stress concentration factors for unloading portion of initial loading cycle in dual amplitude cyclic loading test on a plate.

Nominal Stress lbf/in^2	Local Strain (1) μin/in	Local Strain (2) μin/in	Mono. Data		DAL Data	
			$K_t(1)$	$K_t(2)$	$K_t(1)$	$K_t(2)$
35185	10861	11337	2.88	2.84	2.75	2.84
31481	9637	10060	2.80	2.77	2.67	2.77
21296	6884	7186	2.76	2.71	2.64	2.71
10185	3518	3992	2.24	2.48	2.14	2.48
926	1530	1757	1.76	2.64	1.68	2.64
0	1377	1517	0	0	0	0
-5556	0	319	2.64	2.20	2.53	2.20
			2.51	2.61	2.40	2.61

Mono.-Monotonic data from cyclic stress-strain curve test.
$\sigma_m = 78{,}000\ \text{lbf/in}^2$ $E = 10.67 \times 10^6\ \text{lbf/in}^2$

DAL - Dual Amplitude cyclic loading test data.
$\sigma_m = 78{,}000\ \text{lbf/in}^2$ $E = 10.19 \times 10^6\ \text{lbf/in}^2$

TABLE 26

Stress, strain, and cycle number data from dual amplitude cyclic loading test on a plate.

Cycle	Nominal Load Volts	Nominal Strain Volts	Local Strain (1) Volts	Local Strain (2) Volts	Nominal Stress lbf/in^2	Nominal Strain μin/in	Local Strain (1) μin/in	Local Strain (2) μin/in
1	3.9	2.25	7.05	7.05	36111	3431	10785	11258
2	2.5	1.45	4.85	4.85	23148	2211	7419	7745
3	3.9	2.30	7.15	7.05	36111	3507	10938	11258
4	2.5	1.35	4.85	4.85	23148	2059	7419	7745
5	3.9	2.15	7.15	7.25	36111	3278	10938	11258
6	2.5	1.35	4.85	4.85	23148	2059	7419	7745
7	3.9	2.15	7.15	7.05	36111	3278	10938	11258
8	2.5	1.35	4.85	4.85	23148	2059	7419	7745
9	3.9	2.15	7.15	7.05	36111	3278	10938	11258
10	2.5	1.35	4.85	4.85	23148	2059	7419	7745
11	3.9	2.15	7.15	7.05	36111	3278	10938	11258
12	2.5	1.35	4.85	4.75	23148	2059	7419	7585
13	3.9	2.15	7.15	7.05	36111	3278	10938	11258
14	2.5	1.30	4.85	4.75	23148	1982	7419	7585
15	3.9	2.15	7.05	7.05	36111	3278	10785	11258
16	2.5	1.30	4.75	4.75	23148	1982	7266	7585
17	3.9	2.15	7.05	7.05	36111	3278	10785	11258
18	2.5	1.30	4.75	4.75	23148	1982	7266	7585
19	3.7	2.15	7.05	7.05	34259	3278	10785	11258
20	2.5	1.30	4.75	4.75	23148	1982	7266	7585
21	3.7	2.05	7.05	7.05	34259	3126	10785	11258
22	2.3	1.25	4.75	4.75	21296	1906	7266	7585
23	3.6	2.05	7.05	7.05	33333	3126	10785	11258

Table 26 (Cont'd)

Cycle	Nominal Load Volts	Nominal Strain Volts	Local Strain (1) Volts	Local Strain (2) Volts	Nominal Stress lbf/in^2	Nominal Strain μin/in	Local Strain (1) μin/in	Local Strain (2) μin/in
24	2.3	1.30	4.75	4.75	21296	1982	7266	7585
25	3.6	2.05	7.05	7.05	33333	3126	10785	11258
26	2.3	1.30	4.75	4.75	21296	1982	7266	7585
27	3.6	2.05	7.05	7.05	33333	3126	10785	11258
28	2.3	1.25	4.75	4.75	21296	1906	7266	7585
29	3.6	2.05	7.05	7.05	33333	3126	10785	11258
30	2.3	1.30	4.75	4.75	21296	1982	7266	7585
31	3.6	2.05	7.05	6.95	33333	3126	10785	11098
32	2.3	1.30	4.75	4.75	21296	1982	7266	7585
33	3.6	2.05	7.05	6.95	33333	3126	10785	11098
34	2.3	1.25	4.75	4.75	21296	1906	7266	7585
35	3.6	2.10	7.05	6.95	33333	3203	10785	11098
36	2.3	1.25	4.75	4.75	21296	1906	7266	7585
37	3.6	2.05	7.05	6.95	33333	3126	10785	11098
38	2.3	1.15	4.75	4.75	21296	1754	7266	7585
39	3.6	2.05	7.05	6.95	33333	3126	10785	11098
40	2.3	1.15	4.75	4.75	21296	1754	7266	7585
41	3.6	2.10	7.05	6.95	33333	3202	10785	11098
42	2.3	1.15	4.75	4.75	21296	1754	7266	7585
43	3.6	2.05	7.05	6.95	33333	3126	10785	11098
44	2.3	1.15	4.75	4.75	21296	1754	7266	7585
45	3.6	2.05	7.05	6.95	33333	3126	10785	11098
46	2.3	1.15	4.75	4.75	21296	1754	7266	7585
47	3.7	1.95	7.05	6.95	34259	2973	10785	11098
48	2.3	1.15	4.75	4.75	21296	1754	7266	7585

Table 26 (Cont'd)

Cycle	Nominal Load Volts	Nominal Strain Volts	Local Strain (1) Volts	Local Strain (2) Volts	Nominal Stress lbf/in^2	Nominal Strain μin/in	Local Strain (1) μin/in	Local Strain (2) μin/in
49	3.7	1.95	7.05	6.95	34259	2973	10785	11098
50	2.1	1.15	4.75	4.75	19444	1754	7266	7585
51	3.5	1.95	7.95	6.95	32407	2973	10785	11098
52	2.1	1.15	4.75	4.75	19444	1754	7266	7585
53	3.5	1.95	7.05	6.95	32407	2973	10785	11098
54	2.0	1.15	4.75	4.75	18519	1754	7266	7585
55	3.5	1.95	7.95	6.95	32407	2973	10785	11098
56	2.1	1.20	4.75	4.75	19444	1830	7266	7585
57	3.5	1.95	7.05	6.95	32407	2973	10785	11098
58	2.1	1.15	4.75	4.75	19444	1754	7266	7585
59	3.5	1.95	7.05	6.95	32407	2973	10785	11098
60	2.0	1.15	4.75	4.75	18519	1754	7266	7585
61	3.5	1.95	7.05	6.95	32407	2973	10785	11098
62	2.0	1.15	4.75	4.75	18519	1754	7266	7585
63	3.5	1.95	7.05	6.95	32407	2973	10785	11098
64	2.0	1.15	4.75	4.75	18519	1754	7266	7585
65	3.5	1.95	6.95	6.95	32407	2973	10632	11098
66	2.0	1.15	4.75	4.75	18519	1754	7266	7585
67	3.5	1.95	7.95	6.95	32407	2973	10785	11098
68	2.0	1.15	4.75	4.75	18519	1754	7266	7585
69	3.5	1.95	6.95	6.95	32407	2973	10632	11098
70	2.0	1.05	4.75	4.75	18519	1601	7266	7585
71	3.5	1.95	6.95	6.95	32407	2973	10632	11098
72	2.0	1.05	4.75	4.75	18519	1601	7266	7585
73	3.5	1.95	6.95	6.95	32407	2973	10632	11098

Table 26 (Cont'd)

Cycle	Nominal Load Volts	Nominal Strain Volts	Local Strain (1) Volts	Local Strain (2) Volts	Nominal Stress lbf/in^2	Nominal Strain μin/in	Local Strain (1) μin/in	Local Strain (2) μin/in
74	2.0	1.05	4.75	4.75	18519	1601	7266	7585
75	3.5	1.95	6.95	6.95	32407	2973	10632	11098
76	2.0	1.05	4.75	4.75	18519	1601	7266	7585
77	3.5	1.90	6.95	6.95	32407	2897	10632	11098
78	2.0	1.05	4.75	4.75	18519	1601	7266	7585
79	3.5	1.90	6.95	6.95	32407	2897	10632	11098
80	2.0	1.05	4.75	4.75	18519	1601	7266	7585
81	3.5	1.85	6.95	6.95	32407	2821	10632	11098
82	2.0	1.05	4.75	4.75	18519	1601	7266	7585
83	3.5	1.85	6.95	6.95	32407	2821	10632	11098
84	2.0	1.05	4.75	4.75	18519	1601	7266	7585
85	3.3	1.90	6.95	6.95	30556	2897	10632	11098
86	2.0	1.05	4.75	4.75	18519	1601	7266	7585
87	3.3	1.90	6.95	6.95	30556	2897	10632	11098
88	1.9	1.10	4.75	4.75	17593	1677	7266	7585
89	3.3	1.85	6.95	6.95	30556	2821	10632	11098
90	1.9	1.10	4.75	4.75	17593	1677	7266	7585
91	3.3	1.85	6.95	6.95	30556	2821	10632	11098
92	1.9	1.05	4.65	4.75	17593	1601	7113	7585
93	3.3	1.90	6.95	6.95	30556	2897	10632	11098
94	1.9	1.05	4.65	4.75	17593	1601	7113	7585
95	3.3	1.85	6.95	6.95	30556	2821	10632	11098
96	1.9	1.05	4.65	4.75	17593	1601	7113	7585
97	3.2	1.85	6.95	6.95	29630	2821	10632	11098
98	1.9	1.05	4.70	4.75	17593	1601	7190	7585

Table 26 (Cont'd)

Cycle	Nominal Load Volts	Nominal Strain Volts	Local Strain (1) Volts	Local Strain (2) Volts	Nominal Stress lbf/in^2	Nominal Strain μin/in	Local Strain (1) μin/in	Local Strain (2) μin/in
99	3.3	1.90	6.95	6.90	30556	2897	10632	11018
100	1.9	1.05	4.65	4.75	17593	1601	7113	7585
101	3.20	1.85	6.95	6.85	29630	2821	10632	10938
102	1.9	1.05	4.65	4.75	17593	1601	7113	7585
103	3.3	1.90	6.95	6.85	30556	2897	10632	10938
104	1.9	1.00	4.65	4.75	17593	1525	7113	7585
105	3.3	1.85	6.95	6.85	30556	2821	10632	10938
106	1.9	0.95	4.65	4.75	17593	1449	7113	7585
107	3.3	1.85	6.95	6.85	30556	2821	10632	10938
108	1.9	0.95	4.65	4.75	17593	1449	7113	7585
109	3.3	1.85	6.95	6.85	30556	2821	10632	10938
110	1.9	0.95	4.65	4.75	17593	1449	7113	7585
111	3.3	1.85	6.85	6.85	30556	2821	10479	10938
112	1.9	0.95	4.65	4.75	17593	1449	7113	7585
113	3.2	1.75	6.85	6.85	29630	2668	10479	10938
114	1.9	0.95	4.65	4.75	17593	1449	7113	7585

CALIBRATION

Load: 1.0 VDC = 10,000 lbf

Strain: Strain Gage (1) 1.0 VDC = 1529.76 μin/in

Strain Gage (2) 1.0 VDC = 1596.83 μin/in

Stress: 1.0 VDC = 9259.26 lbf/in^2

TABLE 27

Data for calculation of local stress for stress relaxation behavior of dual amplitude cyclic loading test on a plate on high stress cycles.

		Mono. Data		DAL Data	
Cycle	Nominal Stress lbf/in^2	Local Stress(1) lbf/in^2	Local Stress(2) lbf/in^2	Local Stress(1) lbf/in^2	Local Stress(2) lbf/in^2
1	36111	78000	78000	78000	78000
5	36111	78000	78000	78000	78000
9	36111	78000	78000	78000	78000
13	36111	78000	78000	78000	78000
17	36111	78000	78000	78000	78000
21	34259	72277	72129	72537	72388
25	33333	69416	69194	69805	69853
29	33333	69416	69194	69805	69853
33	33333	69416	69194	69805	69853
37	33333	69416	69194	69805	69853
41	33333	69416	69194	69805	69853
45	33333	69416	69194	69805	69853
49	34259	72277	72129	72537	72388
53	32407	56555	66258	67073	66777
57	32407	56555	66258	67073	66777
61	32407	56555	66258	67073	66777
65	32407	56555	66258	67073	66777
69	32407	56555	66258	67073	66777
73	32407	56555	66258	67073	66777
77	32407	56555	66258	67073	66777
81	32407	56555	66258	67073	66777
85	30556	60835	60391	61613	61168
89	30556	60835	60391	61613	61168
93	30556	60835	60391	61613	61168
97	29630	57974	57455	58881	58363
101	29630	57974	57455	58881	58363
105	30556	60835	60391	61613	61168
109	30556	60835	60391	61613	61168
113	29630	57974	57455	58881	58363

$Sm = 36111\ lbf/in^2$

$\sigma m = 78{,}000\ lbf/in^2$

Mono. - Monotonic data from cyclic stress-strain curve test.
$E = 10.67 \times 10^6\ lbf/in^2$

DAL - Dual amplitude cyclic loading test data.
$E = 10.19 \times 10^6\ lbf/in^2$

TABLE 28

Data for calculation of local stress for stress relaxation behavior of dual amplitude cyclic loading test on a plate on low stress cycles.

		Mono. Data		DAL Data	
Cycle	Nominal Stress lbf/in^2	Local Stress(1) lbf/in^2	Local Stress(2) lbf/in^2	Local Stress(1) lbf/in^2	Local Stress(2) lbf/in^2
2	23148	37944	36907	39759	38722
6	23148	37944	36907	39759	38722
10	23148	37944	36907	39759	38772
14	23148	37944	36907	39759	38772
18	23148	37944	36907	39759	38772
22	21296	32222	31036	34296	33111
26	21296	32222	31306	34296	33111
30	21296	32222	31036	34296	33111
34	21296	32222	31036	34296	33111
38	21296	32222	31036	34296	33111
42	21296	32222	31036	34296	33111
46	21296	32222	31036	34296	33111
50	19444	26499	25166	28832	27499
54	18519	23641	22233	26104	24696
58	19444	26499	25166	28832	27499
62	18519	23641	22233	26104	24696
66	18519	23641	22233	26104	24696
70	18519	23641	22233	26104	24696
74	18519	23641	22233	26104	24696
78	18519	23641	22233	26104	24696
82	18519	23641	22233	26104	24696
86	18519	23641	22233	25104	24696
90	17593	20779	19298	23372	21890
94	17593	20779	19298	23372	21890
98	17593	20779	19298	23372	21890
102	17593	20779	19298	23372	21890
106	17593	20779	19298	23372	21890
110	17593	20779	19298	23372	21890
114	17593	20779	19298	23372	21890

$Sm = 78,000$ lbf/in^2

$\sigma m = 36111$ lbf/in^2

Mono. - Monotonic data from cyclic stress-strain curve test.
$E = 10.67 \times 10^6$ lbf/in^2

DAL - Dual amplitude cyclic loading test data.
$E = 10.19 \times 10^6$ lbf/in^2

TABLE 29

Initial stress and stress relaxation rate parameter data from uniaxial and plate cyclic loading tests.

Initial Stress, lbf/in^2	Relaxation Rate Parameter	Type of Test		
		Plate		
		Data from uniaxiam specimen cyclic stress-strain curve test		
79220	3.427	SAL test	K_t=2.85	Strain Gage (1)
79470	3.752		K_t=2.95	Strain Gage (2)
78080	2.593	DAL test	K_t=3.09	Strain Gage (1)
78100	2.671	(high)	K_t=3.17	Strain Gage (2)
39030	6.350	DAL test	K_t=3.09	Strain Gage (1)
38120	6.843	(low)	K_t=3.17	Strain Gage (2)
		Data from uniaxiam specimen single amplitude test		
79470	3.324		K_t=2.66	Strain Gage (1)
79470	3.470		K_t=2.76	Strain Gage (2)
		Data from uniaxial specimen dual amplitude tests		
78060	2.457	(High)	K_t=2.95	Strain Gage (1)
78070	2.534	(High)	K_t=3.03	Strain Gage (2)
70650	5.594	(Low)	K_t=2.95	Strain Gage (1)
39720	6.010	(Low)	K_t=3.03	Strain Gage (2)
		Uniaxial Specimen		
73160	3.177	SAL		
76930	3.168	DAL (High)		
45600	7.572	DAL (Low)		

REFERENCES

1. Neuber, H., "Theory of Stress Concentration for Shear-Strained Prismatical Bodies with Arbitrary Nonlinear Stress-Strain Law," Journal of Applied Mechanics, p. 544-550, December 1961.

2. NASA Langley Research Center Technical Note D-6558, Effects of Loading Sequence for Notched Specimens Under High-Low Two-Step Fatigue Loading, by John H. Crews, Jr., November 1971.

3. NASA Langley Research Center Technical Note D-5253, Elastoplastic Stress-Strain Behavior at Notch Roots in Sheet Specimens Under Constant Amplitude Loading, by John H. Crews, Jr., June 1969.

4. Wetzel, R. M., "Smooth Specimen Simulation of Fatigue Behavior of Notches," Journal of Materials, v. 3, no. 10 p. 646-657, September 1969.

5. Morrow, JoDean, Wetzel, R. M., and Topper, T. H., "Laboratory Simulation of Structural Fatigue Behavior," Effects of Environment and Complex Load History on Fatigue Life, ASTM STP 462, p. 74, January 1970.

6. Landgraf, R. W., Morrow, JoDean, and Endo, T., "Determination of the Cyclic Stress-Strain Curve," Journal of Materials, v. 4, no. 1, p. 176-188, March 1969.

7. NASA Langley Research Center Technical Note D-1584, Evaluation of the Influence of Load Randomization and of Ground-Air-Ground Cycles on Fatigue Life, by Eugene C. Naumann, October 1964.

8. NASA Langley Research Center Technical Note D-2629, Fatigue Under Random and Programmed Loads, by Eugene C. Naumann, February 1965.

9. Schijve, J., "Fatigue Tests with Random Flight-Simulation Loading," Advanced Approaches to Fatigue Evaluation, NASA SP 309, May 1971.

10. Natioanl Aeronautics and Astronautics Research Institute AFFDL-TR-66-143, Fatigue Tests with Random and Programmed Load Sequences, with and without Ground-to-Air Cycles, by J. Schijve, D. Brock, P. Derijk, A Nederveem, and P. J. Sevenhuysen, October 1966.

11. Potter, J. M., "The Effect of Load Interaction and Sequence on the Fatigue Behavior of Notched Coupons," Cyclic Stress-Strain Behavior-Analysis, Experimentation, and Failure Prediction, ASTM STP 519, p. 109-132, 1973.

12. ASTM, Annual Book of ASTM Standards, Part 10, "Tentative Recommended Practice for Constant Amplitude Axial Fatigue Tests of Metallic Material," E466-72T, 1975.

13. MTS Systems Corporation, Operator's Manual, Series 810, Material Test System, No. 976.01-30.

14. Volterra, E., and Zachmanoglov, E. C., Dynamics of Vibrations, p. 15-17, Charles E. Merrill Books, Inc., 1965.

15. Vindrine, D. M., A Sequential Strain Monitor and Recorder for Use in Aircraft Life Prediction, Master's Thesis, Naval Postgraduate School, Monterey, California, June 1975.

16. Stanfield, W. C., Microprogrammable Integrated Data Acquisition System-Fatigue Life Data Application, Master's Thesis, Naval Postgraduate School, Monterey, California, March 1976.

17. Butler, C. L., Software Design for a Fatigue Monitoring Acquisition System, Master's Thesis, Naval Postgraduate School, Monterey, California, September 1976.

18. Rourk, R. J., Formulas for Stress and Strain, p. 284, McGraw-Hill Book Company, 1965.

INITIAL DISTRIBUTION LIST

		No. Copies
1.	Defense Documentation Center Cameron Station Alexandria, VA 22314	2
2.	Library, Code 0212 Naval Postgraduate School Monterey, CA 93940	2
3.	Department Chairman, Code 67 Department of Aeronautics Naval Postgraduate School Monterey, CA 93940	2
4.	Associate Professor G. H. Lindsey, Code 67ln Department of Aeronautics Naval Postgraduate School Monterey, CA 93940	1
5.	LT George Michael Horne, USN 601 South Church Street Brookhaven, MS 39601	1

14 MAR 77 24304

Thesis
H8024 Horne
c.1 An investigation of stress determination for aircraft fatigue life estimation from in-flight strain data.

166560

24304

14 MAR 77

Thesis
H8024 Horne
c.1 An investigation of stress determination for aircraft fatigue life estimation from in-flight strain data.

166560

thesH8024
An investigation of stress determination
3 2768 002 06698 7
DUDLEY KNOX LIBRARY